The Abdus Salam International Centre for Theoretical Physics

United Nations Educational, Scientific and Cultural Organization

IAEA International Atomic Energy Agency

Workshop on Indian Ocean Variability and Teleconnections | (SMR 3592)

15 Mar 2021 - 17 Mar 2021
Virtual, Virtual, Italy

---

01 - ADIAHA Monday Sunday

02 - ALABI Oluwasola Benjamin

03 - ALI Shaukat

04 - ARORA Anika

05 - BEHRAVESH Milad

06 - BIBI Amna

07 - BRACCO Annalisa

08 - CHOUDHURY Abida Begum

09 - DA SILVA Leidinice Maria

10 - DEGORSKI Peter

11 - DESHPANDE Aditi

12 - DING Ruibin

13 - DIXIT Ajit Shivsai

14 - DONNER Reik

15 - FRANCIS Feba

16 - GORJA Mohan Murali Krishna

17 - GUPTA Anu

18 - HEMPEL Tim

19 - HUSSAIN Zaheer Syed

20 - HU Xinjia

21 - IACOVONE Florencia María

22 - IKUYAJOLU Olawale James

23 - JAYAPRAKASH SUDHA Deepa

24 - JEGANATHAN Anushiya

25 - JIMA Legese Wogayehu

26 - KADIR Kadir Mokrane

27 - KAKATKAR Arun Rashmi

28 - KANG In Sik

29 - KARREVULA Narayana Reddy

30 - KARYPIDOU Maria Chara

31 - KULKARNI Ravindra Akshay

32 - MARATHE Manas Shamal

33 - MOHANTY Shyama

34 - MOIHAMETTE Foupouapegnigni

35 - MOTSUMI Oreeditse

36 - MUKHOPADHYAY Soumya

37 - NAGARAJAN Kowshika

38 - OROZCO MONTOYA Alonso Ricardo

39 - PANDEY Pushpa

40 - PATEKAR Dasharath Darshana

41 - PATTERSON Ross Matthew

42 - REBOITA Simões Michelle

43 - SAFAR Mahmoud

44 - SANKAR Guganesh

45 - SARTHI Parth Pradhan Parth

46 - SEBASTIAN Anila

47 - SENAN Retish

48 - SHAHI Namendra Kumar

49 - SHAHZAD Kamil

50 - SWAIN Madhusmita

51 - SYED Faisal Saeed

52 - THALLAM Reddy Venugopal

53 - VIBHUTE Suresh Amol

54 - VITA SANCHEZ Sergio Maximiliano

55 - WANG Jiabao

56 - WELDEKIDANE Mamo Ephrem

57 - WOROU Loumovi Amèwuho Koffi

58 - ZAHAN Yasmin

P01

USING SEASONAL AND TEMPORAL PRECIPITATION CONCENTRATION INDEX FOR CHARACTERIZING RAINFALL DISTRIBUTION: A STRATEGY TOWARDS HYDROMETEOROLOGICAL FORECASTING FOR CLIMATIC MODULATION, AGRICULTURAL AND ENVIRONMENTAL MONITORING

Monday S. ADIAHA* and Effiom E. OKU+

*Department of Planning, Research Extension & Statistics,
Nigeria Institute of Soil Science (NISS)
E-mail: mondaysadiaha@gmail.com , sundaymonday@niss.gov.ng
https://orcid.org/0000-0002-2645-3687 Mobile: +2348062627551

+Department of Soil Science, Faculty of Agriculture
University of Abuja, Nigeria
E-mail: eessienoku@gmail.com
https://orcid.org/0000-0002-5043-6457

ABSTRACT

Increase in ocean variability, human-animal ill-health, environmental pollution, land fragmentation, low food production including intensive land disputes have been projected to rise with the current fluctuation and variability in the earth climatic system. The intensity and frequency of this problem has been shown to be worsen and caused by natural and anthropogenic factors including hydrometeorological imbalance, burning of fossil fuel among other triggering factors like unsustainable agricultural practices that contributes to greenhouse gas emission which has resulted in the continues increase in the mean temperature of our planet. Incidence of flood disaster has been recorded globally as part of the resultant impact in the variation that occurs in the earth climate. Flood hazard has been on an increasing alarming frequency, statistics has indicated more than 60% death, ecosystem degradation, economy distortion among other heart-breaking happenings resulting from this disaster, there have also been undocumented impact of this hazards especially in poor-resources Nations. As a strategy towards hydrometeorological forecasting for climatic modulation, agricultural and environmental monitoring this study becomes imperative. Meteorological data was obtained for Federal Capital Territory of Nigeria from Nigeria Meteorological Agency, Seasonal and Temporal Precipitation Concentration Index (PCI) models were applied after data processing. Analysis was done using Geographic Information System models. Seasonal and Temporal map of the study area was developed from where interpolation was done. Descriptive statistics was applied in the study. Result of the study indicated that the study area has recorded a value range of (PCI = 13.28 – PCI = 15.56) which was ranked to show that the area possesses flooding tendency. Ecological engineering with the use of Vetiver Grass Technology (VGT) was recommended for the area to reduce flow intensity and damage impact during a flood outburst.

Keywords: *Climatic Variability; Precipitation Concentration; Hydrometeorological Forecasting; Climatic Modulation; Environmental Monitoring*

P02

SENSITIVITY OF FIVE CUMULUS SCHEMES IN SIMULATING WEST AFRICAN MESOSCALE CONVECTIVE SYSTEMS' CHARACTERISTICS

ALABI B.O.* and ADEFISAN E.A.

Department Of Meteorology, Federal University of Technology, Akure, Ondo State, Nigeria.

ABSTRACT

This research work evaluated the performances of five cumulus parametrization schemes (CPSs) in Weather Research and Forecasting (WRF) model for simulating the initiation, propagation and rainfall delivery capacity of mesoscale convective systems (MCSs) over West Africa. Five simulations were conducted using five different cumulus schemes, for the whole of September, 2012 with the initial and lateral boundary conditions from ERA-Interim reanalysis data. The five cumulus parameterization schemes used are the Kain-Fritsch (KF), Grell-3Dimension ensemble (Grell 3D), Tiedtke (TKE), Grell-Freitas (GF), and New Simplified Arakawa-Schubert (NSAS). Infra-red brightness temperature from the satellite imagery was used for the performance evaluation while TRMM rain rate were used as observed to compare rain rate of the five CPSs. However, based on the subjective verification and objective evaluation, it can be concluded that the performance of the five schemes is highly case-and local-dependent, and the performance of the better TKE and NSAS schemes cannot be generalised over West Africa.

Keywords: Mesoscale Convective Systems, Cumulus Parameterization Schemes, Verification and Evaluation.

P03

21st Century Precipitation and Monsoonal Shift over Pakistan using High-Resolution Models

Shaukat Ali[1], Michelle S. Reboita[2*] and Rida Sehar Kiani[1]

[1]*GCISC, Ministry of Climate Change, Government of Pakistan, Islamabad, Pakistan*

[2]*Instituto de Recursos Naturais, Universidade Federal de Itajubá, Brazil*

Abstract

There is research evidence that due to global warming, global precipitation and monsoon area have shown a shift which needs to be analyzed at local scale. This study analyses future precipitation and monsoon spatial shift over Pakistan and adjoining areas based on CORDEX-CORE projections for the South Asian domain. Three global climate models from CMIP5 provided the lateral boundary conditions for the Regional Climate Model (RegCM4) under RCP2.6 and RCP8.5 scenarios. Results indicate an increase in June-July-August precipitation over north/northeast Pakistan for RCP2.6 and RCP8.5. The results also show a projected expansion in the monsoon area of Pakistan which corresponds with future precipitation increase in the area. The changes in monsoon precipitation and domain are also correlated with low and upper level circulation patterns.

Keywords: precipitation, monsoon area, Pakistan, atmospheric circulation, Arabian Sea, Indian ocean

P04 On the role of the Arabian Sea thermal variability in governing rainfall variability over the Western Ghats

Many previous studies have documented the changes in rainfall patterns along the Western coast of India. The Western Ghats of India comprising of coastal regions of Maharashtra, Karnataka, and Kerala regions are facing the worst floods and droughts in recent years. Changes in low-level horizontal wind circulation due to the change in sea surface temperature over the northern Arabian Sea have been reported by many studies. This work highlights the role of surface-subsurface variations in temperature over the Arabian Sea in governing rainfall variability over the Western Ghats. The subsurface flow of water masses from the Southern Indian Ocean into the Arabian Sea or vice versa along the Somalia-Oman coast can increase or decrease depth of the thermocline. Deepening or shoaling of thermocline depth in the central Arabian Sea can further lead to the changes in the surface temperatures. The rainfall variability over the Western Ghats is predominantly governed by the sea surface temperature (SST) variations over the Arabian Sea. The shoaling of thermocline due to an increase in Ekman upwelling and decrease in the subsurface water flow has decreased SST in the Arabian Sea in the recent decade. This decrease in SST can lead to a decrease in the rainfall over the Western Ghats. This study also reports an interdecadal oscillation in the surface-subsurface coupling over the Arabian Sea.

P05

Investigating the effects of the extratropical transition of North Indian Ocean Cyclones over Iran in four case studies

Milad Behravesh and Mahmoud Safar
Department of Space Physics, Institute of Geophysics, University of Tehran, Iran
(milad.behravesh@ut.ac.ir)

The extratropical transition of tropical cyclones (ETTCs) significantly impacts the midlatitude flow predictability in operational weather forecast models. Knowing ETTCs mechanisms is an essential subject to prevent or reduce hazards associated with them, especially in the coastal areas. The interaction between the involving processes in ETTCs can occur over various space and time scales. The effects of ETTCs on the midlatitude are ambitious in the North Indian Ocean and the Arabian Sea. This study delineates an objective assessment of four North Indian Ocean Cyclones (NIOCs) over the Arabian Sea and investigates their impacts on midlatitudes, specifically Iran, during and after their activities, in various atmospheric levels.

Four NIOCs, Chapala (27 October to 3 November 2015), Megh (4-10 November 2015), Phet (30 May to 7 June 2010), and Ashobaa (6-12 June 2015), have been selected to study here. The Weather Research and Forecasting (WRF) model has been used to simulate those events. The selected tropical cyclones were somewhat similar in their underlying path two by two (Chapala with Megh and Phet with Ashobaa). Moreover, the NIOCs in this study categorized as the monsoon-season cyclones (Phet and Ashobaa) and the post-monsoon-season cyclones (Chapala and Megh).

It was noticeable that the surface pressure at higher latitudes (in the selected domain for this study, especially between 40°N to 50°N) has decreased in all simulations after finishing the cyclones activity, especially over some parts of Europe and Russia. Changes in the maximum wind speed position in the post-monsoon-season cyclones have been noticed in the 500 hPa trough from downstream to upstream. Also, a similar wind speed pattern displacement was noticed at 300 hPa jet stream.

All simulations have proved the transfer of the potential vorticity (small amounts up to 0.5 PVU) into the midlatitudes by ascending on the 320 K isentropic surface. Moreover, a similar pattern was noticed in the relative humidity by ascending on the 320 K isentropic surface into the midlatitudes, especially towards the west of Iran in Chapala and south of Iran in Megh. It seems that the humidity transfer was more evident in the pos-monsoon-season due to the lack of vast amounts of humidity in that area compared to the monsoon-season.

The results confirm the remarkable effects of the tropical cyclones in the North Indian Ocean and the Arabian Sea on the midlatitudes. It seems the post-monsoon season cyclones with the westward movement toward the coast of Yemen (considering the topography of that region) have more indirect impacts on Iran.

Keywords: extratropical transition of tropical cyclones, WRF, North Indian Ocean, potential vorticity, relative humidity

P06

The Mechanism and Prediction of the Torrential Rainfall over Northern Pakistan

AMNA BIBI

PAKISTAN METEOROLOGICAL DEPARTMENT (PMD) ISLAMABAD

Keywords: Westerly Jet; Potential vorticity, Absolute vorticity, Torrential rainfall; Monsoon; Northern Pakistan

Abstract

Deadly events such as runoff, flash flooding, and mudslides may trigger by torrential rainfall events that pose a significant threat to human assets. In the past, Pakistan has experienced major meteorological disasters such as flash floods caused by torrential rainfall events. Previous studies have shown precipitation characteristics in Pakistan, but upper level circulations dynamics during extreme rainfall events by using high resolution models over this region are still warranted. For improvement of forecasting accuracy and mitigate flood hazards, the main objective is to study the dynamics of westerlies that play a key role in the enhancement of extreme rainfall over northern Pakistan during the summer monsoon. WRF model version 3.7 developed by the National Oceanic and Atmospheric Administration (NOAA) and the National Center for Atmospheric Research (NCAR) is used for simulated data of precipitation and circulation products, to study the dynamics of westerlies associated with flood-producing extreme rainfall events. To claculate percentage departure, PMD observational dataset was used for a period of 31 years (1985-2016) containing a record rainfall of 14 meteorological stations. Moreover, CRU TS4.01 and GPCC datasets with 0.5º× 0.5º and 0.25º× 0.25º grid resolutions were used to determine the similarity and suitability of different precipitation datasets as well as for the verification of model simulation.

The area factor for PMD station data was calculated by applying Thiessen's (1911) polygon method commonly used in meteorology as suggested by Rhynsburger (1973). Area-weighted rainfall for PMD along with GPCC is also used to analyze the precipitation events. By analyzing observational data, it is found that precipitation was slightly higher than the GPCC precipitation in certain years during 1985–2016, but the trend and variability were the same. Furthermore, the spatial analysis reveals that there is a high correlation (R = 0.7816) between the two datasets. Moreover, the Standardized Precipitation Index (SPI) is used for extreme precipitation events over northern Pakistan using precipitation data from 1985-2016 to identify flood/drought years. The procedure used by McKee et al. (1993) for SPI calculation has been adopted. SPI values have been computed and used to analyze flood events. Three wet years of extreme precipitation 1988, 2010 and 2013 were undertaken in this study on the basis of the seasonal and monthly analysis of percentage departure and SPI values

.

Results evidenced that the selected extreme rainfall events are accompanied by interactions of moist monsoon circulations and penetration of mid-latitude westerly troughs over northern Pakistan. Analysis of the horizontal distribution of rainfall showed that Pakistan has received maximum rainfall exceeded upto 120mm/day during all events. Jet streams at 200 hPa were observed for all three selected events that had caused the sucking of warm moist air from the Indian Ocean. Maximum values of absolute vorticity have been observed associated with cyclonic depression. Vertical cross-section of potential vorticity along with potential temperature was taken for a detailed analysis of vertical structure at the upper and lower tropospheric levels. Negative PV shows potential instability at the upper level and deep convergence at a lower level which is linked with westerlies trough between pressure levels 750 hPa to upper troposphere respectively. To find the deep convection relative humidity and vertical velocity has also been plotted at 500 and 850 hPa which gives information about the rising and sinking of air. Negative values of vertical velocity at 500 hPa have been observed over Afghanistan, India and adjoining areas along with high values of relative humidity which is a significant progenitor of the warm moist air from the Arabian Sea and cause of convection leading to precipitation. In the presence of westerlies, a blocking signature over Eurasia along with Tibetan anticyclone was present 4-2 days prior to rainfall events. It is an important element to forecast such events in the future. The high-resolution models like WRF are not being in practice for better assessment of daily forecast of upper-level circulation patterns which also considered as a vital element in triggering the extreme rainfall events over complex topography. This study will be helpful for understanding the processes that can be responsible for generating heavy rainfall over northern Pakistan and its neighboring regions.

P07

Using part of the abstract of a recently submitted work. If the student leading this work applies, he can present it. I would rather not. Annalisa Bracco

Information entropy and climate predictability in the Indo-Pacific basin

Olawale J. Ikuyajolu[1,2], Fabrizio Falasca[1], Annalisa Bracco*[1,2]

[1]School of Earth and Atmospheric Sciences, Georgia Institute of Technology, Atlanta, GA, USA

[2]Program in Ocean Sciences and Engineering, Georgia Institute of Technology, Atlanta, GA, USA

In this work, we build upon recent advances in nonlinear dynamical systems theory and introduce the climate community to an information entropy quantifier based on recurrence. The entropy, or complexity, and therefore potential predictability, of a system is associated with microstates that recur over time in the time-series that define the system.

A computationally fast method to evaluate the entropy of multi-dimensional fields is applied to the investigation of the predictability potential of sea surface temperature in the tropical Pacific and Indian Oceans, focusing in boreal fall. In this season the predictability of the basins is linked to two regularly varying nonlinear oscillations, the El Niño-Southern Oscillation and the Indian Ocean Dipole. We compute and compare the entropy in simulations from the CMIP5 catalog from the historical period and RCP8.5 scenario, and in reanalysis datasets. Discrepancies are found between the models and the reanalysis, and no robust changes in predictability can be identified in future projections. The Indian Ocean and the equatorial Pacific emerge as areas where the modeled entropy differs the most from that of the reanalysis in many models. A brief investigation of the bias origin points to a poor representation of the ocean mean state and, for some of the models, of the basins' connectivity at the Indonesian Throughflow among the causes.

P08

Rapid Drying of Northeast India in the Last ThreeDecades: Climate Change or Natural Variability?

B. Abida Choudhury[1,3], Subodh Kumar Saha[2], Mahen Konwar[2], K. Sujith[2],and Atri Deshamukhya[1]

[1]Department of Physics, Assam University, Silchar, India
[2]Indian Institute of Tropical Meteorology, Pune, India
[3]Cotton University, Guwahati, Assam, India

Abstract

Northeast India (NEI), the wettest place on the Earth, has experienced a rapid decrease in summer monsoon rainfall (about 355 mm) in the last 36 years (1979–2014), which has serious implications on the ecosystem and the livelihood of the people of this region. However, it is not clear whether the observed drying is due to anthropogenic activities or it is linked with the global natural variability. A diagnostic model is employed to estimate the amount of recycled rainfall, which suggests that about7% of the total rainfall is contributed by the local moisture recycling and decrease in recycled rainfall is about 30–50 mm. Using gridded observed rainfall and sea surface temperature data of the last 114 years(1901–2014), here we show that the recent decreasing trend of NEI summer monsoon rainfall is rather associated with the strong interdecadal variability of the subtropical Pacific Ocean. The strong interdecadal variability over NEI suggests a possibility of skillful decadal prediction of the monsoon rainfall, which may have important implications in terms of long-term planning and mitigation.

P09

Dynamic downscaling of climate simulations and projections in tropical South America

Maria Leidinice da Silva

Climate Sciences Post-graduate Program, Federal University of Rio Grande do Norte, Av. Senador Salgado Filho, 3000, 59078-970, Lagoa Nova, Natal, Brazil.

Abstract: High resolution simulations of the Regional Climate Model version 4.7 (RegCM4.7) coupled with the Community Land Model version 4.5 (CLM4.5) under the scenarios RCP2.6 and RCP8.5, which interact with the Fifth Evaluation Report of the Intergovernmental Panel on Climate Change (IPCC AR5), were carried out on tropical South America (TSA). These simulations were produced through initial and boundary conditions from simulations conducted by the Global Climate Model HadGEM2-ES. With the objective of verifying the Added Value (AV) of the regional model by reproducing in an appropriate and coherent way the regional aspects of influence in the recent climate (1986-2005), as well as evaluating the regional aspects simulated by the model in the scope of the projections of changes for the future (2080-2099). For this study, the climate in the TSA was characterized based on the variables of precipitation and air temperature close to the surface. For the evaluation of the spatial representation, frequency and extremes of the regional simulation during the recent climate, the high resolution observational database of the Climate Research Unit version ts4.02 (CRU-ts4.02) was used. Although some differences and biases still persist, RegCM4.7 presents VA in the spatial representation of precipitation and temperature over the Northeast Brazil region and part of the Andes. However, it does not adequately represent precipitation over the Amazon basin, especially during the southern summer season. Preliminary results for future projections indicate that the more refined simulation of RegCM4.7 improves the projected change patterns of the coarser resolution simulation of HadGEM2-ES and even modifies the temperature signal in some cases, for example, during the southern autumn season. In general, HadGEM2-ES simulates the main aspects of the climate sufficiently to consider forcing RegCM4.7 to generate simulations with better performance and more realistic climate projections.

Keywords: Dynamic Downscaling; RegCM4.7; HadGEM2-ES; Climate Change.

P10

South Atlantic Indian Ocean Teleconnection – contribution to Indian ocean variability?

Peter Degorski (peter.degorski@gmail.com)

The tropical casual pathway between Atlantic and Indian ocean is understood and its impact on Indian ocean basin has been reviewed [1]. More recently an extratropical bridge between the Atlantic and Indian ocean (SAIO) has been demonstrated to impact the variability of Indian ocean tropical cyclones [2]. Following work which details the mechanism that drives this extratropical connection [3]. I've looked into the skill with which seasonal models are able to forecast the atmosphere teleconnection between the Atlantic and Indian ocean.

It remains an open question the impact this extratropical teleconnection has on tropical Indian ocean dynamics.

[1] Wang, Chunzai, et al. "Teleconnections of the tropical Atlantic to the tropical Indian and Pacific Oceans: A review of recent findings." *Meteorologische Zeitschrift* 18.4 (2009): 445-454.

[2] Lin, Zhongda. "The South Atlantic–South Indian Ocean pattern: A zonally oriented teleconnection along the Southern Hemisphere westerly jet in austral summer." *Atmosphere* 10.5 (2019): 259.

[3] DeBlander, Evan, and Jeffrey Shaman. "Teleconnection between the South Atlantic convergence zone and the southern Indian Ocean: Implications for tropical cyclone activity." *Journal of Geophysical Research: Atmospheres* 122.2 (2017): 728-740.

P11

Study of the evolution and simulation of Arabian Sea monsoon eddy systems in CMIP models.

Aditi Deshpande*

***Savitribai Phule Pune University**

aditid84@gmail.com

Arabian Sea monsoon eddy systems, namely, Southern Gyre, Great Whirl and Socotra eddy are unique oceanic features which are observed over coastal Arabian Sea during Indian Summer Monsoon. Their simulations in the CMIP models are being studied to understand its changes and their relationship with the Indian Summer Monsoon in the ocean warming scenario is being investigated. An increase in extreme precipitation events over the Indian subcontinent have put a spotlight on the changing behaviour of Indian Summer Monsoon. The circulation over Arabian Sea is vital component of the Indian Summer Monsoon variability. This study aims to improve the understanding of the relationship between the Arabian Sea circulation and the Indian Summer Monsoon. Since the Indian subcontinent relies heavily on the consistency of the monsoon precipitation, it is of fundamental importance to study the dynamics and behaviour of the circulation that plays a significant role in monsoon variability. In this way, this study will contribute significantly to improving our understanding of Arabian Sea circulation and its impact on summer monsoon rainfall.

P12

The internal and ENSO-forced variability of the Indian Ocean sea surface temperature

Ruibin Ding[1], In-Sik Kang[1,3†], Farneti Riccardo[2], Jiliang Xuan[1,4], Fabio Di Sante[2], Feng Zhou[1,3], Tao Zhang[1]

[1] State Key Laboratory of Satellite Ocean Environment Dynamics, Second Institute of Oceanography, Ministry of Natural Resources, Hangzhou, China

[2] Physics of Weather and Climate Group, Abdus Salam International Centre for Theoretical Physics, Trieste, Italy

[3]Institute of Oceanography, Shanghai Jiao Tong University, Shanghai, China

[4]Lab of Marine Ecological Environment Monitoring and Prediction, Fourth Institute of Oceanography, Ministry of Natural Resources, Beihai, China

† Corresponding author: In-Sik Kang (kang@sio.org.cn)

Abstract

The internal and ENSO-forced variability of the Indian Ocean sea surface temperature (SST) was investigated by using four different sets of simulations with a regional coupled model. Those simulations were performed by controlling the atmospheric and oceanic boundary conditions, prescribed with combinations of historical reanalysis data and its climatological cycle. The Indian Ocean Basin (IOB) and Dipole (IOD) modes appear as the first and second eigenvectors of SST in all four simulations, although the amplitudes of ENSO-forced modes are larger than those of internal mode. The major period of the IOB is mainly determined by ENSO through the atmosphere, while that of IOD is mainly determined by internal mode but modulated by ENSO, particularly at 1−2 year period. Also investigated is the seasonal dependency of the IOB and IOD, especially under ENSO atmospheric influence.

P13

An empirical, self-sustained, generic, nonlinear oscillator model for the slow manifold of climate oscillation indices

Shivsai Ajit Dixit[1] and B. N. Goswami[2]
[1]Indian Institute of Tropical Meteorology, Pune
[2]Cotton University, Guwahati

The slow manifolds of the time series of climate oscillation indices typically present quasi-periodic oscillations. However, they exhibit rather broadband spectra and strongly non-Gaussian probability density functions. These attributes, therefore, indicate strong departures from linearity in the underlying dynamics that create these oscillations. Time series analysis using delay-coordinate embedding, routinely used in nonlinear dynamics, shows that the time-localized behaviour of the underlying system in the neighbourhood of the present state may be better described in terms of a self-sustained nonlinear oscillator. The oscillator may be empirically derived from a (discrete) nonlinear regression model that describes the nonlinear relationship between the present state and the past states of the system to an excellent accuracy. The hindcast skill of the discrete and oscillator models in predicting the slow manifold is tested in the context of the Dipole Mode Index (DMI) which describes the temporal variation of the intensity of the Indian Ocean Dipole mode.

P14

Complex network and causal discovery approaches for disentangling monsoon dynamics across regions and timescales

Reik V. Donner

Magdeburg-Stendal University of Applied Sciences, Magdeburg, Germany

Potsdam Institute for Climate Impact Research (PIK) – Member of the Leibniz Association, Potsdam, Germany

Tropical climate variability exhibits complex features in time and space originating from the nonlinear interaction of different processes in the atmosphere and ocean along with other components of the Earth system that are characterized by diverse spatial and temporal scales. In such a setting, classical methods of statistical climatology may miss important information on relevant dynamical characteristics.

One way to address this issue is applying concepts from complex network theory for disentangling large-scale spatial patterns of climate variability, which is demonstrated for the spatiotemporal organization of strong rainfall events in the South American [1], Indian [2] and East Asian monsoon domains [3]. For the specific example of the East Asian summer monsoon, the Baiu frontal system as a main characteristic of the associated seasonal circulation pattern is found not to present synchronized extremes over large spatial scales. In turn, two regions north and south of the front exhibit co-occurring daily precipitation maxima (pointing to an associated – at least episodic – dynamical coupling), despite the fact that the corresponding regions are controlled by remote large-scale circulation patterns that are commonly considered independent – the South Asian Anticyclone and the Northwestern Pacific Subtropical High [3].

To further improve our process understanding of monsoon dynamics, causal discovery tools are exploited to test hypotheses on mechanistic pathways associated with drivers of monsoon systems and quantify the strength of different competing causal effects. For the specific case of the Indian summer monsoon, regional (tropical) and remote (extratropical) drivers are found to both contribute significantly to intraseasonal variability in monsoonal rainfall, with the extratropical influence manifested by the circumglobal teleconnection pattern reaching a strength comparable with that of tropical MJO-related drivers [4,5].

Taken together, both presented techniques – functional climate network analysis and causal effect network analysis – provide deep insights into tropical climate variability and are readily applicable to study also other phenomena associated with climate dynamics in both, tropics and extratropics.

References: [1] Wolf et al., Chaos, 2020; [2] Odenweller & Donner, Phys. Rev. E, 2020; [3] Wolf et al., Earth Syst. Dyn., in press; [4] Di Capua et al., Earth Syst. Dyn., 2020; [5] Di Capua et al., Weather Clim. Dyn., 2020.

P15

Decadal Prediction of Indian Ocean Dipole

Feba Francis[1], Ashok Karumuri[1], and Matthew Collins[2]

[1]University of Hyderabad, Centre for Earth, Ocean and Atmospheric Sciences, India

[2]University of Exeter, College of Engineering, Mathematics and Physical Sciences, UK

Decadal Prediction is the prediction of climate for the next 5–20 years. Decadal Prediction has gained great importance as it tries to bridge the gap between seasonal and Centennial (50-100 year) predictions creating a balance between initial conditions and boundary conditions. We analysed the model output from CMIP5 decadal runs of nine models. Our results show that two of the decadal hindcasts show prediction skills of significance for the **Indian Ocean Dipole** for up to a decade. The Indian Ocean Dipole is one of the leading modes of climate variability in the tropics, which affects global climate. As already established, the models also show year-long lead predictability of the El Niño Southern Oscillation. We found no significant skills for the Indian Summer Monsoon. We are presently looking for the source of the lead predictability of Indian Ocean Dipole which appears to be due to links from **the Southern Ocean**. These decadal prediction skills and predictability for a climate driver like the Indian Ocean Dipole have immense helpfulness for climate science and society in general.

P16

Investigating the Role of Ocean-Atmospheric Interactions during Climate Extremes

Gorja Mohan Murali Krishna & Naresh Krishna Vissa

Department of Earth & Atmospheric Sciences

National Institute of Technology – Rourkela, Odisha, India – 769001

Planned Research:

Ocean-atmosphere interactions in the tropics have a profound influence on the climate system. El Niño–Southern Oscillation (ENSO) occurring in the tropical Pacific is the Earth's most vigorous mode of climate variability at interannual times scales. This dominant mode is observed with maximum SST anomalies in the Central and Eastern Pacific. A strong consensus prevailing in the literature that Tropical Indian Ocean warming (TIOW) induced by El Nino influencing the global circulation pattern and mainly coupled inter-basin ocean phenomena. The relationship between variability of these two oceans is time-varying, which is needed to be explored further. This has motivated me to understand the theoretical studies on dynamics of tropical interactions linking the two oceans and to use modelling approaches.

P17

Spatial extent of extreme precipitation systems over the Indian summer monsoon region

Anu Gupta[1] and Hiroshi G. Takahashi[1]
Department of Geography, Tokyo Metropolitan University
Minami-Osawa, Hachioji-shi, Tokyo, Japan
Email: gupta-anu@ed.tmu.ac.jp

Abstract

This study considers the long-term change in the Indian monsoon rainfall and investigates its spatial-temporal aspects. We examines extreme rainfall events (ERE) spatial characteristics over India during the summer monsoon season. By using the Indian Meteorological Department gridded daily rainfall dataset, we found different coherent ERE precipitation system patterns named as precipitation system approach (PSA). Using the different spatial sizes the EREs were categorized into three groups, sporadic, intermediate, and massive rainfall systems based on their spatial extent. From the long term (118 years;1901-2018) analysis, we found that ERE frequency based on conventional grid approach showed impractical interannual and decadal variability, whereas PSA based EREs showed practical relevance. In the long term change, only sporadic systems frequency is increasing, whereas intermediate and massive frequency is decreasing or no change, respectively. Further, we investigated the composited of massive EREs in the recent 40 years (1979-2018) spatial climatology of rainfall, moisture, winds and vorticity to understand the mechanism of these events. It clearly showed a large circulation over the Central India which could be associated with the low-pressure systems developing over the Bay of Bengal.

Key words: Spatial Extent, Extreme Rainfall Events, Precipitation system approach, Dependency of ERE rainfall on land surface temperature(LST).

P18

Teleconnections of the Indian Ocean Dipole in the 20.th Century in Models and Reanalysis

Tim Hempel[1]

Affiliation:

[1] Atmospheric, Oceanic and Planetary Physics, University of Oxford, Oxford, UK

Disclaimer:

The research in this abstract is still in progress, has not been published, and not been reviewed yet.

Abstract:

The Indian Ocean Dipole (IOD) is the strongest mode of sea surface temperature (SST) and precipitation variation in the Indian Ocean. Studies have shown that the extremely warm and wet winter of 2019/2020 in northern Europe and the strong positive NAO can be linked to the strong positive IOD event of that winter. The SST and precipitation in the Indian Ocean in this year where both very pronounced and incited a wave-train from the Indian Ocean to the North Atlantic, which led to more favourable conditions for the development of a strong positive NAO.

We use reanalysis data and model runs of the 20^{th} century to investigate this teleconnection between the Indian Ocean and the North Atlantic and to identify how likely a scenario like the 2019/2020 winter is. Using ensemble reforecasts from the Integrated Forecasting System (IFS) from the European Centre for Medium-Range Weather Forecasts (ECMWF) of the 20^{th} century we analyse how well the model can simulate this teleconnection. Additionally we use the Coupled ECMWF Reanalysis of the 20^{th} century (CERA-20C) to compare the model results to and to find out how the IOD - North Atlantic teleconnection looked like in the last century.

We find that the IOD teleconnection of 2019/2020 was so strong, not only because the IOD event was so strong, but also because of the absence of any ENSO event that winter. Most positive IOD events are accompanied by a positive ENSO event and vice versa. While a positive IOD event increases the likelihood of a positive NAO, the opposite is the case for a positive ENSO event. In the reanalysis only few and weak IOD events in the 20^{th} century were not accompanied by ENSO events and these events were too weak to develop a strong teleconnection. Thus it is very difficult to identify the typical IOD - NAO teleconnection with reanalysis data. In the model runs some ensemble members showed strong IOD events without an ENSO event in the same year and we identified a wave train that is similar to the one of the year 2019/2020.

P19

Testing of Sentinel 5P and 3A Data for Climate Monitoring and Ocean Variability over the Indian Ocean

Abstract

The main purpose of the study is to correlate the Climate Data with Ocean Variability in the Indian Ocean from 2018 to 2021. For this purpose Sentinel 5P data is used with the 3A data. Sentinel-5P mission perform Climate Monitoring with high spatial-temporal resolution while Sentinel-3A collect Observations like variability of Global Ocean using the technique of Altimetry. The correlation provides the more confidence and accuracy in the observational results and way forward to work in high resolution on Regional level.

P20

Benchmarking prediction skill in climate network-based ENSO prediction

Abstract Reliable El Nino Southern Oscillation (ENSO) prediction at seasonal-to-interannual lead times would be critical for different stakeholders to conduct suitable management. In recent years, new methods combining climate network analysis with ENSO prediction claim that they can predict ENSO up to 1 year in advance by over-coming the spring barrier problem (SPB), the main problem in conventional ENSO forecast limiting prediction lead time. Usually this kind of method develops an index representing the relationship between different nodes in El Nino basins or outside basins, and the index crossing a certain threshold will be regarded as the warning of an ENSO event in the next year or 18 months. How well the prediction performs should be measured in order to estimate any improvements. However, the amount of ENSO recordings in the available empirical data is limited, so that it is difficult to val-idate whether these methods are truely predictive or whether their success is merely a result of chance. We propose a benchmarking method by new surrogate data for a quantitative forecast validation for small data sets and illustrate it using a toy model. We then apply this method to a na¨ıve prediction of El Nino events based on the ONI and Nino3.4 index time series, where we build a data-based prediction scheme using the index series itself as input. In order to assess the network-based ENSO prediction method, we reproduce two different climate network-based forecasts and apply our method to compare the prediction skill of all these. Our benchmark shows that using the ENSO index itself as input to the forecast does not work for moderate lead times, while at least one of the two climate network-based methods has predictive skill well above chance at lead times of about one year.

P21

Indian Ocean Dipole and ENSO, and their teleconnection to extreme rainfall events in South America

Iacovone, M.Florencia (PhD Student. Atmospheric Science. UBA. CONICET. Argentina)
PhD Penalba, Olga C. & PhD Pántano, Vanesa C. (Directors. UBA. CONICET. Argentina)

Climate extremes have become an issue of concern in recent years, due to observed and projected changes that affect society and its economic, productive, and recreational activities. Furthermore, the sea surface temperature (SST) anomalies in the equatorial Pacific and the Indian Oceans can have substantial remote effects on climate in South America (SA).

In view of the relative predictability of El Niño-Southern Oscillation (ENSO) and Indian Ocean Dipole (IOD) episodes, the aim of this research is to understand the IOD two-ways interactions with ENSO, and the spatial relationship between IOD and two indices derived from daily rainfall: maximum number of consecutive dry days (CDD) and wet days (CWD). This work is carried out in the trimester October–December, for the period 1979–2005, in SA.

The following databases were used in this research: a) Daily gridded rainfall derived from meteorological observations worldwide from the Climate Prediction Center (CPC) Gauge-Based Analysis of Global, from the National Center for Environmental Prediction (NCEP); b) time series of the IOD index was obtained from https://psl.noaa.gov/gcos_wgsp/Timeseries/DMI/ ; c) monthly NOAA Extended Reconstructed SST (ERSST), version 5, from the National Center for Atmospheric Research (NCAR). This database was used to calculate the Oceanic Niño Index (ONI) which is the standard index that the National Oceanic and Atmospheric Administration (NOAA) uses to characterize warm (El Niño) and cold (La Niña) SST anomalies in El Niño 3.4 region (5° N–5° S, 120°–170° W).

This research studies the relationship between ENSO- CDD and ENSO-CWD, and between IOD in september (IOD_{sep}), october (IOD_{oct}) and november(IOD_{nov}) with CDD and CWD in the trimester October–December. For example, Figure 1 shows the correlation coefficient patterns between IOD_{oct}-CDD indices (left) and IOD_{oct}- CWD (right). A significant negative correlation of IOD_{oct}- CDD is apparent over the Buenos Aires and Mesopotamia of Argentina, north of Uruguay and south of Brazil; suggesting that negative (positive) IOD index are associated with longer (shorter) consecutive dry days. On the other hand, the east coast of Brazil shows significant positive correlation. An opposite signal is observed in IOD_{oct} - CWD correlation; this suggests that positive (negative) IOD index is associated with longer (shorter) consecutive wet days.

These results indicate a potentially strong relationship between IOD and South American extreme rainfall, which will contribute to improve the predictability of extreme indices in the study region.

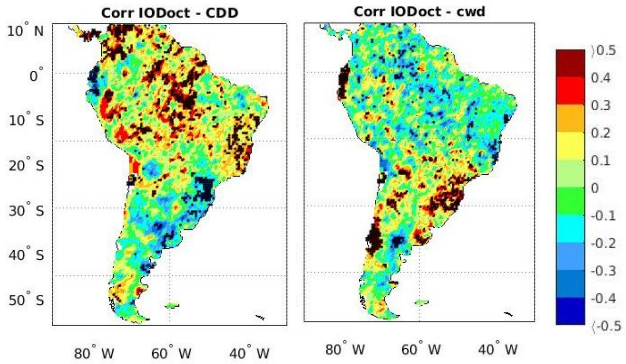

Figure 1: Correlation fields between CDD (CWD) and IOD_{oct} indices in the left (right) panel, over South America. The black dots indicate regions where the correlation is significant at 95% confidence level ($|r| \geq 0.38$).

P22

Using part of the abstract of a recently submitted work with Professor Annalisa Bracco

Information entropy and climate predictability in the Indo-Pacific basin

Olawale J. Ikuyajolu[1,2], Fabrizio Falasca[1], Annalisa Bracco*[1,2]

[1]School of Earth and Atmospheric Sciences, Georgia Institute of Technology, Atlanta, GA, USA
[2]Program in Ocean Sciences and Engineering, Georgia Institute of Technology, Atlanta, GA, USA

In this work, we build upon recent advances in nonlinear dynamical systems theory and introduce the climate community to an information entropy quantifier based on recurrence. The entropy, or complexity, and therefore potential predictability, of a system is associated with microstates that recur over time in the time-series that define the system.
A computationally fast method to evaluate the entropy of multi-dimensional fields is applied to the investigation of the predictability potential of sea surface temperature in the tropical Pacific and Indian Oceans, focusing in boreal fall. In this season the predictability of the basins is linked to two regularly varying nonlinear oscillations, the El Niño-Southern Oscillation and the Indian Ocean Dipole. We compute and compare the entropy in simulations from the CMIP5 catalog from the historical period and RCP8.5 scenario, and in reanalysis datasets. Discrepancies are found between the models and the reanalysis, and no robust changes in predictability can be identified in future projections. The Indian Ocean and the equatorial Pacific emerge as areas where the modeled entropy differs the most from that of the reanalysis in many models. A brief investigation of the bias origin points to a poor representation of the ocean mean state and, for some of the models, of the basins' connectivity at the Indonesian Throughflow among the causes.

P23

The decadal sea level variability observed in the Indian Ocean and its association with global climate modes

J.S. Deepa[1] and C. Gnanaseelan[1,*]

[1]Indian Institute of Tropical Meteorology, Pune-411008, Ministry of Earth Sciences, India.

Abstract

Decadal sea level variability of the Indian Ocean is studied using long-term tide gauge observations. Analysis revealed the existence of close association between Indian Ocean sea level and the global decadal climate modes, such as Pacific Decadal Oscillation (PDO) and/or Atlantic Multidecadal Oscillation (AMO). An anti-phase sea level evolution with PDO index is identified in the regions such as west coast of India, east coast of India and the western coast of Australia. Moreover, the PDO related sea level variability is found to be stronger at the tide gauge stations along the west coast of India compared to that along the east coast of India. On the other hand, the tide gauge station at Mumbai with more than 100 years of data shows an in-phase relationship with AMO index on the decadal timescales. The analysis of sea level pressure (SLP), rainfall and winds over the tropical Indian Ocean indicates existence of strong relationship with AMO especially over the Arabian Sea region, strongly suggesting that the variability observed at the tide gauge station Mumbai may have larger spatial signatures. During the positive phase of AMO, the Arabian Sea region is characterized by large fall in SLP and a strong cross equatorial flow towards the Indian land mass, which are primarily responsible for the positive sea level anomalies (SLAs) at the Mumbai tide gauge station and the adjacent regions.

P24

Global climate indices' teleconnection with monsoons of Tamil Nadu

Abstract

The present study makes an attempt to find the long term rainfall trends of Tamil Nadu and influences of global climate indices on it. Nearly 143 years' data (1871-2013) are taken for climatological analysis. The results show increasing trends in annual and post- monsoon rainfall. A post - monsoon season which brings an average of 49.1% of the total rainfall increases its contribution to 54.6% during 1991-2013. While, southwest monsoon contributes 33.1% of total annual rainfall shows slight decreases during 1991-2013. The teleconnection of both monsoon rainfalls with global climate indices are studied. Post monsoon rainfall shows significant high correlation with Multivariate ENSO Index and Nina 3.4 and insignificant, weak positive correlation with other climate indices. The south west monsoon shows negative correlation with almost all indices and the negative correlation is significant with Nina 3.4 and Multivariate ENSO Index. Then, excess and deficient monsoon years are calculated as per IMD criteria and influences of Nina effect on excess/deficient monsoons are also calculated. During the entire study period, 59 excess and 66 deficient post monsoon seasons are identified, while 50 excess and 61 deficient south west monsoon years are recognized. Interestingly, 72% of the El Nino years had excess rainfall in the post monsoon season, 69% El Nino years had deficit rainfall during southwest monsoon. On the other hand, 61% of the La Nina years had deficit in rainfall during the post monsoon season and 57% La Nina years experienced excess rainfall in southwest monsoon season.

P25

Title: The Climatology and Interannual Variability of Greater Horn of Africa Seasonal Rainfall in CMIP6 Historical and Future Simulations.

The Short Description of my Dissertation:

Understanding fundamental processes of regional climate change and variation are incomplete and need to be improved to support climate projection effort to solidify the practical framework for extended-range forecasting capability. Atmospheric circulation, Sea surface temperature (SST) variability, and ocean-atmosphere coupling of a surrounding ocean of Greater Horn of Africa (GHA) derive the variability of seasonal rainfall at various time scale over the region. Biases within CMIP models, such as CMIP5, are well known and regularly documented in the region. However, the origin of errors and their effects on the models' ability to reproduce climatology and interannual variability are rarely considered. A recent study demonstrated that biases in the CMIP5 models' mean states can drastically influence their ability to correctly represent the atmospheric response to anomalies from the mean state.

Given considerable errors in coupled climate models' skill to simulate the current climate, it remains an open question as to whether or not the future climate in GHA will become wetter as a result of anthropogenic forcing. It is, therefore, necessary to improve these validation products by evaluating them against available field and satellite observations. There is also no clear consensus regarding climate change's far-reaching impact on the mean precipitation and interannual variability and how these will be driven by potential changes in El Niño-Southern Oscillation (ENSO) and Indian Ocean Dipole (IOD).

The overall objective of this PhD project is to analyze climatology, interannual variability, atmospheric dynamics, and a variety of large-scale influences on seasonal rainfall over GHA. The observation and reanalyses dataset will be used to evaluate the performance of coupled models from the World Climate Research Programme (WCRP) Coupled Model Intercomparison Project Phase 6 (CMIP6). The results that would be generated from this study could, therefore, contribute to the planning and management strategies of all rainfall dependent activities/sectors in the GHA. Besides, it could be used to advise which CMIP6 coupled models needs to be used, which policy development needs to account for errors in coupled climate models, while the best numerical modeling results to be transferred to adaptation/mitigation strategies and to support policy for climate compatible development strategies for countries in GHA.

P26

Using convergent cross mapping method and fuzzy analytic hierarchy process to explore causes of streamflow alteration: A case study of Isser catchment, Algeria

Authors and affiliations:

Mokrane Kadir[1]

University of Science and Technology of Houari Boumediene (USTHB)

Abstract:

The water resources of Mediterranean countries are strongly affected by climate change and anthropogenic activities, which exerts a considerable pressure on the overall water security. Understanding the relative contributions of each of the possible causal factors to the hydrological alteration is pivotal to design sustainable water resources management strategies. In this study, the hydrological alteration of the Isser catchment in Algeria is assessed and explained in terms of possible explanatory factors. A long-term hydrometeorological dataset was reconstructed and the nonparametric Mann-Kendall test was used to detect the alteration of streamflow and the possible causal factors. To identify the role of causal factors in the hydrologic alterations, two techniques were used. First, Convergent Cross Mapping (CCM), which is an advanced data based nonlinear time-series analysis tool, was used to identify causality in time-series. Second, a Fuzzy Analytical Hierarchical Process (FAHP) expert based model was applied to assess the possible underlying causes for hydrologic alterations and to quantify the potential influences of human activities and climate change. The results of the trend analysis show a significant downward trend for streamflow ($p_{value} < 0.05$) for the period 1971-2010. The CCM method shows that the streamflow alteration is unidirectionally caused by changes in precipitation, temperature, irrigation, evapotranspiration, and NDVI patterns and that there is little feedback from streamflow alteration to these causing factors. The FAHP suggests that climate change is dominating the decreasing trend in streamflow, being responsible for 60 % of the alterations as compared to 40 % of the alterations caused by changes in the land use patterns and intensive water extraction.

Keywords: hydrological alteration, climate change, FAHP, Mediterranean, causality.

P27

The subsurface temperature variability in the Tropical Indian Ocean

Rashmi Kakatkar, C. Gnanaseelan and J. S. Chowdary

Indian Institute of Tropical Meteorology, Pune-411008

The empirical orthogonal function (EOF) analysis of subsurface temperature shows a dominant north-south mode of interannual variability in the Tropical Indian Ocean (TIO) at around 100 m depth (at around thermocline depth). This subsurface mode (SSM) of variability evolves in September-November (SON) as a response to Indian Ocean Dipole (IOD) and intensifies during December-February (DJF). The evolution of the SSM and its association with the anomalous sea surface temperature and surface wind patterns is analysed in detail using reanalysis/observation products as well as using coupled models. The asymmetry in the evolution of positive and negative phases of SSM and its impacts on the modulation of surface features is studied using reanalysis data. The possible mechanisms behind this asymmetry are examined. During the positive phase of SSM, downwelling Rossby waves generated by anticyclonic wind stress curl propagate towards the southwestern TIO, the thermocline ridge region of mean upwelling. The warmer subsurface water associated with the downwelling Rossby waves upwells in the region of mean upwelling and warms the surface resulting in strong subsurface-surface coupling. Such interaction processes are however weak during the negative phase of SSM. The asymmetry in the subsurface-surface interaction during the two phases of SSM and its impact on the modulation of surface features of TIO are also reported. In addition to the ENSO forcing, self-maintenance of SSM during DJF season is evident in the positive SSM years.

P28

Multi-decadal modulations of the Indian Ocean-ENSO-Atlantic relationship: Implication to Arabian Climate

In-Sik Kang[1], Fred Kucharski[2]

[1]*Indian Ocean Center, Second Institute of Oceanography, Hangzhou, China,*

[2] *International Centre for Theoretical Physics, Trieste, Italy*

Abstract

Multi-decadal changes of the relationship between the Indian Ocean SST and ENSO are investigated using the observed data for the 60 years of 1950-2010 and various AGCM experiments. For the early 30 year period of 1950-1979, the ENSO accompanied relatively strong SST anomalies all over the tropical Oceans and thus relatively large SST anomalies in the Indian Ocean. On the other hand, for the recent 30 years of 1980-2010, the strong ENSO SST anomalies were more-or-less confined in the Pacific and relatively small SST anomalies in the Indian Ocean. Associated with the changes of Indian Ocean SST anomalies during ENSO, the relationship between the Arabian rainfall and the ENSO has been changed for the two periods; The Arabian rainfall was negative correlated to the ENSO for the early 30 year period and positively correlated to the ENSO for the recent period. It is found that the atmospheric anomalies in the Arabian region during the ENSO are the combined responses to the Pacific and Indian Ocean SST anomalies, which offset each other during the ENSO. These observed findings are confirmed by various AGCM experiments. Also shown is the multi-decadal changes of the relationship between the Arabian rainfall and the North Atlantic Oscillation (NAO), which could be a result of the ENSO amplitude changes associated with the Atlantic Multi-decadal Oscillation (AMO).

P29

Flavors of El Nino and associated genesis with special emphasis to 2006-07

Abstract:

The temporal and spatial evolution of westerly wind events (WWE) and El Niño evolution in last century are explored using observations and reanalysis data in this study. The formation of El Niño is mostly associated with the WWE in the equatorial Pacific and changes in the Warm water volume. To identify WWE, European Reanalysis 20 Century (ERA-20C) daily zonal wind data for the period 1900-2010 is used. In addition, Extended Reconstructed Sea Surface Temperature (ERSSTv5) data set is used to estimate Niño indices as well as to understand the eastern and central Pacific SST anomaly evolution associated with El Niño. The study period is divided into four epochs, with a 30 year period, namely, 1895-1924, 1925-1954, 1955-1984, and 1985-2014. The spatial patterns of SST variability displayed strong modulations in the central Pacific along with eastern Pacific in recent era than earlier, when a higher magnitude of SST variability was confined to eastern Pacific. This spatial pattern of SST variability in the central Pacific is consistent with occurrence of more El Niño Modoki events than earlier in recent period. Analysis also suggests that the regional and temporal features of WWE varies, hence they are classified in western Pacific, central Pacific and eastern Pacific WWE. It is noted that the central and eastern Pacific WWE contributes noticeably to the formation of the canonical or modoki El Niño. The frequency of these events is found to be high during the recent period of 1956-2010 as compared to 1900-1955, mostly during the fall and winter season. Our results suggest that five El Niño events are formed without the WWE during the study period, out of which three events are El Niño Modoki, one canonical El Niño and the other one is 2006-07, its spatial pattern is unlike canonical and El Niño Modoki. Further, to understand the role of oceanic adjustments during 2006-07, a detailed analysis of terms involved in temperature tendency (averaged at upper 50m) was carried out.

The zonal advection, that is mean temperature zonal gradient multiply by anomalous currents ($u'\partial T/\partial x$), for Nino1+2 and Nino 3.4 is seen to contribute positively during transition to peak phase of 2006-07. Two Ocean General Circulation Model experiments are carried out by interchanging the momentum flux forcing, in first experiment momentum forcing of 1997-98 is used for the 2006-07 ocean features and in second experiment 2006-07 momentum forcing is used for 1997-98. These two experiments using Modular Ocean Model version 5 (MOM5) conclude that the temporal and spatial evolution of eastern and central Pacific temperature anomaly associated with El Niño is dependent on the WWE strength, pattern and frequency.

P30

Intercomparison of the spatiotemporal precipitation patterns in CORDEX-Africa, CMIP5, CMIP6, gauge-based and satellite products over southern Africa

Maria Chara Karypidou[1], Eleni Katragkou[1] and Stefan Pieter Sobolowski[2]

[1] Department of Meteorology and Climatology, School of Geology, Faculty of Sciences, Aristotle University of Thessaloniki, Thessaloniki, Greece
[2] NORCE Norwegian Research Centre, Bjerknes Centre for Climate Research,
Bergen, Norway

Abstract

The region of southern Africa is identified as a highly vulnerable region to the impacts of climate change and is expected to experience severe drought events and precipitation shortages in the coming decades. In the current work, a set of satellite precipitation products along with gauge-based datasets are analysed. In addition, regional climate simulations performed in the context of the Coordinated Regional Climate Downscaling Experiment over Africa (CORDEX-Africa), along with global circulation models performed in the context of the Coupled Model Intercomparison Project Phase 5 (CMIP5) and Phase 6 (CMIP6) are investigated with regards to precipitation, over southern Africa. The analyzed period is 1986-2005. The standard deviation (SD) of precipitation during the rainy season (October - March) for satellite and gauge-based products displayed a significant disagreement between satellite products that merge with rain gauges and satellite products that do not. In addition, the CORDEX-Africa ensemble displayed lower SD values and thus, higher within-ensemble agreement, than the CMIP5 ensemble. The behavior of CMIP6 was similar to CMIP5, however CMIP6 displayed smaller SD values. When the annual cycle was examined, the CORDEX-Africa displayed a substantial improvement for monthly precipitation relative to the CMIP5 and CMIP6 ensembles. This observation is also valid for indices characterizing the interannual variability of precipitation amount and severity for all datasets. With regards to observed precipitation trends during 1986-2005, there was a substantial agreement between satellite and gauge-based products concerning the spatial pattern of signal and strength for each month. Nevertheless, both the CORDEX-Africa and the CMIP5 ensembles failed to reproduce monthly precipitation trends as displayed in satellite and gauge-based products. CMIP6 displayed drying trends throughout the whole rainy season.

P31

Simulations and Projections of Monsoon studies in coupled climate models (CMIP): A Review

Influence of South west Monsoon rainfall on economy and society is far beyond the expectations and its impact on agricultural and public as well as private sectors account more than two-third of populations around the world. In the global warming context, mean monsoonal rainfall exhibited significant changes in spatial patterns and epochal variations accompanied by significant increase in extreme rainfall events in terms of its intensity and frequency over the regions. In this paper we provide a glimpse of literature review of coupled climate model (CMIP) simulations for the past changes and forecasts. Physical and dynamical processes associated with the monsoon and key outcomes from the literature review along with the challenges in prediction in climate models are discussed in this paper. Monsoon rainfall activities showed the epochal variability over the northern part of global land points however quantification and effect of natural and anthropogenic forcing in modulating the monsoon rainfall is still challenge to scientific community. CMIP has made an approach to simulate past and future atmosphere of earth systems which evolved and improved with enhancing the performance over time. In terms of monsoon frequency and its intensity, presently models participating in CMIP6 (most recent Phase of coupled model intercomparison project) simulating well on the other hand persistence of intermodal variability and spatial distribution of rainfall bias is noted. Spatially varying climate patterns over time period determines the significant increase in intensity and frequency of extreme monsoon rainfalls, besides increase in drought like situations as well over certain regions.

With consideration of interannual variability of Indian summer monsoon rainfall (ISMR) in recent two epochs, significant amplification of intensity and frequency of extreme rainfall events over the central India noted in observed trends which need to be investigated to mitigate hazards associated with it in upcoming decades. [1]

1. Goswami, B. N., Venugopal, V., Sangupta, D., Madhusoodanan, M. S. & Xavier, P. K. Increasing trend of extreme rain events over India in a warming environment. *Science (80-.).* **314**, (2006).

P32

Tropical Indian Ocean and ENSO relationships in a changed climate

Marathe Shamal[1,*], Pascal Terray[2], Karumuri Ashok[3]

[1]Centre for Climate Change Research, Indian Institute of Tropical Meteorology, Pune, India.

[2]CNRS-IRD-MNHN, LOCEAN Laboratory, Sorbonne Universités (UPMC, Univ Paris 06), 4 Place Jussieu,75005 Paris, France.

[3]Centre for Earth, Ocean and Atmospheric Sciences, University of Hyderabad, Hyderabad, India.

*Corresponding Author's address:

Dr. Shamal Marathe

Centre for Climate Change Research,

Indian Institute of Tropical Meteorology, Pune-411008.
Phone: 91-90-1167-8048

e-mail: shamal.marathe@tropmet.res.in, 27shamal.m@gmail.com

Abstract

We explore the current (1958-2005 period) and near future (2006-2050 period) teleconnections between El Niño Southern Oscillation (ENSO), Indian Ocean Basin Mode (IOBM), and Indian Ocean Dipole (IOD) as simulated in historical and Representative Concentration Pathway (RCP8.5) simulations of 32 coupled models that participated in the phase five of Coupled Model Intercomparison Project (CMIP5). A set of 16 CMIP5 models out of 32 models, which perform best to simulate tropical climate variability in recent decades, is first selected using a robust method based on the Empirical Orthogonal Function analysis for detailed analysis.

Most of these models show modest capability in reproducing the seasonal cycle of ENSO types in the current period. Further, amplitude of Indian Ocean (IO) modes is overestimated by the 16 models along with large inter-model spread. Based on these results, a subset of 9 models is formed, which simulate a realistic seasonal phase-locking of ENSO for a robust assessment of future teleconnections.

No significant change in El Niño amplitude is detected in near future. However, the IOBM is projected to be weaker during late spring and early summer. The IOD is projected to be stronger during boreal summer in the future relative to the current period. We also investigate if there are any changes from historical to RCP 8.5 simulations in the strength of the IO negative feedback on ENSO with a multiple linear regression approach. The IO negative feedback strengthens significantly in the RCP8.5 scenario due to the increasing role of IOBM in speeding the transition from El Niño to La Niña, despite its reduction of amplitude, In contrast, IOD loses its predictive value in the future projections.

P33

A case study of Extremely Severe Cyclonic Storm Fani (2019) from the prediction view of land-ocean-atmosphere coupled model

Shyama Mohanty[1], and UC Mohanty[1]

Abstract

Tropical cyclone (TC) Fani (April-May 2019) over the Bay of Bengal was the first TC to strike Odisha coast as an extremely severe cyclonic storm (ESCS) with 185 kmph wind speed in last 130 years. It could sustain for around 24 hours with intensity of cyclonic storm or more after landfall thus classifying it as a unique case of land interaction. Therefore, an attempt is made to predict the cyclone with available best state-of-the-model Weather Research Forecast (WRF) modeling system and understand physical processes using land surface inputs from United States Geological Survey (USGS) land data. The high resolution model with the ability of vortex following telescoping nested domains could produce the track and intensity forecast of the cyclone with reasonably good accuracy with India Meteorological Department (IMD) best track and intensity estimations. The model performance in predicting landfall time, position and intensity was remarkable. The positional and temporal error estimations were 9 km and 0 hour respectively. Effort has been made to understand the land condition. Greater insight to the convection pattern that influence the evolution and sustenance of the storm intensity in terms of latent flux, sensible heat, mass flux and other diagnostic parameters is attempted.

Key words: Fani, Tropical cyclones, intensity

P34

Indian Ocean Dipole and rainfall variability over Central Africa

The Indian Ocean (IO) has been identified as the main source of ocean moisture for Central African rainfall. It is well known that the Indian Ocean Dipole (IOD) affects the atmospheric circulation over the IO. At the state of the art, the IOD constitutes an important driver of global climate variability due to the impact it has on the climate of neighbouring regions as well as on remote areas at the IO.
This study examined the possible influence of IOD on rainfall in Central Africa (CA) from September to December of the period 1980-2016. The results show that CA rainfall exhibits an opposite pattern between positive IOD (pIOD) and negative IOD (nIOD) events. Indeed, both observational and reanalysis data reveal that pIOD events are associated with above-normal rainfall while nIOD events result in a rainfall deficit over CA. However, some regions present opposite responses to those corresponding to the phase of the IOD examined. The analysis of the composites of rainfall anomalies shows an asymmetry in the magnitude of the anomalies of the two phases of the IOD, with stronger pIOD events anomalies compared to those of nIOD events.

To further quantify the statistical relationship between IOD and rainfall in Central Africa, we performed the regression of CA rainfall onto Dipole Mode Index (DMI). This shows that rainfall intensity increases with the strength of the DMI, although some regions show the opposite pattern. Given that most of the years used in this study as IOD events coincided with ENSO events, we regressed CA rainfall onto DMIs in which the linear relationship with the Niño-3.4 index was removed, to find out how the relationship between CA rainfall and pure IOD DMIs behaves. The resulting findings show stronger regressions than those carried out with DMIs including the ENSO signal. Although the discrepancy between the magnitudes of these regressions is not significant, regressions of CA rainfall on DMIs with ENSO removed indicate that phases of similar nature (warm or cold) of IOD and ENSO are associated with opposite impacts on rainfall in Central Africa from September to December, with above (below) mean rainfall during pIOD (El Niño) events.

Transport of the moisture flow presented a strengthening (weakening) of the moisture flux convergence over the entire troposphere. Rainfall variability during both phases appears to be influenced by changes in circulation, with moisture flux from the equatorial and eastern Indian Ocean above (below) normal during pIOD (nIOD) events. Moisture advection from the Southern Indian Ocean, on the other hand, is weakened (strengthened) during pIOD (nIOD). During nIOD events, this circulation is characterised by a strengthening of the westerly flow leading to further advection of moisture away from CA. On the other hand, during pIOD events, the westerly flow present over the central equatorial Indian Ocean is weakened from September and then reversed into an easterly flow in October to December with stronger flow recorded in November which contributes to more inflow from the central equatorial Indian Ocean and consequently more rainfall in CA. Inflow is strongest in the lower troposphere (1000-850 hPa) over the ocean while it is strongest in the midtroposphere (700-600 hPa) over CA because much of the inflow is blocked by the topography associated with the Great Rift Valley.

P35

LEVEL: Project report submitted in partial fulfilment of the requirements for the degree of Bachelor of Science in Physics with Meteorology.

TITLE: Possible impacts of extreme events on seasonal weather changes in southern Africa: Case study of cyclone Elita.

INSTITUTION: University of Botswana

ABSTRACT

Southern Africa has experienced changes in seasonal weather patterns like changes in rainfall patterns, temperature and wind field .These changes are due to various reasons such as the El-nino Southern Oscillation, cyclones, sea surface temperatures and changes in the wind patterns. This study focused on changes in rainfall patterns in Southern Africa due to cyclone Elita, which was an usual cyclone that made landfall in Madagascar three times on January 2004.Through research from literature it was found that cyclone Elita brought heavy rainfalls to some countries of southern Africa including Madagascar ,Mozambique and Malawi. It was not certain that cyclone Elita had an impact on seasonal rainfall patterns of Botswana because there was no information from literature that linked this cyclone to any changes in the local weather in 2004.In order to check if Elita had impacted rainfall patterns in Botswana, rainfall data of the years 2001 to 2007 for four selected weather stations obtained from Botswana Meteorological Services was used to plot graphs in order to detect changes in the rainfall amounts in 2004.From the graphs it was evident that the rainfall amounts received in 2004 were higher than those of the previous years especially during the months in which Elita was expected to make an impact and this signified that possibly Elita impacted the local rainfall, but this was not conclusive.

P36 **Heat distribution in the Tropical Indian Ocean during the prolonged La-Niña events during 1958–2017**

Soumya Mukhopadhyay, C. Gnanaseelan, J.S.Chowdary, Sandeep Mohapatra

Abstract:

In the present study, heat distribution in the Tropical Indian Ocean (TIO) associated with the prolonged La-Niña events during 958–2017 is examined using reanalysis/observations. A detailed analysis revealed that in response to prolonged La-Niña forcing, prominent the east-west thermocline gradient in the equatorial Indian Ocean and the eastward extension of thermocline ridge in the southwestern TIO (TRIO) are noted. Anomalous subsurface warming, thermocline deepening, and sea-level increase are also evident in the eastern and southeastern TIO and Bay of Bengal (BoB) during the prolonged La-Niña events. Cross equatorial volume transport near the eastern boundary during the prolonged La-Niña years especially at 50m—150m depth levels indicates the pathways of Pacific water entering the north Indian Ocean (NIO), a feature that has a strong impact on the BoB dynamics and thermodynamics. Intense cooling of TRIO and the Arabian Sea and the eastward extension of TRIO are some of the characteristic features of the prolonged La-Niña years. These may have strong implications on the air-sea interaction associated with inter-annual and intra-seasonal variability over this region. Further, the subsurface heat content (50m–150m) in the eastern and southeastern TIO in general dominated by inter-annual variability, the TRIO region experienced the decadal variability. Interestingly, in recent years, the strength of decadal variability is found to be comparable with that of inter-annual variability in the TIO heat content, moreover similar variability is evident in the sea level anomaly as well. Subsurface heat content variations associated with prolonged La Niña years are discussed. This study shows that the warming and cooling events of TIO are closely tied to the internal dynamics of the IO driven remotely by the Pacific through modulation of surface winds.

Keywords: Prolonged La-Niña, North Indian Ocean; volume transport; cross equatorial flow; wind curl; Reanalysis; Decadal variability.

P37

Hydrology and its impact on crop yields using SWAT under CMIP6 climate projections

Water is an essential component in all life forms, especially in agricultural sector. Hydrological models can be efficient in assessing water resources, determining best management practices, climate and land use changes *etc*. SWAT (Soil and Water Assessment Tool) model is one such kind to understand the inflow and outflow of any water resource and further help in responding to changes that affect the resource and its quality. Pioneer works have been done in water budgeting and crop yield simulations by embedded EPIC model in the perspective of water component using this model. World Climate Research Programme (WCRP), is now in its sixth phase being named as CMIP6- Coupled Model Inter-comparison Project. CMIP6 coordinates somewhat independent model inter-comparison activities and their experiments, which have adopted a common infrastructure for collecting, organizing, and distributing output from models after performing common sets of experiments. Working for the projections of CMIP6 would be an advancement in research, especially in hydrological response arena that is gaining momentum under changing climate.

Objectives:

- Project hydrological changes in a watershed under CMIP6 future projections.
- Analyse the impact of hydrological changes on yields of major crops for the selected watershed using SWAT (Soil and Water Assessment Tool) model
- Develop efficient cropping pattern for the watershed on climate change conditions of future.

Methodology:

- A watershed will be chosen to understand the stream flow. Following this, future sensitivities on changing climate using CMIP6 projections would be simulated.
- The impact of hydrological changes in future will be studied using the simulations of SWAT model for major crops of the selected watershed.
- The model tends to incorporate climate data from selected Global Circulation Models (GCM) downscaled through a Regional Climate Model (RCM) for the selected area.
- These climate models will be chosen based on their suitability for Indian conditions to derive future responses of the watershed in climate change scenario.
- The crop yield simulations for the accounted hydrological changes encountered in watershed will be the resultant outcome.
- Further suggestion on managing the watershed can be provided using model output for sustaining yields in the watershed against changing climate.

Significance

Hydrological models have been in usage to simulate crop yield as a response to hydrology and water budget. The recent CMIP6 projections would provide a strength in understanding the hydrological changes and its impact on crop yield for aiming adaptations.

Prospects of this work for extending it as a long-term project

The proposed research work can further be extended to any watershed of concern; crop yield responses, best management options, influence of weather disturbances can be studied and recommended to the policy makers towards efficient planning and monitoring of watersheds.

P38

Relationship between the Indian Ocean and ENSO with precipitation in the Caribbean of Costa Rica, applied to the pineapple and banana crops.

Orozco-Montoya, Ricardo. A. [1], Penalba, Olga. C. [1]
[1]Department of Atmospheric and Ocean Sciences, University of Buenos Aires, Argentina.

In the framework of the doctoral research, one of the goals is to improve the knowledge of the physical mechanisms responsible for the spatio-temporal variability of the occurrence of extreme rainfall events in the Caribbean region of Costa Rica with focus in pineapple (*ananas comosus*) and banana (*musa spp,)* main crops exported in the country. Due to the relative predictability of the Indian Ocean Dipole (IOD) episodes and El Niño-Southern Oscillation (ENSO), the aim of this research is to understand the teleconnectivity of the Dipole Mode Index (DMI) and the Oceanic Niño Index (ONI) with the rainfall in December, critical month for pineapple and banana crops.

28 monthly rainfall series located in the Caribbean region of Costa Rica were analyzed in 2 periods: 1985-2009 (23 stations) and 1997-2019 (5 stations, strategically located for crop analysis). For each period, the correlation between December rainfall and the DMI for October and November, and correlation between December rainfall and ONI in ASO, SON and OND were analyzed. In some stations, as the case of Limón, it was possible to analyze both periods in order to perform if the teleconnection change in time.

The teleconnection analysis shows an inverse relationship between DMI of October and November and December rainfall. The significant signal is located in the southern of the study area and to the north close to the coast (Figure 1, left). The correlation associated with the ONI is also present in the region mainly in SON in the southern (Figure 1, right). The Limón station shows changes in the correlations between both periods, being higher for the most recent period in both indices.

These results indicate a potentially relationship between IOD and rainfall in Caribbean region of Costa Rica, which will contribute to improve its predictability in the study region.

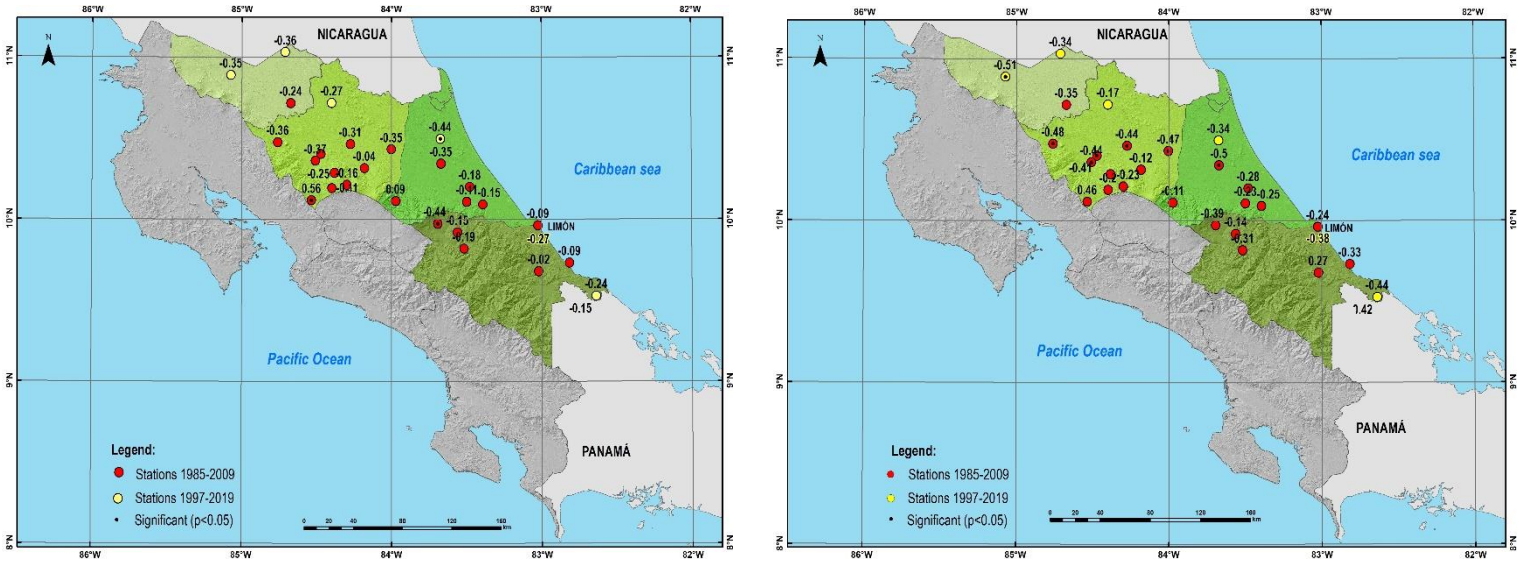

Figure 1. Correlation between December rainfall and November DMI (left); and ONI-SON (right).

Impact of Tropical South Atlantic Sea Surface Temperature on the Atmospheric Circulation Variability over the Indian Ocean

Pushpa Pandey[1*], Suneet Dwivedi[1], Fred Kucharski[2]

[1]K Banerjee Centre of Atmospheric and Ocean Studies and M N Saha Centre of Space Studies, University of Allahabad, Allahabad, UP 211002, India.

[2] The Abdus Salam International Centre for Theoretical Physics, Earth System Physics Section, Trieste, Italy.

* Corresponding Author: pandeypushpa82@gmail.com

Abstract

The variability of the atmospheric circulation over the Indian Ocean has been studied in response to the changes in the Tropical South Atlantic Sea Surface Temperature (TSASST) in a warming world. The atmospheric circulation over the Indian Ocean is represented in terms of the Webster-Yang Index (WYI). Out of a total of 32 CMIP6 models taken for the study, 21 models are found to correctly simulate the observed negative relationship between the TSASST index and WYI for the period 1955-2014. It is found that the inverse relationship between the TSASST and WYI shall weaken in the high greenhouse gas concentration future projection scenario SSP5-8.5 of CMIP6 models during the period 2015-2100. It has been further observed that the weakening of the vertical wind shear over the Arabian Sea in response to increase in TSASST leads to the intensification of tropical cyclones over the region, which shall result into the reduction of Indian summer monsoon rainfall (ISMR) during 1955-2014. It is noticed that the ISMR shall increase in a warming world of SSP5-8.5 scenario with relative strengthening of the vertical wind shear and reduced cyclonic circulation over the Arabian Sea.

P40

Decadal variability of IPOC mode and its influence on Indian summer monsoon rainfall

Year to year variability of the Indo-Western Pacific Ocean Capacitor (IPOC) mode influence on summer climate over the South Asian region has been studied. The present study examines the interdecadal modulations of interannual variability of IPOC mode and its impact on the Indian Summer Monsoon (ISM) precipitation fluctuation. The study is carried out for boreal summer season (June-July-August; JJA).

El-Niño Southern Oscillation (ENSO) amplitude and non-ENSO factors, such as Pacific Decadal Oscillation (PDO) contributes to the decadal variations of the Indo-Western Pacific climate. Thus it is very important to investigate the factors responsible for decadal variability of IPOC mode in summer and the subsequent influences on ISM.

In this study, for a long period of 129 years (1886-2014), IPOC mode is extracted by performing Singular Value Decomposition (SVD) analysis of tropical Indian ocean sea surface temperature (TIO SST) and Western North Pacific (WNP) 850 hPa relative vorticity anomalies in JJA. Variance explained by the leading SVD mode is 65.2%. Analysis suggests that the IPOC mode induces a southwest-northeast dipole pattern in the Indian subcontinent rainfall with significant positive anomalies over the southern peninsular India and negative anomalies over the eastern parts of the Indo-Gangetic plains during the positive phase of IPOC. Depending upon the 21-year sliding correlation coefficients between ISM rainfall anomalies and leading principal component of SVD analysis (SVD-PC1), it is analysed that IPOC mode and ISM rainfall relationship exhibits significant interdecadal variability.

Good relationship of IPOC mode with rainfall anomaly in Epoch-1 (1895-1926) and Epoch-3 (1976-2007) is weaker in Epoch-2 (1932-1972). For each epoch, IPOC mode impact on Indo-Western Pacific climate is separately studied. In epoch-1 and epoch-3, anomalous TIO SST and the Pacific–Japan (PJ) pattern/WNP circulation both are well organized as part of the IPOC mode. However, in epoch-2 vigorous warm SSTs over the equatorial central Pacific and cyclonic circulation over the north Pacific accompanied by SST cooling around 40°N are noticed. Positive SST anomalies and associated low-level convergence in central equatorial Pacific limit the extension of northeasterlies from the southern edge of WNP anticyclone to TIO. As a result, WNP anticyclone is squeezed/twisted between them, thereby weakening and shifting it northeastward. This in turn weakens the PJ mode and the inter-basin interaction of WNP circulation and TIO SSTs, causing disorganized IPOC pattern in epoch-2. This work enables us to understand the decadal modulation of interannual variability of IPOC mode in epoch-2.

P41

The effect of Indian and Pacific Ocean SSTs on decadal variability of the East Asian summer jet

Indian and Pacific Ocean variability is known to have a considerable influence on summer East Asian climate on an inter-annual timescale, particularly through modulation of the East Asian Summer monsoon and upper level jet stream. However, it is not yet clear the extent to which this variability has an effect on longer timescales, particularly given the relatively short period of available observations and the complications of aerosol and greenhouse gas forcing.

In this study we have examined the long pre-industrial control runs in CMIP6 models to try to understand the extent to which Indian and Pacific Ocean SSTs modulate decadal variability of the East Asian summer jet. We show that in the models, unlike on inter-annual timescales, the Indian Ocean tends to have only a weak influence on the decadal variability, though the Pacific plays a larger role.

P42

An interactive online tool for monitoring the influence of teleconnection patterns over South America

Michelle Simões Reboita and Christie Andre de Souza
Centro de Estudo e Previsão do Tempo e do Clima de Minas Gerais - CEPreMG
Universidade Federal de Itajubá - UNIFEI - Itajubá - Minas Gerais - Brasil

Until nowadays a great challenge in meteorology is to provide a good seasonal climate forecast. This kind of forecast involves both numerical modeling and knowledge of the teleconnection patterns that affect a region. In order to help the seasonal climate forecasters in South America, we developed a website, called *online tool for teleconnection patterns*, that put together 24 climate indices. Some of these indices are classical in the literature such as Oceanic Niño Index (ONI), Pacific Decadal Oscillation (PDO), Madden-Julian Oscillation (MJO) and Indian Ocean Dipole (IOD). Others, such as the South Atlantic Subtropical Anticyclone Index (IASAS) and Sea Surface Temperature Index (ITSMRG2), were created by us. The indices that are available in the meteorological centers, such as the National Oceanic and Atmospheric Administration (NOAA), are automatically obtained while others are calculated by the online tool. The website has an interface that allows the users to visualize the current value of the indices and their time series, maps of different atmospheric variables and their anomalies, statistics, as well as other products. The online tool for teleconnection patterns is available at meteorologia.unifei.edu.br/teleconexoes.

Keywords: teleconnection indices, South America, online tool

P43

The cyclone Chapala was one of the strongest (the second) tropical cyclones formed over the Arabian Sea. On 28 October 2015, the cyclone Chapala developed over the western India from the monsoon trough. After peak intensity (on 30 October, 2015) it started to move toward the Yemeni island of Socotra and then on 2 November 2015, it entered the Gulf of Aden and it became the strongest cyclone developed in that water area. Finally, on 4 November 2015 the cyclone Chapala dissipated.

In the present work the extra tropical transient effect of cyclone Chapala on development of mid-latitude jet stream over western part of Iran is studied. In fact, the main objective of this work is to find out whether there is an indirect relation between the heavy rainfall over western Iran and the cyclone Chapala via the extra tropical transient effect of cyclone on development of mid-latitude jet stream.

In this work, the Weather Research and Forecasting (WRF) model is used to simulate the cyclone Chapala during its development and dissipation. The advanced research WRF model is a fully compressible, Euler non-hydrostatic mesoscale numerical weather prediction model. This model has been developed at National Center for Atmospheric Research (NCAR). For the ARW dynamical core an Arakawa-C horizontal grid is used and for temporal integration of governing equations, a Runge-Kutta scheme is used in which uses a smaller time step for fast waves (such as sound waves).

WRF model simulations are performed for period 1 to 11 of November 2015. To perform the WRF model simulations, the NCEP FNL (Final) Operational Global Analysis data which are available operationally every six hours are used to prepare the initial and lateral boundary conditions. In this study, the ARW dynamical core of the WRF model is used. The WRF model is configured with one nest with 45000 m horizontal grid resolutions in a Lambert projection. The computational domain of the WRF model covers Iran, the Persian Gulf, the Oman Sea and the Arabian Sea.In addition, the physical parametrizations used are as follows. The WSM3 scheme for the microphysics, the RRTM scheme for the longwave radiation, the Dudhia scheme for the shortwave radiation, the MM5 method for the surface layer, the Noah method for the land surface, the YSU scheme for the planetary boundary layer and the Kain-Fritsch scheme is used for the parametrization of the convection.

In addition, to simulate the air parcel trajectories the Hybrid Single Particle Lagrangian Integrated Trajectory Model (HYSPLIT) is used. The HYSPLIT model can be used for numerical simulation of air parcel trajectories, as well as complex transport, dispersion, chemical transformation, and deposition simulations. Here, HYSPLIT is coupled with the WRF model to forward and backward simulation of air parcel trajectories over Iran during the period of cyclone Chapala.

Computation of some diagnostics such as potential vorticity form the numerical results of the WRF model and air parcel trajectory simulations by HYSPLIT model show that there is a transfer of mass and energy form the lower troposphere over tropical region to the upper troposphere in mid latitude region during the course of development of dissipation of cyclone Chapala.

P44

CLIMATE CHANGE IMPACTS ON FLOODING IN URBAN RIVER BASIN

Climate related extreme events are increasing all over the world. Climate change will disproportionately affect urban cities mostly located in climate-sensitive areas such as floodplains and coastal zones. Chennai, fourth-most populous metropolitan area in India, is witnessing increase in extreme rainfall events resulting in severe flooding. Recent heavy rainfall during November December 2015 resulted dreadful flooding throughout the city. This triggered the need for flood risk assessment to cope with changing climate in order to increase urban resilience. The Chennai Basin comprises of the four Rivers namely: Araniar, Kosasthalaiyar, Coovum, and Adyar River, besides a number of major and minor drains through Buckingham Canal into Sea via Ennore Creek and Kovalam Creek. The terrain of Chennai basin is flat and hence it leads to flooding during every monsoon rain. Hence, flood risk assessment and mitigation strategies are inevitable for Chennai basin to increase its resilience. In this study, we analysed the impacts of projected climate change on flooding in Chennai basin. Global Climate Models of RCP 4.5 were selected to develop future climate change projections. A Hydrological model (HEC-HMS) was used to estimate the basin runoff. The two-dimensional (2D) hydraulic model is an important tool in understanding the flood events. Due to the continuous representation of the terrain, two-dimensional models were able to characterize the lateral interaction of flow between the main channel and the floodplain. HEC-RAS 2D model was used for this study. It is one of the powerful and widely used hydraulic models. A high resolution terrain model was created using HEC-RAS Mapper. Upstream and downstream boundary conditions were provided. Additional details like Lateral structures, Bridges and Reservoirs were incorporated into the model. The inundation extend and inundation depth over the basin were calculated using HEC-RAS. ArcGIS software was employed for the creation of flood inundation maps. The flood vulnerability maps were prepared for different return periods under present and future climate scenarios. This study has identified the high flood risk zones in terms of climate change scenario and also suitable adaptation measures were suggested.

P45

Variability of Indian Summer Monsoon in CMIP3 and CMIP5 models

P. Parth Sarthi,
Department of Environmental Science,
School of Earth, Biological and Environmental Science
Central University of South Bihar (CUSB)
Gaya- Panchanpur Road, Gaya, Bihar, India
Email: ppsarthi@cub.ac.in,
Alternate Email: drpps@hotmail.com

The Indian SummerMonsoon (ISM) spans four months starting from June and ending in September and produced wide spread rainfall over Indian continents mainly due to land–sea heating contrast between Indian Ocean and large Asian land mass. ISM is controlled by semi-permanent features such as heat low over northwest sector of India, cross-equatorial flow and the low level westerly jet over the Arabian Sea at 850 hPa, the tropical easterly jet over the Indian Ocean at 200 hPa, Mascarene High, and anti-cyclone over the Tibet. Any fluctuation in Indian Summer Monsoon Rainfall (ISMR) during ISM on intra seasonal to inter annual is manifestation of change in wind circulation and temperature distribution. Therefore, in order to understand the change in magnitude and pattern of ISMR under warmer climate, it is necessary to qualitatively and quantitatively assess the change in associated monsoon wind circulation and temperature distribution. The current study examines the changes in magnitude and spatial distribution of ISMR and associated change in wind circulation under forced emission scenarios in selected models of CMIP3 and CMIP5. It is found that under A2, B1 and A1B emission scenarios of CMIP3, future projected change in spatial distribution of ISMR shows deficit and excess of over the lower part of western and eastern coast of India in simulation of HadGEM1, ECHAM5, and MIROC (Hires) model which seems to be manifestation of anomalous anticyclonic flow at 850 hPa in Arabian Sea and anomalous westerly flow at 200 hPa. In CMIP5, the better performed models, for the period of 1961-2005, are used for analyzing the ISMR during 2006-2050 under RCPs 4.5 and 8.5. ISMR may be excess and deficit rainfall over monsoon regions of NWI, NEI, WCI, CNI and PI at 99% & 95% confidence levels. Future projected change of JJASwind shows anticyclonic circulation over Arabian Sea at 850 hPa and cyclonic circulation around 40° N,70°E-90°E at 200 hPa which may be a possible cause of changes in JJAS rainfall over Indian regions.

P46

Epochal changes in the teleconnections between subtropical and tropical Indian Ocean

Sebastian Anila and C. Gnanaseelan

Indian Institute of Tropical Meteorology, Ministry of Earth Sciences, Pune

The second Empirical Orthogonal Function (EOF) mode of sea surface temperature (SST) variability over the subtropical Indian Ocean displays a southwest-northeast structure and is called Subtropical Indian Ocean Dipole (SIOD). During its positive phase, a positive SST anomaly over the south-western box and a negative SST anomaly over the north-eastern box of the subtropical Indian Ocean. The second EOF mode of SST variability over the whole Indian Ocean resembles this dipole structure over the subtropical Indian Ocean region but does not show the Indian Ocean Dipole (IOD) structure over the tropical Indian Ocean. In this study, the relation between tropical and subtropical Indian Ocean and its epochal nature have been investigated. The correlation analysis reveals that the SIOD is positively linked with the following tropical IOD, whereas negatively correlated with the preceding tropical IOD. The SIOD and tropical IOD display seesaw pattern of co-variability. These relationships strengthened after the climate regime shift of 1976/77. The SIOD shows a similar relationship with the subsurface dipole mode (SDM) over the tropical Indian Ocean, which is a north-south dipole mode of thermocline depth variability over the tropical Indian Ocean. Strengthening of this relationship is also evident after the climate regime shift. Therefore, the teleconnections between them have potential impacts on both oceanic and atmospheric processes over the tropical Indian Ocean.

P47

Role of Tropical SST anomalies on the seasonal predictability of the Northern Hemispheric Winter of 2019/20

Retish Senan, Franco Molteni, Magdalena Alonso Balmaseda, Antje Weisheimer, Timothy N. Stockdale and Stephanie Johnson

European Centre for Medium-range Weather Forecasts, Reading, United Kingdom

Seasonal forecasts of the positive North Atlantic Oscillation (NAO) and mild European temperatures during DJF 2019/20 were remarkably skilful. This provides a unique opportunity to identify the mechanisms behind the strong seasonal predictability. The strong European forecast signal occurred despite the absence of significant ENSO anomalies. A major anomaly preceding the season was an exceptionally strong positive Indian Ocean Dipole (IOD) event, whose positive sea surface temperature (SST) anomaly in the west-central Indian Ocean persisted into the December to January (DJF) season and was well captured by the operational ECMWF seasonal forecasting system, SEAS5. Here, a series of deconstruction experiments are performed to separate the impact of various tropical SST anomalies on the DJF 2019/20 northern hemispheric winter response. In these forced SST experiments, the observed anomalies were replaced by climatology over the tropical Indian, Atlantic, and Pacific Ocean basins in order to isolate the impact of regional SST forcing. The results of these attribution experiments show that persistent diabatic heating of the tropical Indian Ocean in DJF associated with the positive IOD was a key driver of the DJF NAO response. The plausible mechanisms associated with the response are discussed.

The prediction of variability in the Indian, Pacific and Atlantic Ocean has been improved in models in the recent decades. However, the prediction of South Asian monsoon is still a challenge for the scientific community of the world even after 25-30 years of advancement in the modelling efforts. The quantification of the predictability of monsoon with reference to the improvement of variability in three major ocean basins in a systematic manner has not been done till date. I am trying to investigate the role of three major ocean basins on South Asian monsoon variability from the Atmospheric Model Intercomparison Project (AMIP)-style models, Coupled models and Intercomparison Project (CMIP) runs. This will provide understanding of monsoon dynamics and predictability coming from the three ocean basins. The assessment of the reasons responsible for the improvement in the predictability of summer monsoon will benefit the scientists working in the area of monsoon research.

P49

Abstract

The interannual precipitation variability over Western Himalaya–Karakoram–Hindukush (WHKH) region has a significant impact on the freshwater resources, energy and agriculture sectors. Midlatitude storms play the role of an atmospheric bridge between large-scale circulation patterns and regional precipitation distributions during the winter (December–April) season. In this study, we investigated long-term changes between El Niño Southern Oscillation (ENSO) and storm activity as well as between ENSO and for precipitation, over WHKH for the period 1950–2015. The Melbourne University Objective Cyclone Identification and Tracking Scheme is used to track the midlatitude storms. A non-linear relationship is identified between the storm track frequency and precipitation over the WHKH region. The correlation between the storm frequency and precipitation increases significantly (95%) after the 1980s and reaches a maximum value of 0.53. Furthermore, 21-year running correlations also show non-linear relationships between ENSO and WHKH's precipitation as well as for storm tracks frequency. The simultaneous correlation between storm tracks frequency (precipitation) and Niño3.4 index was in significant 0.03 (0.25) in the earlier period from 1950 to 1979, which surged to 0.47 (0.60) in recent 30-years period from 1986 to 2015. Composites and regression analysis illustrate that ENSO modulated the midlatitude storm tracks over the WHKH region, which in turns impact more precipitation anomalies in the recent 30-years period. Moreover, Saudi King Abdulaziz University Atmospheric General Circulation Model (Saudi-KAU AGCM) also confirms the change in the relationship between ENSO and WHKH precipitation variability during the winter season between the two periods. These findings may have important implications for the seasonal rainfall predictability of the WHKH region.

P50

Plausible factors responsible for extreme rainfall events in different regions of Odisha

Madhusmita Swain, P. Sinha*, U. C. Mohanty, and S. Pattnaik

School of Earth Ocean and Climate Sciences, Indian Institute of Technology Bhubaneswar

Abstract

The present study examines the dominance large-scale meteorological parameters responsible for extreme rainfall (≥ 204.5 mm/day) and dry events (=0 mm/day) during 1980 – 2013 summer monsoon period over Odisha. India Meteorological Department gridded high-resolution (0.25˚×0.25˚) daily rainfall analysis data and ERA-Interim (0.75˚×0.75˚) daily meteorological parameters are used. Analysis depicts that the Indian Ocean is warmer during extreme rainfall events compared to the dry events, particularly near the seashore of Odisha. The stronger (weak) and cyclonic (anti-cyclonic) flows at 850 hPa are present during extreme rainfall (dry) events. The moisture flux is convergent during extreme rainfall events, while it is reverse during dry events. The monsoon trough is shifted south (north) from its normal position during extreme rainfall (dry) events. All these atmospheric states are favorable conditions for the rainfall extremes over Odisha.

Further, possible reasons for heterogenetic characteristics of rainfall extreme within Odisha are investigated. The study has found that the wind at 850 hPa, omega at 500 hPa, and SST play the important role for Region I, while OLR and omega at 500 hPa are dominating for the Region IV in the occurrence of extreme rainfall. Moreover, for the other regions in Odisha, the role of the dominant climatic parameters for the extreme rainfall occurrence varies. Analysis confirms that the role of dominant meteorological parameters is statistically significant for the extreme rainfall event over the respective region. Although climate change is a global issue, but the changes in extreme rainfall event is local and the responsible factors also differ.

Keywords: Extreme Rainfall; monsoon season; large-scale parameters; local change

P51

Inter-annual variability of moisture transport over the northern Indian Ocean and South Asian summer monsoon

ABSTRACT: We studied the inter-annual variability of the vertically integrated zonal/meridional moisture transport in the lower troposphere over the northern Indian Ocean using observed data from 1971−2016 for the South Asian summer monsoon (SASM) season. The moisture transport variability was dominated by the zonal component associated with the Somali low level jet. For identification of the dominant modes of inter-annual variability, 3-dimensional empirical orthogonal function analysis was performed. The leading mode, associated with suppressed meridional moisture transport in both the Arabian Sea and Bay of Bengal and increased zonal moisture transport over the Bay of Bengal, was linked with the positive phase of the Indian Ocean dipole and El Niño conditions in the Pacific Ocean. The second leading mode was associated with the enhanced zonal moisture flow over the Arabian Sea extending up to the Bay of Bengal allied with the Somali low level jet, and enhanced northeastward moisture transport over the whole region. This enhanced moisture flow results in stronger monsoon circulation and increased rainfall over South Asia.

Role of Indian Ocean Capacitance on Indian Summer Monsoon Rainfall

Venugopal Thandlam, Hasibur Rahaman, Ravichandran.M and Ramakrishna.S.S.V.S

The Indian summer monsoon variability on inter-annual and intraseasonal time scale has puzzled the scientific community due to its complex, regionally heterogeneous variability on inter-annual and intra-seasonal time scale. Even today with cutting edge technological advancement and with so many years of research, still most of the dynamical as well as statistical model fails to predict the extreme as well as intra-seasonal monsoon rainfall variability with a reasonable accuracy. This is largely due to the inherent variability within the monsoon system itself and lack of understanding of the ocean's role on Indian monsoon variability. Nevertheless, despite enhanced availability of observational data especially satellite derived sea surface temperature (SST), sea surface height anomaly (SSHA), sea surface wind (SSW) over global ocean monsoon variability have not been looked extensively. In this paper we have used these data for the recent time to see the large-scale variability of SST, SSHA and SSW over the Indian Ocean to the inter-annual Indian monsoon rainfall variability. This study shows the active role of ocean surface as well as subsurface on inter-annual time scale for the extreme monsoon rainfall variability. Analysis shows the cooler (warmer) anomaly over western Indian Ocean affects rainfall variability adversely (favorably). This is largely due to the reversal of SSW pattern during pre-monsoon period (May).

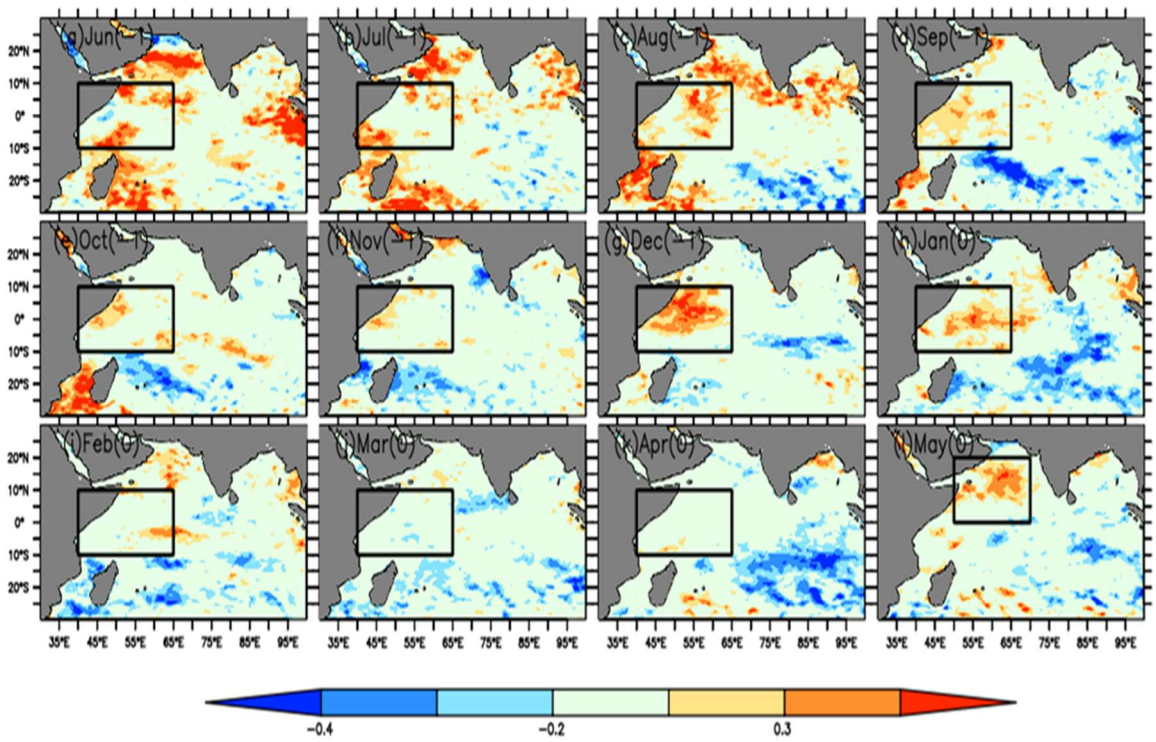

Figure 1: Correlation between SD_ISMR and SSTA

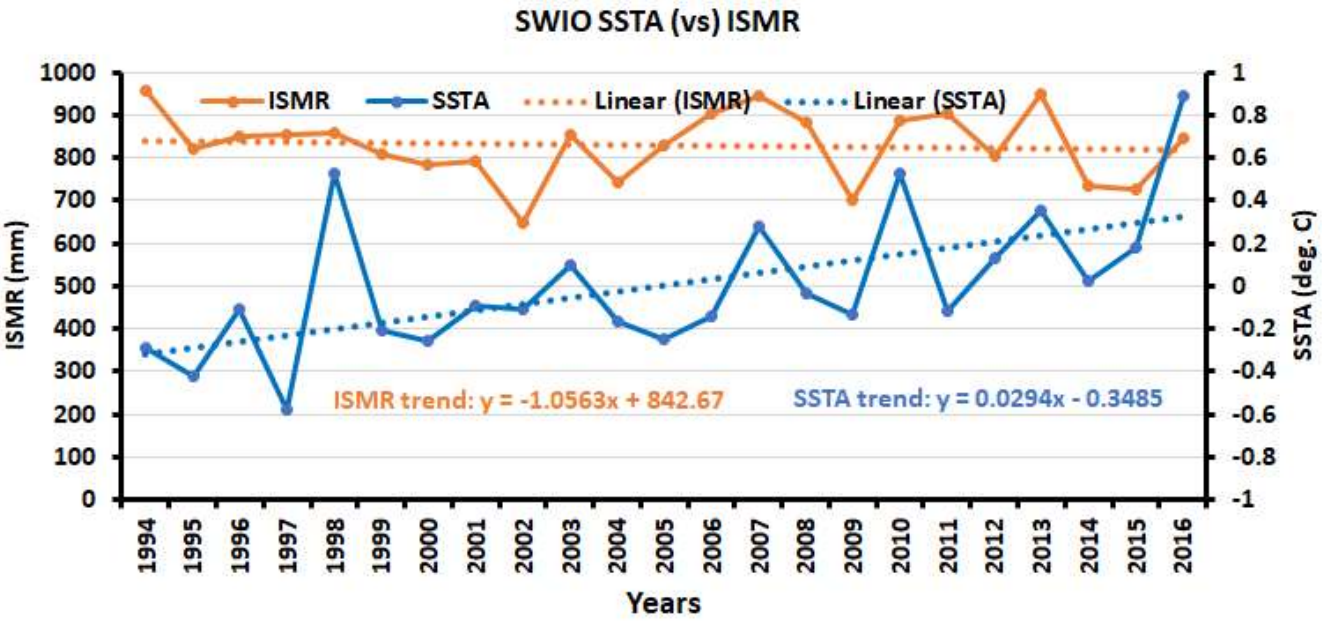

Figure 2: Variability of ISMR with respect to mean SWIO SSTA during June (-1) to May (0)

P53

Decadal variability of Tropical Indian Ocean sea surface temperature and its impact on the Indian summer monsoon

Amol Vibhute[1*], Subrota Halder[1,2], Prem Singh[1], Anant Parekh[1], Jasti S. Chowdary[1] & C. Gnanaseelan[1]

[1]Indian Institute of Tropical Meteorology, Ministry of Earth Sciences, Pune 411008, India
[2]Savitribai Phule Pune University, Pune 411007, India

Decadal variability of climate over the Pacific and Atlantic Ocean is well studied. However, the decadal climate variability over the Indian Ocean and its possible impact on the summer monsoon received relatively less attention. The present study aims to explore the decadal variability of the Tropical Indian Ocean (TIO) sea surface temperature (SST) and its associations with the Indian summer monsoon rainfall (ISMR) variability. More than a hundred years of observed monthly SST data from Extended Reconstructed sea surface temperature and rainfall data from India Meteorological Department are used for the analysis. In addition to these, century reanalysis fields of winds, moisture, vertical velocity, tropospheric temperature, and sea level pressure are used for diagnosing different processes. Time series and wavelet analysis confirmed the presence of decadal variability (~ 9 to 30 years) in the TIO SST. The decadal variance of TIO SST is maximum in the eastern equatorial Indian Ocean, followed by the north Arabian Sea. Decadal EOF of TIO SST shows a dominant basin-wide mode explaining about 50% of total variance and has robust decadal variability during 1940 to 1952; wavelet analysis supported this robust signal statistically. Similar analysis for the ISMR reveals that the decadal variance of rainfall has significant strength over the monsoon core zone and Western Ghats. The EOF analysis further confirms this spatial pattern of rainfall decadal variability over India. Correlation between decadal TIO SST and over monsoon core zone (MCZ) rainfall is significant with 2 years lag. To understand how the decadal variability of TIO SST influences the ISMR, monsoon features during strong warm and cold phase are studied. During the warm phase, MCZ and Western Ghats receive more rain than normal and vice versa for cold phase. Which is consistent with strong southwesterly winds, strong pressure gradient, and strong convergence over the MCZ for the warm phase. Also, during the warm phase, positive anomaly of mid-troposphere temperature, vertical velocity, and moist static energy are found to be associated with excess convective activity. Apart from this, larger scale zonal (Walker) and meridional (Hadley) circulation fields are also in phase with the TIO SST and rainfall variability. Our study advocates that decadal variability in TIO SST influences the monsoon dynamics and moist thermodynamics leading to near in-phase changes in the rainfall over the MCZ and Western Ghats region.

P54

An attempt to forecast seasonal precipitation in the Comahue basins (Argentina) to increase productivity performance in the region.

Maximiliano Vita Sanchez [(1) (2),] Marcela Hebe González [(1) (3) (4)] and Alfredo Luis Rolla [(3) (4)]

marcelahebe@gmail.com

(1) Universidad de Buenos Aires, Facultad de Ciencias Exactas y Naturales, Departamento de Ciencias de la Atmósfera y los Océanos. Buenos Aires, Argentina.
(2) Instituto Nacional del Agua, Ministerio de Obras Públicas, Argentina
(3) CONICET – Universidad de Buenos Aires. Centro de Investigaciones del Mar y la Atmósfera (CIMA). Buenos Aires, Argentina.
(4) CNRS – IRD – CONICET – UBA. Instituto Franco-Argentino para el Estudio del Clima y sus Impactos (UMI 3351 IFAECI). Buenos Aires, Argentina.

Precipitation is decreasing in the last century, in southern Argentinian Andes mountain, especially in winter. This fact is relevant since the Comahue basin, compressed by the sub-basins of the Negro, Neuquén and Limay rivers, is characterized by the fruit-horticultural production and by the presence of hydroelectric dams. The negative precipitation trends are expected to continue in the future, generating a significant negative impact on the local and national economy. As the river flows are largely influenced by the interannual variability of autumn and winter rainfall, the availability of a good seasonal forecast provides an efficient tool to minimize risks. The study addresses the analysis of the main climatic forcing of precipitation in order to design some statistical models to forecast autumn rainfall. Using monthly precipitation data for the period 1981-2010 from several national institutions and data of atmospheric variables from the NCEP/NCAR reanalyses, simultaneous and lagged linear correlation maps were obtained to define the best set of predictors. The multiple linear regression methodology was used to create the predictive models and to evaluate their efficiency. The main conclusion was that the South Atlantic Ocean Anticyclone, the sea surface temperature of the Pacific and Indian Oceans, and the polar jet were the most relevant predictors and the designed models had good skill.

P55

Understanding tropical-midlatitude interactions: metrics, dynamical processes, and future change

Jiabao Wang

Center for Western Weather and Water Extremes (CW3E)

Scripps Institution of Oceanography, UCSD, CA

Tropical convections impact remotely on the midlatitude weather events (e.g., precipitation extremes over California) by forcing changes in circulation patterns. These tropical-midlatitude interactions are particularly important to be accurately simulated and predicted on subseasonal timescales since many management decisions fall within this time range. The Madden-Julian oscillation (MJO) is a unique type of organized tropical convection varying on subseasonal timescales and is recognized as an important source of subseasonal predictability for midlatitude weather phenomena. Better understanding of the MJO-midlatitude interactions is important in improving the simulation, prediction, and the understanding of future changes in MJO associated weather events.

As a joint activity between the WGNE MJO Task Force and WMO S2S teleconnection subproject, we developed a set of standardized diagnostics and metrics to characterize the MJO teleconnections and to understand the associated key dynamical processes (Wang et al. 2020a, b). In this talk, application of these diagnostics to CMIP5 and CMIP6 models will be presented. We will discuss the sensitivity of MJO teleconnections to MJO and basic state representations in models and sources of teleconnection biases. Future changes of MJO teleconnections and the underlying mechanisms will also be discussed.

Wang, J., H. Kim, D. Kim, S. A. Henderson, C. Stan, and E. D. Maloney (2020b): MJO teleconnections over the PNA region in climate models. Part II: Impacts of the MJO and basic state, *J. Climate*, 33, 5081-5101. doi: 10.1175/JCLI-D-19-0865.1.

Wang, J., H. Kim, D. Kim, S. A. Henderson, C. Stan, and E. D. Maloney (2020a): MJO teleconnections over the PNA region in climate models. Part I: Performance- and process-based skill metrics, *J. Climate*, 33, 1051-1067. doi: 10.1175/JCLI-D-19-0253.1.

P56

Journal of Sustainable Development; Vol. 11, No. 5; 2018
ISSN 1913-9063 E-ISSN 1913-9071
Published by Canadian Center of Science and Education

Development and Assessment of Localized Seasonal Rainfall Prediction Models: Mapping and Characterizing Rift Valley Fever Hotspot Areas in the Southern and Southeastern Ethiopia

Ephrem Weledekidane[1]

[1] School of Natural Resources and Environmental Sciences, Haramaya University, Haramaya, Ethiopia

Correspondence: Ephrem Weledekidane, School of Natural Resources and Environmental Sciences, Haramaya University, Haramaya p.o.Box: 20, Ethiopia. Tel: 251-9-1341-3420. E-mail: ephratus@gmail.com

Received: May 18, 2018 Accepted: June 16, 2018 Online Published: September 28, 2018

doi:10.5539/jsd.v11n5p102 URL: https://doi.org/10.5539/jsd.v11n5p102

Abstract

Rift Valley Fever disease has been recognized as being among permanent threats for the sustainability of livestock production in Ethiopia, owing to shared boarders with RVF endemic countries in East Africa. Above-normal and widespread rainfall have outweighed as immediate risk factor that facilitated historical outbreaks of the disease in the East Africa. The objective of the present study, thus, was to develop prospective localized seasonal rainfall anomaly prediction models, and assess their skills as early indicators to map high risk localized rift valley fever disease outbreak areas (hotspots) over the southern and southeastern part of Ethiopia. 21 years of daily rainfall data; for five meteorological stations, was employed in diagnosing existences of any anomalous patterns of rainfall, along with a cumulative rainfall analysis to determine if there were ideal conditions for potential flooding. The results indicated that rainfall in the region is highly variable; with non-significant trends, and attributed to be the results of the effects of large-scale climatic-teleconnection. The moderate to strong positive correlations found between the regional average rainfall and large scale teleconnection variables ($r \geq 0.48$), indicated some potentials for early prediction of seasonal patterns of rainfall. Accordingly, models developed, based on the regional average rainfall and emerging developments of El Niño/Southern Oscillation and other regional climate forcings, showed maximum skills (ROC scores ≥ 0.7) and moderate reliability. Deterministically, most of the positive rainfall anomaly patterns, corresponding to El Niño years, were portrayed with some skills. The study demonstrated that localized climate prediction models are invaluable as early indicators to skillfully map climatically potential RVF hotspot areas.

Keywords: Rift Valley fever, prediction, rainfall, models

1. Introduction

The burdens from vector-borne infectious diseases are affecting the least developed countries in Africa disproportionally (LaBeaud, 2008; Hotez & Kamath, 2009). Rift Valley Fever (RVF) is among such mosquito-borne viral zoonotic diseases. Its outbreaks had inflicted pronounced health and economic impacts in much of the countries in sub-Saharan Africa (Anyamba et al., 2010; Rich & Wanyoike, 2007). Since its first isolation in Kenya in 1930 (Daubney & Hudson, 1931), RVF outbreaks have been recorded in many countries in the region (Davies, 2010), and, recently, it has emerged in new geographical areas, with outbreaks reported in Yemen and Saudi Arabia in 2000 (Balkhy & Memish, 2003).

Despite the long perceived high risk for the disease, many countries in Africa, including Ethiopia, have not reported RVF disease. One reason is because most RVF viral activity is cryptic and at a low level and not associated with detectable disease in humans and animals (Davies, 2008). Another reason could be the lack of systematic surveillance activities for such epidemic diseases or, if exists, because they are not necessarily optimal in many of these countries (Davies, 2010). As a result, most of them remain unaware of the circulation of the virus within their territories, which can be validated based on the fact that many African countries have found significant seroprevalence in sheep, goats and cattle for the RVF virus, yet without any clinical signs being reported in humans or animals (Davies, 2008).

Ethiopia is not an exception to that, with RVF virus reported in 1995, following positive serological tests with no clinical disease, suggesting that the virus has been circulating in the country (Bouna, 2015; Teshome, Kasye,

Abiye, and Eshetu, 2016). During the 1997/98 RVF epizootic period in the Horn of Africa (HoA) region, heavy rain fall and floods affected the southern and southeastern parts of Ethiopia, bordering Somalia and Kenya. Later on, in 1998, veterinarian field investigations carried out in Somali region and the Borena zone in Ethiopia, have observed high level of abortion among livestock in the areas (Wondosen, 2003). Furthermore, Aedes vexans arabiensis, belonging to the same subspecies of Aedes vexans and the chief enzootic vector of RVF virus, was recorded in Ethiopia (Bouna, 2015; Teshome et al., 2016; MoARD, 2008). It has, further, been noted that circumstances that allow occurrences of RVF epizootics in RVF endemic countries often prevail, simultaneously, throughout a large part of the African continent (Davies, 2010; Davies, Linthicum, and James, 1985).

Ethiopia, being among the largest countries in Africa, has high population of domestic ruminants, sheep, goats, and camels. The total livestock population in the country has reached more than 88 million in head count, and is the largest in Africa, with the livestock sub-sector's contribution estimated at 14% of the country's total GDP and over 45% of the agricultural GDP. Hence, the critical role the livestock sector plays in the country's economy means that any negative shocks to the sector can have adverse effects on the livelihoods of millions of households and the performance of the wider economy (Gelan, Engida, Caria, and Karugia, 2012). In such regard, widely prevalent livestock diseases have been major constraints to livestock exports, with RVF being the most important disease that has affected the export of live animals and meat to prime markets in Middle East countries. For instance, Since 1997/98 Ethiopia has faced a total of three export bans as a result of RVF epidemic situations in neighboring countries (Teshome et al., 2016).

Outbreaks of several vector-borne diseases have been correlated with anomalous weather patterns and associated Extreme Weather Events (EWEs) (Davies, Linthicum, and James, 1985; LaBeaud, Ochiai, Peters, Muchiri, and King, 2007; Linthicum et.al., 1999; Patz, Epstein, Burke, and Balbus, 1996; Anyamba, et.al., 2009). The same is true for RVF, with its outbreak being episodic and closely linked to climate variability (Davies et al., 1985; Linthicum et.al., 1999). Historically, anomalously above-normal patterns of rainfall, usually associated with El Niño/Southern Oscillation (ENSO), have preceded most of the major RVF outbreaks in the region; as such, ambient climatic situations outweighed as immediate causes that facilitated the spread and transmission of the RVFV in the Horn of Africa (HoA) region (MoARD, 2008; Davies et al., 1985; Linthicum et.al., 1999; Reliefweb, 2010). ENSO is a well-known climate fluctuation that is associated with extremes in the global climate system. It is manifested as episodic anomalous warming and cooling of sea-surface temperatures (SSTs) in the equatorial eastern and central Pacific regions. At global scale, the El Niño phase of ENSO causes distinct and simultaneous patterns of flooding and drought, with a tendency for wetter-than-normal conditions and floods over Eastern Africa, particularly, when coincided with the short rainy season (from October to December). Generally speaking, the co-occurrence of anomalies over the east equatorial pacific and Indian Oceans (Black, Slingo, and Sperber, 2003), and the Zonal Dipole Mode over the Indian Ocean (IOD) (Saji, Goswami, Vinayachandran, and Yamagata, 1999) are known to affect the short season's rains over the equatorial east African region. Hence, the observed strong link between the anomalously above-normal and widespread rainfall and episodic RVF outbreaks in the HoA region has explicitly confirmed some skills in the predictability of a high potential for RVF outbreaks, based on possible early predictions of seasonal patterns of rainfall .

Such RVF outbreaks forecasting models and early warning systems were attempted and made available at the continental level and proved to be efficient in raising alerts before onsets of potential RVF epidemics in the HoA region (Anyamba et al., 2010; Anyamba, et.al., 2009). Early Warning (EW) messages for RVF outbreaks have often been given by international institutions such as the Emergency Prevention System (EMPRES-i), the National Aeronautics and Space Administration (NASA) and the World Health Organization (WHO) (Gikungu, et al., 2016). The RVF risk prediction systems employed by such institutions have mainly been based on interpretations, in the context of the ENSO, of the leading global scale climatic and ecological indicators that would lead to conditions for emergence of RVF vectors and, subsequently, to the disease epizootics/epidemics over time.

However, despite the proven potentials of such systems in identifying continental- and regional- scale eco-climatic conditions associated with potential vector-borne disease outbreaks (Linthicum et.al., 1999; Anyamba, et.al., 2009), there are some discrepancies between the spatial accuracy required by policy makers and actors at local levels and what has been being delivered, mainly because such monitoring and prediction systems have been based on interpretations of remotely sensed proxy variables as a substitution for leading RVF indicator elements; such as the Normalized Diffrence Vegetation Index (NDVI) as a proxy for regional rainfall. Furthermore, several factors, at local levels, including topography, closeness to surrounding water bodies, *etc*., determine how patterns of rainfall at such smaller spatial scales would evolve. Hence, such approaches might open a window for overestimation or underestimation of the leading RVF outbreak indicator variables. For

example, if NDVI is employed, as proxy for rainfall, specifically, in areas maintained with irrigation or where there have been unprecedented changes in land use it may be misleading (Gikungu, et al., 2016). There is, therefore, a real need to further improve the spatial and temporal accuracies of forecasts of the leading RVF indicator variables, and subsequently our skills in predicting RVF outbreaks. The use of high spatial resolution mapping to identify flooded regions in RVF endemic areas at risk or even the use of radar data has been suggested as possible approaches to improve such discrepancies (Anyamba et al., 2010).

Ethiopia has started providing emphasis to RVF disease following a serious of outbreaks of the disease in the neighboring countries. The country has developed RVF Contingency and Preparedness Plan since June 2008, and set active RVF surveillances in place over high risk areas bordering RVF endemic countries. The plan underlines the importance of RVF specific Early Warning (EW) programmes and early outbreak prediction models in mounting appropriate, timely, and cost-effective responses against the disease, based on early predictions for potential above normal seasonal rainfall over high risk areas (MoARD, 2008). However, to date, no single effort, that the author is aware of, were made in an attempt to analyze and explain the coupling between patterns of local climatic variability with risks for potential establishment and spread of the RVFV, let alone an attempt to develop locally relevant RVF prediction models based on any of the leading RVF outbreak indicator variables.

Apart from that, several studies have previously investigated the influence of ENSO and other regional forcings on the patterns of rainfall in Ethiopia. Most of these studies, however, have focused on variability and predictability of the June to September rainfall season, and, merely, for areas over the central and northern half of the country (National Meteorological Service Agency (NMSA), 1996; Bekele, 1997; Shanko, & Camberlin, 1998; Korecha & Barnston, 2007; Gissila, Black, Grimes, and Slingo, 2004). Paradoxically, there are no previous studies, except one by Degefu, Rowell, and Bewket (2017), regarding the influence of such large scale teleconnections on patterns of rainfall for the (September) October – December ((S)OND) season in Ethiopia, which is known as the short rainy season for areas over the southern and southeastern parts of the country. Despite such limitations, the findings of Degefu et al., (2017) depicted statistically significant positive correlations between Sea Surface Temperature (SST) and patterns of the short rainy season's rainfall over the southern and southeastern parts of the country. Furthermore it has been indicated that there are skills in inferring patterns of seasonal rainfall in the country based on those large scale teleconnection variables (NMSA, 1996; Bekele, 1997; Shanko, & Camberlin, 1998; Korecha & Barnston, 2007; Gissila et al., 2004; Degefu et al., 2017). Recognizing such a possibility, the NMA of Ethiopia has started, recently, to provide seasonal rainfall predictions based on such teleconnection patterns, though its importance continues to be somewhat underweighted (Degefu et al., 2017).

Hence, in responding to the quest for better capability for predicting the seasonal pattern of rainfall for areas characterized as having high risk for RVF disease outbreaks in Ethiopia, and for improved early and rapid detection of possible RVF outbreaks at the local levels (MoARD, 2008), this particular study argues and shows that simple empirical prediction models can be efficiently used. The approach can be one way to identify local scale 'rainfall hotspots' (rainfall hotspots, in this study, are defined as areas for which an anomalously above normal and wide spread seasonal rainfall is forecasted for), which can serve as early indicators for areas with high potential risks of RVF outbreaks. Such local scale rainfall prediction models could enhance the efficiency in targeting zones, districts, or provinces to deploy resources, in time, and strengthen efforts for active surveillance, detection, and control of RVF disease. Furthermore, predicting the pattern of rainfall at such finer-local scale, at a reasonable lead-time preceding potential RVF outbreak periods in neighboring countries, could help to prioritize targeted surveillance and mosquito control activities, in accordance with available resources.

The paper begins with a short description of the study area, the data employed, and the methods used in the analysis, followed by the results and discussion section that elaborates on, in order of appearance, results of the quality control process, seasonal and annual trends in the rainfall series, daily and monthly cumulative rainfall totals, and patterns and strengths of seasonal correlations of rainfall with large scale teleconnection indices. The results of subsequent analyses on predictability of the pattern of the regional rainfall are also presented. Finally it ends with the main conclusions drawn from the study.

2. Materials and Methods

2.1 Description of the Study Areas

The study areas are purposefully selected, for this particular study, based on their geographical proximity and climatic similarity to RVF endemic countries in the HoA region (Keneya and Somalia), and the nature of cross-border livestock movement (trade or seasonal migration). Accordingly five districts were selected; Deghabur and Kebridhar (from the Somali regional state), Dire, Moyalle and Yabello (from the Borena zone of

the Oromia regional state). Figure 1, below, portrayed the locations of the districts.

The areas in the Southern (S-) and Southeastern (SE-) part of Ethiopia are generally characterized as arid- to-semi- arid environments. All districts experience bimodal rainfall pattern, the main rainy season, locally termed "Belg" season, running from March to May, and the short rainy season, locally termed "Bega" season, spanning from Sept/Oct to December.

In Ethiopia, the pastoralist and agro-pastoralist areas; such as the "Borena", "Afar", and "Somali", are considered the traditional sources of livestock, supplying 95 percent of livestock destined for export markets. Owing to their proximity and/ or because they share borders with Keneya and Somalia, the inhabitants, along with their animals, traditionally move across the borders for several reasons, one being an access to available grazing and watering points. Livestock trade in these areas is also characterized by informal cross-border trade with adjacent neighboring countries, mainly Somalia and Kenya, where the livestock are used either for re-export or domestic consumptions. All the above factors, combined, thus make the areas at a greater risk to clinical RVF disease during the epizootic/ epidemic periods of the disease in the HoA region.

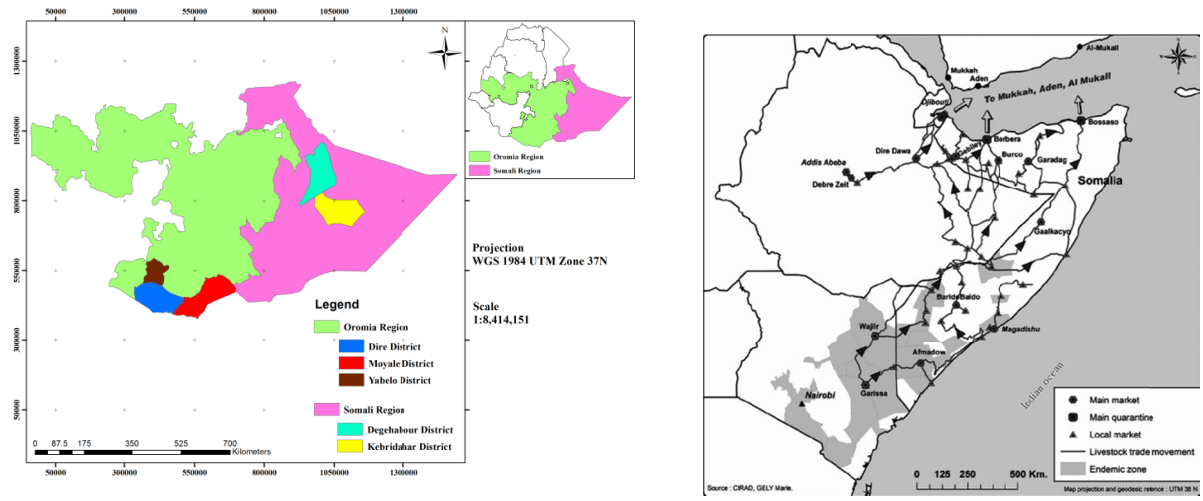

(a) (b)

Figure 1. (a) Locations of the study areas, and (b) Live animals trade movement from Somalia, Kenya, and Ethiopia to Yemen, through Bossaso and Djibouti sea ports (Source: Marie G., in Abdo-Salem et al., 2010). The southern and southeastern parts of Ethiopia are shown as sharing boarders with RVF endemic countries in the HoA region in figure 1 (b)

2.2 Data

Climate data of daily rainfall records for five observing stations from the study areas, for the period 1978-2008, were obtained from the National Meteorological Services Agency of Ethiopia (NMSA). Subsequently, monthly, seasonal, and annual rainfall totals were derived from the daily data for all the stations. To determine a common period to all the rainfall stations, some missing data were calculated using INSTAT+ v. 3.36 software, first and second order Markov-chain simulations for the occurrences and amount of rainfall, respectively (Stern, Rijks, Dale, and Knock, 2006). Time series data for two of the dominant large scale global teleconnection variables (Niño3.4 SST & Indian Ocean Dipole Mode (MDI)), which are known to influence the weather systems of East Africa region, were downloaded and, subsequently, employed in the study. The different environmental and climate data sets that were used in the study, their main characteristics, and sources are provided in appendix A (Table A1).

2.3 Methods

2.3.1 Quality Control

Long term climatic series is rarely free of irregularities, errors and missing values. Thus, it is essential to produce homogeneous and quality controlled climate records before using them in subsequent analysis (Costa & Soares, 2009).

Outlier identification: Identification of outliers has been the primary emphasis to the climate database

development (Gonzalez-Rouco, Luis, Quesada, and Valero, 2001; Štěpánek, Zahradníček, and Fardaet, 2013). Outliers (suspicious data) are observation values very distant from a threshold value of a specific time series data that can be due to measurement errors or to extreme meteorological events (Gonzalez-Hidalgo, Lopez-Bustins, Stepanek, Martin-Vide, and De-Luis, 2009; Göktürk, Bozkurt, Sen, and Karaca, 2008). Several approaches that focus on temporal and/or spatial variability can be applied in order to identify outliers and diagnose whether they are erroneous or not (Barnett & Lewis, 1994; Peterson et al., 1998). In this particular study, the Tukey fence outlined in (Ngongondo, Yu-Xu, Gottschalk, and Alemaw, 2011) was used to censor outliers in the rainfall datasets.

The primary objective of outliers trimming is to reduce the size of the distribution tails in order to make a safer use of the nonresistant homogenization techniques used later (Štěpánek et al., 2013). Hence, rather than rejecting extreme values in the data (suspicious data values) they were replaced by some threshold value that kept the information of an extreme event and yet did not have such an important influence on the nonresistant statistical techniques employed latter in this research.

The Turkey fence is the data range:

$$[Q_1 - 1.5 * IQR, Q_3 + 1.5 * IQR] \quad (1)$$

Where Q_1 and Q_3 are respectively the lower and upper quartile points, 1.5 are standard deviations from the mean, and IQR is the interquartile range.

In this study values beyond these limits were considered as suspicious data points and subjected to further evaluations to check if the trimmed values carried any physical meaning and, hence, for suppression of false alarms. If no plausible interpretations were found, outliers were set to a limit value corresponding to ±1.5×IQR, otherwise, to keep the information from extreme events, suspicious outlier values of each monthly precipitation series were identified as those values trespassing a maximum threshold for each time series (Trenberth, & Paolino, 1980; Peterson, Vose, Schmoyer, and Razuvaev, 1998), defined as:

$$P_{out} = Q_3 + 3IQR \quad (2)$$

Where, Q_3 is the third quartile and IQR the interquartile range. Subsequently, suspicious values were replaced by the corresponding unique Pout values (Gonzalez-Rouco et al., 2001; Göktürk et al., 2008). The original values of the outliers were restored, latter, for specific studies concerning extreme values (e.g. potential flooding). This method has more resistance against outliers because quartiles are used in this method (Gonzalez-Rouco et al., 2001).

Homogeneity tests: The second step of the quality control process involved homogeneity tests. A homogeneous climate series is defined as one where variations are caused only by changes in weather and climate (Conrad & Pollak, 1950). The presence of in-homogeneities is a common problem in climate time series. These irregularities in climate data can deceive the actual results and lead to some wrong conclusions (Vicente-Serrano, Beguería, Lopez-Moreno, García-Verac, and Stepanek, 2010). Thus, to assess some meaningful climate analysis, the climate data must be homogeneous (Stepanek, Zahradnicek, and Skalak, 2009). Although several techniques have been developed for detection of irregularities on a site and their adjustment, no single procedure is explicitly recommended.

In this particular study, due to their lower demands in application and interpretation as well as because the stations are randomly distributed, with poor correlations among the stations, three homogeneity tests; Pettitt test, Buishand Range (BR) test, and Standard Normal Homogeneity Test (SNHT), were used for absolute testing of homogeneity (using stations own data) of the rainfall series. For each of the daily rainfall series, two testing variables, annual mean and annual maximum values, were considered. The following sections outline in detail the methodology for performing these tests.

Pettitt's test: This test is a nonparametric test, which is useful for evaluating the occurrences of abrupt changes in climatic records (Yesilırmak, Akçay, Dagdelen, Gürbüz, and Sezgin, 2008). One of the reasons for using this test is that it is more sensitive to breaks in the middle of the time series (Wijngaard, KleinTank, Können, 2003). The statistic used for the Pettitt's test is computed as follows:

$$U_k = 2\sum_{i=0}^{n} m_i - k(n+1) \quad (3)$$

Where m_i is the rank of the i^{th} observation when the values X_1, X_2 ….. X_n in the series are arranged in ascending order. The statistical break point test (SBP) is as follows:

$$K = \max_{1 \le k \le n} |U_k| \tag{4}$$

When U_k attains maximum value of K in a series then a change point will occur in the series. The value is then compared with the critical value given by Pettitt (1979).

Buishand Range (BR) test: Buishand, (1982) noted that tests for homogeneity can be based on the adjusted partial sums or cumulative deviations from the mean and it is given as follows:

$$S_0^* = 0 \text{ and } S_k^* = \sum_{t=1}^{k} (y_i - \bar{y}), \quad k = 1, 2, \dots, n \tag{5}$$

The term S_k^* is the partial sum of the given series. If there is no significant change in the mean, the difference between y_i and $\bar{y}$ will fluctuate around zero. The significance of the change in the mean is calculated with 'rescaled adjusted range', R, which is the difference between the maximum and the minimum of the S_k^* values scaled by the sample standard deviation (SD) as:

$$R = (\max_{0 \le k \le n} S_k^* - \min_{0 \le k \le n} S_k^* / SD) \tag{6}$$

The critical value for R/ n is calculated by Buishand (1982).

Standard Normal Homogeneity Test (SNHT): A statistic $T_{(y)}$ is used to compare the mean of the first y years with the last of (n - y) years and can be written as below:

$$T_y = y\overline{Z1} + (n - y)\,\overline{Z_2}, \qquad y = 1,2, \dots, n \tag{7}$$

Where,

$$\overline{Z_1} = \frac{1}{y} \sum_{i=1}^{n} \frac{(Y_i - \bar{Y})}{S} \text{ and } \overline{Z_2} = \frac{1}{n-y} \sum_{i=y+1}^{n} \frac{(Y_i - \bar{Y})}{S} \tag{8}$$

The year 'y' consisted of a break if the value of T_y is a maximum. To reject null hypothesis, the test statistic, T_0, should be greater than the critical value, which depends on the sample size. The test statistic, T_0, is given as:

$$T_0 = \max_{1 \le y \le n} T_y \tag{9}$$

Classification of the results of the homogeneity tests: After testing the homogeneity of all the selected stations, for the testing rainfall variables, the results of all the three tests were evaluated. The results were classified following (Schonwiese & Rapp, 1997; Amit & Mohammed, 2013). This classification was based on number of tests rejecting the null hypothesis. Three categories were identified: Class1: 'useful'- one or zero of the tests rejected the null hypothesis; Class 2: 'doubtful'- two tests rejected the null hypothesis; and Class 3: 'suspect'- all the three tests consistently rejected the null hypothesis.

The qualitative interpretations of the categories are as follows:

Class1: 'useful'- No clear signal of an inhomogeneity in the series is apparent. The series seem to be sufficiently homogeneous for trend analysis and variability analysis.

Class 2: 'doubtful'- Indications are present of an inhomogeneity of a magnitude that exceeds the level expressed by the inter-annual standard deviation of testing variable series. The results of trend analysis and variability analysis should be regarded very critically from perspective of the existence of possible inhomogeneities.

Class 3: 'suspect'- It is likely that an inhomogeneity is present that exceeds the level expressed by the inter-annual standard deviation of testing variable series. Marginal results of trend and variability analysis should be regarded as spurious. Only very large trends may be related to a climatic signal. Hence, series falling in class 3 labeled 'suspect' could not be taken as reliable and removed from subsequent statistical analysis.

Randomness and persistence analysis: One of the problems in the analysis and interpretation of trends in hydroclimatic data is the confounding effect of serial dependence (Partal & Kahya, 2006). The existence of a positive serial correlation in a time series could signify a significant trend, while in fact, due to random effects of the data series. A negative serial correlation, on the other hand, could cause an underestimation of the probability of a significant trend (Yu, Yang, and Kuo, 2006). Thus, time series data required for trend analysis should be random and/or non-persistent (Ngongondo et al., 2011).

Hence, before proceeding to trend analysis, the rainfall time series data were tested for randomness and independence using the autocorrelation function (r_1) as described in (Box & Jenkins, 1976) in the following manner:

$$r_1 = \frac{\sum_{i=1}^{n-1}(x_i - \bar{x})(x_{i+1} - \bar{x})}{\sum_{i=1}^{n}(x_i - \bar{x})^2} \tag{10}$$

Where x_i is an observation, x_{i+1} is the following observation, $\bar{x}$ is the mean of the time series, and n is the number of data.

The autocorrelation coefficient provides a measure of temporal correlation between the data points in a series, for different time lags (Brockwell & Davis, 1996). In this study, serial correlation of rainfall series, for all individual stations as well as for the regional average rainfall series, with time, was employed to see the tendency for the series to remain in the same state from one observation to the next or not. Whenever significant serial correlation appeared within a given time series, the data series had been 'pre-whitened', prior to applying the subsequent trend test, following the procedure described in Box & Jenkins (1976). The corrected data series is, thus, obtained as:

$$(x_2 - r_1 x_1, x_3 - r_1 x_2, \ldots, x_n - r_1 x_{n-1}) \tag{11}$$

2.3.2 Trend Analysis

The Mann–Kendall test: is a rank-based method (Mann, 1945; Kendall, 1975) that has been applied widely to identify significant trends in hydroclimatic variables (Yenigun, Gumus, and Bulut, 2008). The test checks the null hypothesis of no trend versus the alternative hypothesis of the existence of increasing or decreasing trend. Furthermore, it is a non-parametric method, which is less sensitive to outliers (temper values of time series) and test for a trend in a time series without specifying whether the trend is linear or nonlinear (Partal & Kahya, 2006; Yenigun, Gumus, and Bulut, 2008).

The Mann-Kendall's test statistic is given as:

$$S = \sum_{i=1}^{N-1} \sum_{j=i+1}^{N} \mathrm{Sgn}\,(x_j - x_i) \tag{12}$$

Where S is the Mann-Kendal's test statistics; x_i and x_j are the sequential data values of the time series in the years i and j (j > i), and N is the length of the time series. A positive S value indicates an increasing trend and a negative value indicates a decreasing trend in the data series.

The sign of the function is given as:

$$\mathrm{Sgn}(x_j - x_i) = \begin{cases} +1 \text{ if } (x_j - x_i) > 0 \\ 0 \text{ if } (x_j - x_i) = 0 \\ -1 \text{ if } (x_j - x_i) < 0 \end{cases} \tag{13}$$

This statistics represents the number of positive differences minus the number of negative differences for all the differences considered. For large samples (N > 10), the test is conducted using a normal distribution, with the mean and the variance as follows:

$$E[S] = 0$$
$$\mathrm{var}(s) = \frac{N(N-1)(2N+5) - \sum_{k=1}^{n} t_k(t_k - 1)(2t_k + 5)}{18} \tag{14}$$

Where n is the number of tied (zero difference between compared values) groups and t_k the number of data points in the k^{th} tied group. For n larger than 10, ZMK approximates the standard normal distribution (Partal & Kahya, 2006; Yenigun, Gumus, and Bulut, 2008) and the standard normal deviate (Z-statistics) is then computed as follows:

$$Z_{MK} = \begin{cases} \dfrac{s-1}{\sqrt{\mathrm{Var}\,(s)}}, & \text{if } s > 0 \\ 0, & \text{if } s = 0 \\ \dfrac{s+1}{\sqrt{\mathrm{Var}\,(s)}}, & \text{if } s < 0 \end{cases} \tag{15}$$

The presence of a statistically significant trend was evaluated using the ZMK value. In a two-sided test for trend, the null hypothesis H_o should be accepted if /ZMK/ < $Z_{1-\alpha/2}$ at a given level of significance. $Z_{1-\alpha/2}$ is the critical value of ZMK from the standard normal table. E.g. for 5% significance level, the value of $Z_{1-\alpha/2}$ is 1.96. All the trend results in this paper have been evaluated at the 5% level of significance to ensure an effective exploration of the trend characteristics within the study areas.

The Sen's estimator of slope: Sen's estimator (Sen, 1968) has been widely used for determining the magnitude of trend in hydro-meteorological time series, depicting the quantification of changes per unit time (Hadegu, Tesfaye, Mamo, and Kassa, 2013). In the method, the slopes ($T_{i)}$ of all data pairs are first calculated as:

$$T_i = \frac{x_j - x_j}{j - k} \text{for } i = 1, 2, \dots, N \tag{16}$$

Where, x_j and x_k are data values at time j and k (j > k), respectively. The median of these N values of T_i is Sen's estimator of slope which is calculated as:

$$\beta = \begin{cases} T_{\frac{N+1}{2}}, & N \text{ is odd} \\ \frac{1}{2}\left(T_{\frac{N}{2}}, \right. & N \text{ is even} \end{cases} \tag{17}$$

A positive value of β indicates an upward (increasing) trend and a negative value indicates a downward (decreasing) trend in the time series.

2.3.3 Cumulative Rainfall Analysis

Since Rift Valley fever outbreaks are known to follow periods of anomalously extended above-normal rainfall and associated potential flooding conditions, cumulative monthly and daily rainfall anomalies, corresponding to the short rainy seasons (OND) of two of the recent RVF outbreak periods (1996/97 and 2006/07), were calculated and plotted. The periods were purposefully selected to encompass the short rainy season for equatorial eastern Africa, which historically preceded or be followed by outbreaks of RVF epidemics.

The cumulative rainfall anomaly index is calculated as:

$$C_n = \sum_{i=1}^{n} R_i - \sum_{i=1}^{n} M_i \tag{18}$$

where C_n is the cumulative rainfall anomaly value for time steps 1to n, Σ is the summation function, R_i was total rainfall at time step i of the series, and M_i is the average total rainfall for time step i.

It has been known that the chances for flooding are enhanced if an ElNiño event coincided with the short rainy season for East Africa (October–December) (De-Luı´s, Gonza´lez-Hidalgo, Raventos, Sanchez, and Cortina, 1999). This study illustrated the occurrences of potential flooding conditions by analyzing whether the calculated C_n values, for the periods preceding and including the first reported RVF outbreak month for east Africa-(December) were consistently positive or not. Accordingly, consistent positive C_n values, for consecutive two to three months, were considered as indicators for potential flooding situations.

2.3.4 Precipitation Concentration Index (PCI)

The monthly Precipitation Concentration Index (PCI) was analyzed following De-Luı´s et al., (1999), which is the modified version of the one given by Oliver (1980). The PCI values are calculated as:

$$PCI = \sum_{i=1}^{n} P_i^2 \Big/ \left(\sum_{i=1}^{n} P_i\right)^2 \tag{19}$$

Where, P_i is the rainfall amount of the i^{th} month. Based on the scale defined in De-Luı´s et al., (1999), PCI values below 10 indicate uniform monthly rainfall distribution; values between 11 and 20 indicate high concentrations of monthly rainfall distribution; and values of 21 and above indicate very high concentration of monthly rainfall distribution. Subsequently the results from the cumulative rainfall analysis and the calculated PCI values were interpreted together. The larger the values of the calculated PCI and the more consistent and positive the C_n values, then the more will be the potential for flooding condition.

2.3.5 Seasonal Teleconnection Patterns and Strengths

Correlation analyses were employed to investigate if the pattern of rainfall in the southern and southeastern

Ethiopia had significant correlations with large scale global and regional teleconnection indices. The correlation tests were set for the two to three months period corresponding to the RVF pre-epidemic and epidemic periods for east Africa. The analyses were based on the regional average SON rainfall totals, calculated as the average of SON rainfall totals for all the five rainfall stations selected from the southern and southeastern Ethiopia, and the two teleconnection indices, the Niño3.4 SST and the Indian Ocean Dipole mode (MDI), which are known to affect the pattern of seasonal rainfall in Ethiopia (Ogallo, 1988). Both positive and negative correlation values equal to and greater than 4.5 ($r \geq 4.5$) were considered as indicatives for moderate to strong relationships.

2.3.6 Predictability of Seasonal Rainfall Patterns

To determine whether the regional average SON rainfall pattern could be predicted with a purely simple statistical model, based on the large scale SSTs data, Multiple Linear Regression (MLR) models were developed and their skills in predicting the regional average SON rainfall anomaly patterns investigated. Model equations were developed by using the MLR option in the Climate Predictability Tool (CPT) of the IRI (http://iri.columbia.edu). The selection of predictor variables for the models was based on the linear strength of the correlations between historical records of Niño-3.4 SST and DMI values and the regional rainfall total anomaly, averaged for the SON period. Both cross validation (Michaelsen, 1987) and retroactive (Barnston et al., 1994) approaches have been widely used in studies involving climate prediction (Korecha & Barnston, 2007; Gissila et al., 2004; Thiaw, Barnston, and Kumar, 1999). In cross validation, a model is developed using all years but excluding each single year, in turn, which is predicted and verified in each case. The retroactive method involves partitioning the time series data into a training period and an independent verification period. Both forecasting approaches are described in-detail in the IRI website (http://iri.columbia.edu). In this study, the retroactive calculation option in the CPT was used to fit a MLR model to an initial subset of the overall model training period, with the models first trained with information from 1987/88 and leading up to and including 1996/97, which resulted in a first training set of 10 years long. The seasonal rainfall of the next year (1997/98) was subsequently predicted using the trained models. This procedure had continued until the 2006/07 regional SON rainfall anomaly was predicted, using the models trained with data from 1987/88 to 2006/07, which resulted in 10 years (1997/98–2006/07) of independent forecast data. All the models, developed for regional average SON rainfall anomaly forecasts, were cross validated (5-years-out window) over the 20 years period from 1987/88 to 2006/07.

2.3.7 Forecast Verifications

In estimating skills of the models in predicting the regional average SON rainfall total anomaly over S- & SE-Ethiopia, the observed and predicted fields were separated into three categories defining above-normal, near-normal, and below-normal rainfall total anomalies. The three-category design employed in this study was based on threshold values as defined by the 33rd (below-normal) and 67th (above- normal) percentile values of the climatological record.

Seasonal climate is inherently probabilistic, hence two attributes of interest for probabilistic forecasts were considered, i.e., discrimination (can the forecasts successfully distinguish different outcomes?) and reliability (is the confidence communicated in the forecast appropriate?) (Landman, Beraki, DeWitt, and Lötter, 2014). These two attributes were analyzed by using two of the outputs of the CPT MLR model fitting procedure as forecast verification measures, the Relative Operating Characteristic (ROC) (Mason & Graham, 2002) and the Reliability Diagram (Hamill & Colucci, 1997; Wilks, 2006). The ROC indicates how frequently the forecasts can successfully distinguish different below-normal from normal and above- normal, or above-normal from normal and below-normal. Specific to this study, it can also be translated as whether the forecasted probability for wetter condition, for the average SON period, was higher when an El Niño occurs, compared to when it did not occur. ROC scores for the three rainfall categories (above normal (AN), normal (N), and below normal (BN)) represent the respective areas beneath the ROC curve that are produced by plotting the forecast hit rates against the false alarm rates. If the area is ≤ 0.5, the forecasts have no skills, and for a maximum ROC score of 1.0, perfect discrimination has been obtained (Landman et al., 2014). The forecasts are considered reliable if there is consistency between the predicted probabilities of the defined rainfall categories and the observed relative frequencies of the observed rainfall being assigned to these categories.

3. Results and Discussion

3.1 Quality Control

Outliers Identified: The results of the outlier trimming process are given in Table 1, in which Pout values and periods of extreme data values corrected for each station are tabulated. The result of the outlier identification depicts that the seasons that reach maximum values correspond to the rainy seasons of the respective sites in the

eastern and southeastern parts of the country. The number of outliers identified has a clear periodic cycle. For all of the observing stations, a higher number of outliers were detected for the respective months in the 'MAM' and 'OND' seasons, while only three extreme data value were detected during the 'JJAS' season for Deghabur (1992) and Kebridhar (1992 & 1993). Furthermore, almost all of the months for which outliers were detected coincided with an El Niño episode; none has occurred during a La Niña episode. Such coincidences of anomalous data points with ENSO is not a matter of arbitrary chance, as the ENSO state is known to modulate the seasonal pattern of rainfall in some regions, particularly in the Tropics (Hastenrath, 1995). Specifically, for East Africa, it has been well known that an El Niño episode during the OND period is associated with an above-normal rainfall, with chances for flooding. The effects of ENSO on the SOND seasonal rainfall in the study areas is assessed more quantitatively latter.

Thus, in the background of such mechanisms as a possible explanation for possibilities of anomalous weather patterns, specifically during the SOND periods; the overall agreement of the temporal distribution and seasonal characteristics of the rainfall and timing of outliers, with extreme data points occurring concurrent with ENSO episodes, supports the idea of the existence of a plausible physical mechanism, which can be attributed as a cause for the detected anomalous data, rather than taking such outliers as, merely, human-induced errors. Hence, in this particular study, outliers' adjustments have been carried out by trimming only very extreme data points (values > Pout), with the aim of reducing large distribution tails, as a means of preprocessing previous to testing the rainfall series for homogeneity and subsequent corrections, if any.

Table 1. Results of the outlier trimming process

Stations Name	Periods, for which, outlier values replaced by Pout									
	JJAS						OND			
	Aug	Pout (mm)	Sept	Pout (mm)	Oct	Pout (mm)	Nov	Pout (mm)	Dec	Pout (mm)
Deghabur	1992	19.2			-		1997	46	2006	0
Kebridhar	-	-	1992/ 93	14.0	-	-	1997	151.7	-	-
Moyale	-	-	2006	43.8	1997	396.6	-	-	-	-
Yabello	-	-			-	-	1997	188.5	2002	111.3
Mega	-	-			-		-	-	-	-

* Pout = UQ + 3IQR, where UQ is the upper quartile and IQR is the inter quartile range

Despite great care was taken to conserve as much information as possible about the extreme events, by removing data points that are only greater than the corresponding Pout values, the process followed might inflict the possibility of dismissing interesting climatological information about extreme events. Hence, in the background of a plausible physical mechanism as a possible explanation for such anomalous extreme events, as explained above, and considering the basic objective of the study, i.e., identifying RVF hotspots (areas with anomalously high rainfall), the original values of the extreme data points were restored, latter, and employed in specific studies concerning extreme values, as for example in cumulative monthly and daily rainfall analysis.

Homogeneity of rainfall series: Previous studies outlined that because of the inherent noise in a given time series, statistical homogeneity tests render results with some degree of uncertainty (Cheung, Senay, and Singh, 2008). However, the use of various statistical tests (Buishand Range, Pettitt's, and SNHT tests) and different testing variables (annual rainfall total and annual maximum rainfall total) employed, under the current study, enabled to assess the homogeneity more reliably. Table 2 lists the results of the homogeneity tests for rainfall series and comparative test statistics calculated by the three techniques. It is clear from the table that out of the five stations analyzed for homogeneity, for annual mean and maximum rainfall series, not a single station was categorized as class 2 and/or class 3. Accordingly, the rainfall data series of all the stations were deemed sufficiently homogeneous for subsequent analysis, trend analysis.

Table 2. Comparison of results of the various homogeneity tests

Variable	Station	Buishand Range (BR) test		Pettitt's test		Standard Normal Homogeneity Test		Classification
		P value	Break Point	P value	Break Point	P value	Break Point	
Mean Annual Rainfall Total	Deghabur	0.201	1989*	0.238	1989*	0.280	1987*	Class 1
	Kebridahar	0.538	1997*	0.799	1992*	0.724	1997*	Class 1
	Moyale	0.185	1988*	0.107	1990*	0.133	1988*	Class 1
	Mega	0.749	1997*	0.443	1993*	0.770	1990*	Class 1
	Yabello	0.868	1990*	0.674	1997*	0.920	1990*	Class 1
Annual Max Rainfall Total	Deghabur	0.087	1994*	0.174	1989*	0.246	1994*	Class 1
	Kebridahar	0.395	1997*	0.376	1997*	0.476	1987*	Class 1
	Moyale	0.266	1989*	0.307	1989*	0.307	1988*	Class 1
	Mega	0.193	1990*	0.262	1990*	0.016	1988**	Class 1
	Yabello	0.391	1999*	0.385	1999*	0.312	1989*	Class 1

*Indicates non- significant change points at 0.05 significance level; **indicates significant change points at 0.05 significance level

Autocorrelation and persistence: For all the autocorrelations fallen within 95% confidence limits and standard errors of 0.1 (Figure 2) there was no apparent pattern observed (such as a sequence of positive autocorrelations followed by a sequence of negative autocorrelations). This means that there was no associative ability to infer from a current value of the time series to the next value. Such non-association was the essence of randomness; in that adjacent observations did not "correlate", and that no dependency and periodicity apparently existed in the time series from one year to the next.

3.2 Trends

Annual and seasonal rainfall trends: The Mann–Kendall trend test shows that there was no significant trend towards wetter or drier conditions in in the southern and southeastern part of the country, for more than two decades, either for the annual or seasonal rainfall totals. This might be due to large inter-annual fluctuation of rainfall in the region. However, while interpreting the results of trend analysis, it is well noted that trends are real, yet insignificant, with, for example, a decreasing trend of annual rainfall depicted in most of the stations. In regard to the main rainy season in the region ('MAM' season), a notable observation was depicted with a decreasing trend in the rainfall totals for, almost, all of the stations studied, with the exception that an insignificant increasing trend was noted at Kebridahar station. Another interesting observation from the trend analysis was the consistent increasing trends of rainfall portrayed for the small rainy season (OND) for all of the stations studied (Table 3).

Despite the fact that the trends are insignificant, the results indicated a general increase in the OND rainfall total over the southern and southeastern part of the country, with the OND rainfall at the stations of Deghabur, Kebridahar, Mega, Moyale and Yabello had increased by 41.54, 41.78, 54.42, 25.90, and 73.31 mm, respectively, for over the last two decades.

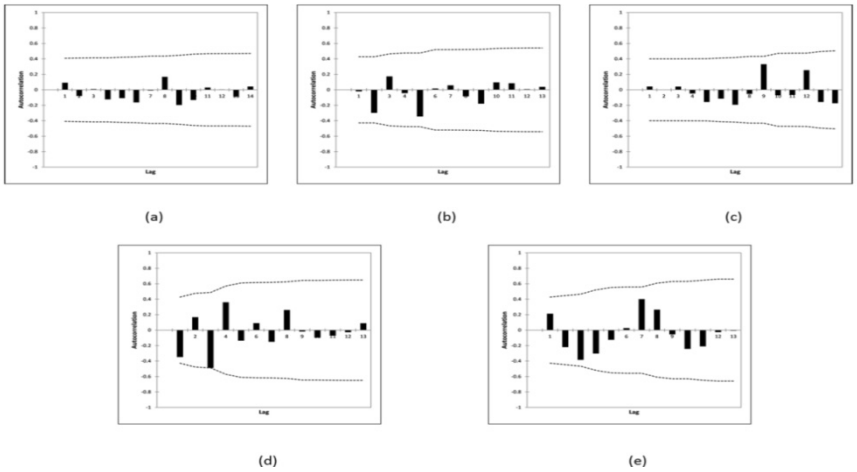

Figure 2. Autocorrelation of long-term annual rainfall totals for (a) Deghabur (b) Kebridahar (c) Mega (d) Moyale (e) Yabello

Monthly rainfall trends: Considering rainfall during months of the small rainy season, encompassing the two months prior to the outbreaks of the RVF in eastern Africa (October and November) and the first two months of the RVF epidemic periods (December and January), an increasing trends were observed at most of the stations in the region, for all the months, except for November, for which a decreasing trend were depicted for Moyale and Mega stations, and December, with decreasing trend observed at Kebridahar station (Table 4).

Table 3. Trends of annual and seasonal rainfall totals in southern and southeastern Ethiopia for the period 1987-2007

Stations	Annual		Belg (JFMAM)		Kiremt (JJAS)		Bega (OND)	
	ZMK	Slope	ZMK	Slope	ZMK	Slope	ZMK	Slope
Deghabur	-0.26	-0.79	-1.43	-3.72	1.00	1.21	1.43	1.81
Kebridahar	0.63	2.25	0.03	0.23	-0.69	-0.02	0.97	1.74
Moyale	-1.41	-5.72	-1.61	-6.43	0.07	0.02	0.27	1.08
Mega	-1.18	-4.62	-1.42	-5.48	-0.57	-0.60	0.45	2.27
Yabello	-0.36	-2.11	-0.82	-3.80	-1.30	-1.80	1.60	3.49

*ZMK is Mann–Kendall trend test; slope (Sen's slope) is the change (mm)/year; bold values indicate statistical significance at 95% confidence level according to the Mann–Kendall test

Table 4. Trends of monthly rainfall totals and mean PCI values for selected five stations for the period 1987-2007

Stations	October		November		December		January		PCI
	ZMK	Slope	ZMK	Slope	ZMK	Slope	ZMK	Slope	
Deghabur	0.96	1.37	0.73	0.0	0.39	0.0	0.08	0.0	30
Kebridahar	0.78	1.61	0.49	0.53	-0.58	0.0	1.04	0.0	34
Moyale	0.29	0.61	-0.55	-0.99	0.62	0.28	1.40	0.0	1.2
Mega	0.69	1.62	-1.06	-1.45	1.00	1.45	-0.51	-0.07	1
Yabello	1.09	0.83	1.60	1.36	0.0	0.0	-0.24	-0.14	20

*ZMK is Mann–Kendall trend test; slope (Sen's slope) is the change (mm)/year; bold values indicate statistical significance at 95% confidence level according to the Mann–Kendall test

Despite the very little variability of the stations with regard to the magnitude and direction of trends, increasing trends, yet insignificant, of rainfall were observed for all stations and for all the months preceding and concurrent with the reported RVF outbreak months for East Africa.

In general, there was a positive trend in rainfall of the small rainy season over the southern and southeastern part of the country. However, neither of the trends was statistically significant. This result agrees with previous findings regarding the trends and spatial distribution of annual and seasonal rainfall in Ethiopia (NMSA, 1996; Cheung, Senay, and Singh, 2008). Cheung et al., (2008) argued that there are no significant changes or trends in annual rainfall at the national level in Ethiopia. It has also been confirmed that, between 1951 and 2006, no statistically significant trend in mean annual rainfall was observed in any season in the country (NMSA, 1996). However, several previous time-series studies of rainfall patterns in Ethiopia carried out at various spatial (e.g., national, regional, local) and temporal (e.g. annual, seasonal, monthly) scales have depicted many contradictions regarding their findings on annual and seasonal rainfall trends and climate extremes in the country. Both Seleshi & Zanke, (2004) and Verdin, Funk, Senay, and Choularton, (2005) have reported a decline in trend of annual rainfall totals in southern and southeastern Ethiopia. Seleshi & Zanke, (2004) have, further, indicated a decline in Kiremt rainfall in those areas. Despite such contrasting reports, on larger spatially aggregated scales, the result of rainfall trend analyses in the current study were found to be quite consistent and in agreement with most of previous similar studies that have concluded that there is no significant trend in annual and seasonal rainfall totals over the country.

3.3 Monthly and Daily Cumulative Rainfall Totals

Historically, for East Africa, the first reported case of Rift Valley fever disease outbreaks paralleled with or followed the short-rainy season (October–December). Such patterns were attributed to the influence of ENSO and other large scale teleconnections that is found to consistently result in anomalously above normal rainfall and flooding in the region, creating conducive climatic conditions for the vectors that carry or transmit the RVFV. In this study, for all the stations studied, similar pattern of consistent and above-normal rainfall is depicted in the monthly and daily rainfalls accumulated over the three-months period (OND) of the recent RVF outbreak periods in East Africa (1997/98 and 2006/07) as well, which indicates ideal ecological conditions for Rift Valley fever mosquito vectors emergence and survival. The daily and monthly rainfall totals accumulated over the three months (September - November), preceding the reported outbreak period of the RVF activity for east Africa (outbreaks in December 1997/98 and 2006/07), and including the actual outbreak month (December, 1997/98 and 2006/07) were shown in Figure 3, for Deghabur, Mega, Yabello, and Moyale stations.

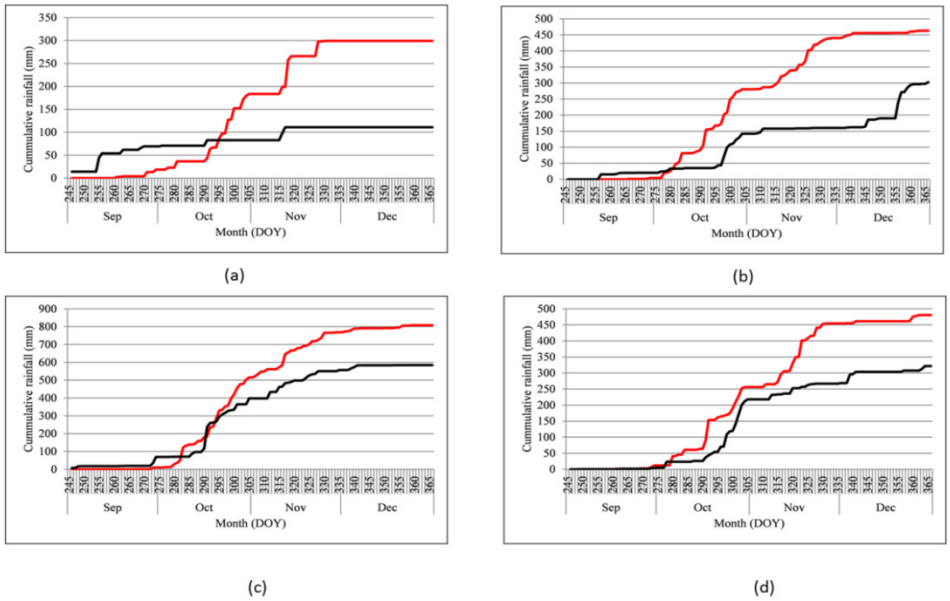

Figure 3. Daily cumulative SOND rainfall totals (mm) for 1997/98 (dark black line) and 2006/07 (deep red line); (a) Deghabur (b) Mega station (c) Moyale station (d) Yabello

Figure 3 further indicated that rainfall during both the 1997/98 and 2006/07 short rainy season (SOND) was poorly distributed in the study areas, with high concentration of the rains close to the actual reported RVF outbreak month (December) for the HoA region. The cumulative rainfall for September and early October were very much low (less than 150 mm), depicting the previously drier conditions prevailed in the region. The increase above 200 mm cumulative rainfall had only occurred closer to the month of December.

The ten-day cumulative rainfall anomaly for each of the months from October- to- December 1996/97 and 2006/07 (Figure 4) also depicted that the OND seasonal rainfall was anomalously high, and that most of the individual months had received anomalously above normal rainfall. Moreover, the results for the Precipitation Concentration Index (PCI) analyses for Deghabur, Kebridhar, and Yabello depicted a high to very high concentration of the monthly rainfall distribution (PCI > 20%), in agreement with the findings of the cumulative rainfall analyses. However the PCI values for the remaining two stations, Mega and Yabello, indicated uniform monthly distribution of rainfall in the areas. The calculated mean PCI values, for all stations, are portrayed in Table 4.

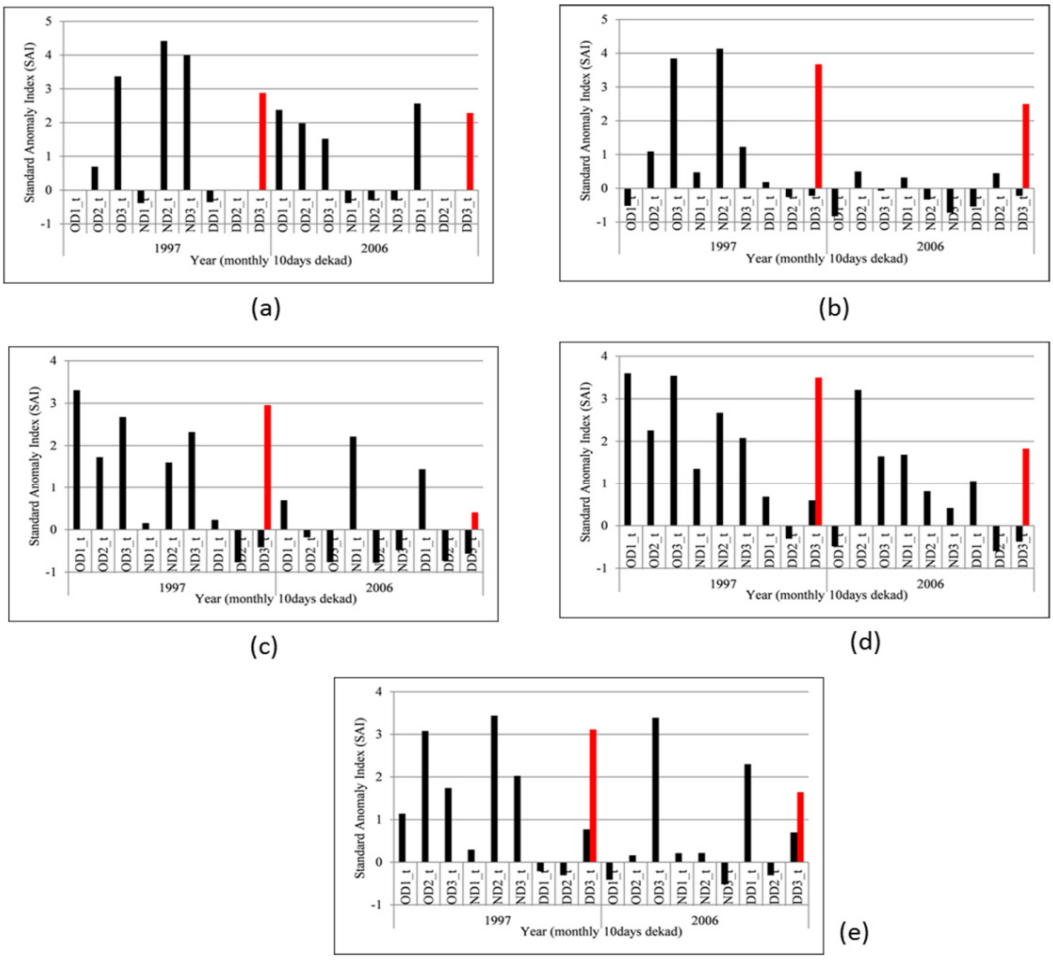

Figure 4. Cumulative ten-day rainfall anomaly for the 1996/97 and 2006/07 OND short rainy season a) Deghabur b) Kebridahar c) Mega d) Moyale e) Yabello stations, respectively. Black bars indicate 10days cumulative rainfall anomaly for each ten-day period of the Oct. to Dec. months and deep red bars indicate the cumulative seasonal (OND) rainfall total anomalies for the years 1996/97 and 2006/07, respectively, in order of appearances within the figures

Thus, the persisted tendency for wetter-than-normal conditions during the 1997/98 and 2006/07 small rainy seasons (ONDJ) were an ideal condition for potential flooding in the region. Furthermore, the probability of persistence of RVF virus in the study areas, owing to the perceived high risk for the RVFV infection to enter into

the greater mosquito vector population of these areas was, thus, much higher owing to the conducive climatic conditions depicted in the findings of this study. Hence, had the infection entered in the grater mosquito population of the study areas, a significant risk of transmission of the diseases to livestock raised along communal grazing lands and to those which are kept in areas close to the over flooded areas would have been evident.

3.4 Seasonal Teleconnection Patterns and Strengths

The seasonal rainfall variability for the selected study areas in the S-and SE- Ethiopia, and the associated modes of SSTs (Niño3.4 and IOD), are shown in Figure 5, depicting a similar pattern of variability in the seasonal (SON) average regional rainfall as that of the equatorial east Pacific SST anomaly and the Indian Ocean Dipole (IOD) mode index (MDI). The strengths of linear relationship between the regional average rainfall total and the Niño-3.4 SST anomaly index and the Indian Ocean MDI, for all individual months and for the average of the SON period, are also shown in Table 5 and 6, respectively.

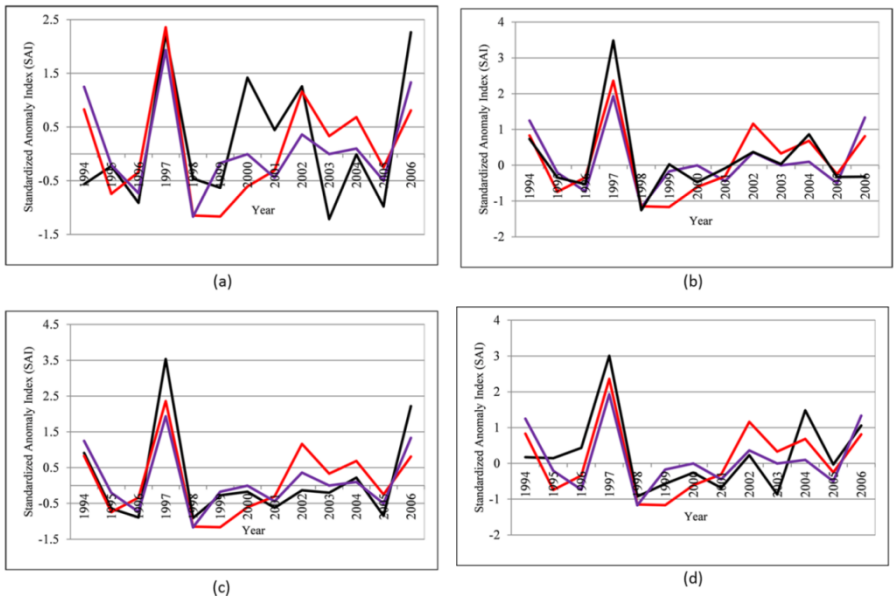

Figure 5. Time series plots of standardized regional rainfall total and SSTs anomalies for (a) Deghabur (b) Mega (c) Moyale, and (d) Yabello. The figure depicts time series plots of the regional rainfall total anomaly (dark black line), Niño3.4 SST anomaly (deep red lines), and Indian Ocean Dipole Mode Index (deep purple lines), all averaged for the SON season and for the period 1994–2006; The SST indices are computed for the same period as the rainfall indices

Table 5. Correlations between regional average SON rainfall total anomaly and the Niño-3.4 SST index for individual months from January to December, and for average SON SST

Jan	Feb	Mar	Apr	May	Jun	Jul	Aug	Sep	Oct	Nov	Dec	SON
-0.35	-0.33	-0.30	-0.13	0.08	0.24	0.37	**0.52***	**0.57***	**0.50***	**0.51***	**0.49***	**0.53***

*Values in bold are significant at significant level of 0.05

Table 6. Correlations between regional average SON rainfall total anomaly and the Indian Ocean Dipole mode index (DMI) for individual months from January to December, and for average SON DMI

Jan	Feb	Mar	Apr	May	Jun	Jul	Aug	Sep	Oct	Nov	Dec	SON
-0.28	-0.08	0.23	0.01	-0.12	-0.04	**0.51***	**0.48***	**0.60***	**0.72***	**0.84***	**0.50***	**0.77***

*Values in bold are significant at significant level of 0.05

The physical mechanisms through which the large scale teleconnection signals from the Pacific Ocean, or from

any other location, arrive in Ethiopia and subsequently influence the spatial and temporal pattern of rainfall in the country is outside the scope of this paper. As depicted in Table 5 and 6, the association of the regional average SON rainfall totals with both ENSO and IOD modes, in early months (January–July), is weak, and increases progressively as the time of the ENSO and IOD states approaches the beginning of the small rainy season (OND) in the southern and southeastern Ethiopia. The correlations are moderate, 0.57 and 0.52 for August and September ENSO modes and 0.51, 0.48, and 0.60 for the July, August, and September Indian oceans' DMI, respectively, suggestive of some predictability of the average regional rainfall patterns two to three months in advance of the month for the first reported case of RVF in East Africa (December), based, solely, on the ENSO and IOD states of the respective individual months. In a similar manner the moderate positive correlations (> 0.5) between the regional average SON rainfall totals and the Nina3.4 SST and the Indian Oceans mode indices, happening simultaneously for the respective months (SON), also indicated the possibility for predicting the pattern of the average regional rainfall for SON, corresponding to the period preceding the reported RVF epidemic month (December) in East Africa, given that the large scale ENSO and MDI indices for the respective SON months are predicted and made available two to three months in advance. The correlation results for individual stations also indicated a persistent and statistically significant positive correlation (significant level= 0.05) among the average SON rainfall total anomalies for each of the individual stations and the average of the ENSO (Table 7) and IOD (Table 8) modes occurring nearly simultaneously (in SON). The stronger correlation for the regional average SON rainfall totals than the correlations for any of the individual stations could be due to the filtering effects of spatial aggregation with respect to the random variability present in single location rainfall.

The stronger patterns of relations between the small rainy seasons' rainfall in the southern and southeastern Ethiopia and global SST indices (both ENSO and IOD) depicted in this study were similar with the findings of Degefu et al., (2017), except for the length of the season considered. Degefu et al., (2017) indicated that rainfall variations during October and November depicted similar statistically significant patterns of positive correlation between the Niño3.4 and IOD indices and gridded rainfall over southern Ethiopia. It is also in agreement with the findings of similar studies reported for equatorial east Africa, mainly for Kenya and Tanzania (Black et al., 2003; Saji et al., 1999).

Table 7. Correlations between average SON rainfall total anomalies and Niño-3.4 SST index for the study areas, for the period 1987-2007

Stations	Jan	Feb	Mar	Apr	May	Jun	July	Aug	Sept	Oct	Nov	Dec	SON
Deghabur	-0.10	0.18	0.25	0.08	-0.07	-0.13	0.17	0.18	**0.56***	**0.51***	**0.63***	0.24	**0.651***
Mega	-0.44	0.06	0.24	-0.07	-0.27	-0.15	**0.55***	**0.41***	**0.41***	**0.58***	**0.65***	**0.44***	**0.766***
Moyale	-0.22	-0.25	0.14	0.07	0.02	0.18	**0.57***	**0.59***	**0.67***	**0.77***	**0.89***	**0.49***	**0.829***
Yabello	-0.25	-0.05	0.18	-0.08	-0.30	-0.23	0.28	0.25	**0.46***	**0.53***	**0.66***	**0.47***	**0.723***

*Values in bold are significant at significant level of 0.05

Table 8. Correlations between average SON rainfall total anomalies and the Indian Ocean Dipole Mode Index (DMI) for the study areas, for the period 1987-2007

Stations	Jan	Feb	Mar	Apr	May	Jun	July	Aug	Sept	Oct	Nov	Dec	SON
Deghabur	-0.49	-0.44	-0.43	-0.25	-0.05	0.14	0.24	**0.39***	**0.45***	**0.38***	**0.38***	**0.35***	**0.563***
Mega	-0.27	-0.26	-0.23	-0.14	0.01	0.15	0.30	**0.39***	**0.43***	**0.39***	**0.40***	**0.40***	**0.828***
Moyale	-0.19	-0.18	-0.15	0.01	0.18	0.30	0.38	**0.53***	**0.60***	**0.54***	**0.55***	**0.54***	**0.565***
Yabello	-0.35	-0.34	-0.37	-0.27	-0.07	0.11	0.26	**0.40***	**0.44***	**0.38***	**0.39***	**0.39***	**0.787***

*Values in bold are significant at significant level of 0.05

3.5 Predictability of the Regional Average SON Rainfall Total Anomaly

Predictive models developed: Different models are fitted for the regional-average SON rainfall total anomaly. For example, the first model regresses the regional average SON rainfall total anomaly over both the Niño-3.4

SSTs anomaly index and the Indian Ocean MDI, averaged for the same period (SON), while the fifth model diagnose the predictability of the regional SON rainfall anomaly by fitting a MLR model with Niño3.4 SST anomalies and the Indian Ocean MDI, with different monthly lags, expressed as combinations of atmospheric and oceanic predictors whose values are available upon completion of the September month to predict the regional average SON rainfall total anomaly. In general, the predictability of the regional average SON rainfall total anomaly is investigated by using either of the Niño3.4 SST and MDI, independently, or in combination of both as potential predictors.

Historical records for the Niño-3.4 SST and Indian Ocean MDI indices over 1987-2006, which showed moderate to stronger correlation ($r \geq 0.4$) with the regional average SON rainfall total anomaly (Table 5 and 6), were included in the respective models, as predictors. The retroactive calculation procedure, employed in this study, resulted in 10 years (1997/98–2006/07) of independent forecast data. The MLR fitting procedure also provided stable estimates for the coefficients of the resulting model equations, for both the cross validation and the retroactive hindicasts.

The performances of the models over the 20 years period are presented, here, in terms of the Kendall rank correlation coefficients, which is commonly referred to as Kendall's tau (Thiaw, Barnston, and Kumar, 1999). Kendall's tau is a measure of rank correlation, and is considered a robust (to deviation from linearity) and resistant (to outliers), alternative to Pearson's or "ordinary" correlation. Kendall's correlation measures the discrimination skills of the respective models (do the forecasts increase and decrease as the observations increase and decrease?). The model equations are presented in Table 9, along with the respective Kendall's tau correlation coefficients. As depicted in the table, the discrimination skills of the models improved from the first (Model#1) to the last model (Model#5), in response to addition or removal of the large scale predictor variables.

3.6 Forecast Verifications

Retroactive forecast skills: The findings of the forecast verification process, over the 10 years retroactive period, from 1997/98 to 2006/07, using the 'verification' option in the IRI's CPT, are outlined in the following sections.

Table 9. Model equations and the corresponding performance scores for each of the models

Models	Predictors employed	Model Equation	Kendall's tau
Model#1	Sept_DMI & Avg_SON_DMI	Regional_SON_Rainfall_Anomaly = 0.04671 – 0.8813Sep-DMI + 1.7135AvgSONDMI	0.347
Model#2	Avg_SON_DMI	Regional_SON_Rainfall_Anomaly = -0.00552 + 1.00256AvgSON_DMI	0.347
Model#3	Sept_DMI	Regional_SON_Rainfall_Anomaly = -0.0377 + 0.601Sep-DMI	0.284
Model#4	Avg_SON_DMI & Avg_SON_ Niño3.4 SST	Regional_SON_Rainfall_Anomaly = -0.00049 + 1.05414Avg_SON_DMI -0.05640Avg_SON_ Niño3.4 SST	0.189
Mode#5	Sept_DMI & Sept_ Niño3.4 SST	Regional_SON_Rainfall_Anomaly = -0.0564 + 0.4067Sept_DMI + 0.360446207985Sept_ Niño3.4 SST	0.074

[+] The coefficients and the overall "goodness of fit" of the models are statistically significant at the 95% level

Relative operating characteristics: All the models showed maximum skills (ROC scores > 0.7) in successfully distinguishing the above normal and below normal rainfall categories as opposed to the normal category, for the SON period, as shown in the Relative Operating Characteristic (ROC) diagrams for the categorical forecast measures (Figure 6). Figure 6 also presented the ROC scores (in the right bottom panels in the diagrams) obtained by retroactively predicting the regional average SON rainfall total anomaly for the S- and SE- Ethiopia over the 10 years retroactive period from 1997/98 to 2006/07. The ROC scores for the normal category are less or around 0.5 for all models, except for the second model, which employed the average SON DMI as the only predictor of the regional average SON rainfall total anomaly.

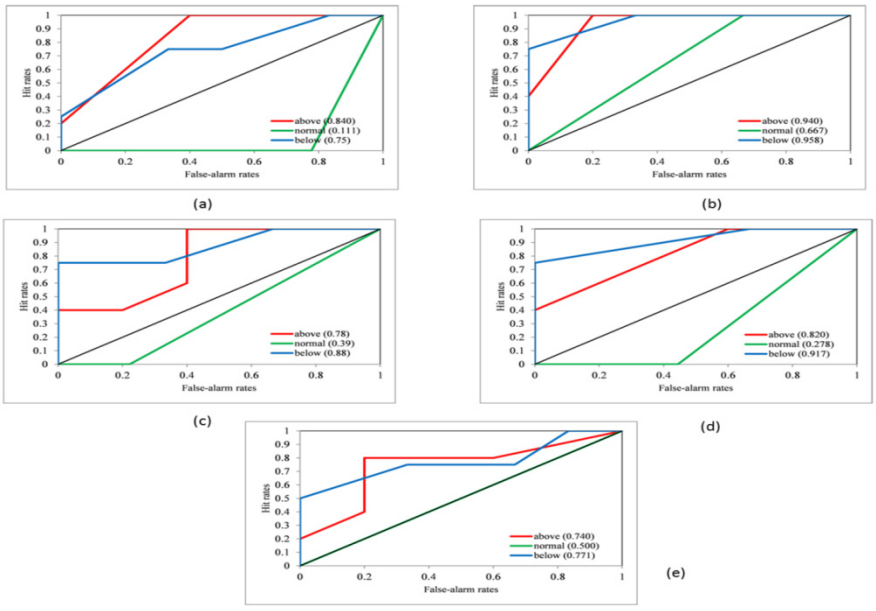

Figure 6. ROC diagrams and scores obtained by retroactively predicting the regional average SON rainfall total anomaly for (a) Model#1; (b) Model#2; (c) Model#3; (d) Model#4; and (e) Model#5

Reliability: Among the five models constructed to forecast the regional average SON rainfall total anomaly over the S- and SE- Ethiopia, the highest ROC scores were obtained for Model#1. This section, thus, elaborates on verifying how reliably this specific model could discern the pattern of the SON rainfall anomaly in the region. Figure7 shows the reliability diagrams for forecasts of the regional average SON rainfall total anomalies produced by Model#1.

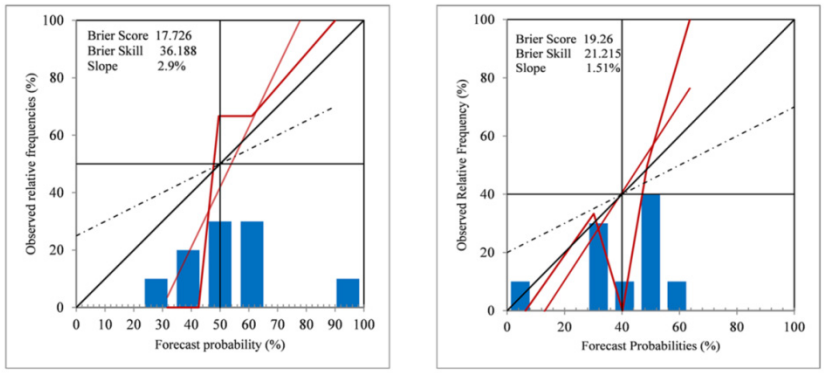

Figure 7. Reliability diagrams and frequency histograms for the regional average SON rainfall total anomaly forecasts; (a) for above-normal (>67th percentile) and (b) for below-normal (<33rd percentile) categories. The predictors are the Indian Ocean MDI index for the month of September and for the seasonal (SON) average. The thick Red curves represent the observed relative frequencies for the above- and below- normal categories and the thin red line is the weighted least squares regression line for respective reliability curves

The figure presented the reliability curves for the above and below normal categories along with weighted least squares regression lines for the two categories. The weighting is relative to how frequently forecasts are issued at a given confidence level (Landman, DeWitt, Lee, Beraki, and Lötter, 2012). Regression lines along the diagonal of the reliability diagram imply perfect reliability, while regression lines above (below) the diagonal imply that observed wet (dry) SON rainfall season tend to occur more (less) frequently than predicted. Furthermore,

histograms plotted within the reliability diagrams outlined the frequencies with which the two categorical forecasts occurred and revealed how strongly and frequently the issued forecast probabilities departed from the climatological probabilities.

Deterministic skills: The previous section presented verification statistics for the probabilistic forecasts using the models developed. Similar to the discussion for reliability, the deterministic forecast performance for the model which showed the highest ROC score (i.e., Model#1) is presented here.

Figure 8 shows the plot of observed regional average SON rainfall anomaly index and the retroactive and cross-validated predictions for the regional average rainfall anomaly, for the same period, obtained by regressing the observed regional average SON rainfall anomaly with the Indian Ocean Dipole MDI values over the 10 years retroactive period, from 1997/98 to 2006/07. The model performed well in portraying most of the positive anomalous rainfall pattern (wettest condition) for the SON period corresponding to the three El Niño years (1997/98, 2002/03, and 2006/07), and the driest condition for the 1999/00 La Niña event, with the signs of the predicted rainfall anomaly during these years captured by the forecasts, emphasizing the already demonstrated strong positive correlation between the average regional SON rainfall total anomaly and the teleconnection anomalies. These findings are also in agreement with the results of the correlation analyses presented, which outlined that the rainfall anomaly in the region is highly correlated with a positive Indian Ocean Dipole mode (Table 6). The results from both hindcasting techniques are depicted in Figure 8.

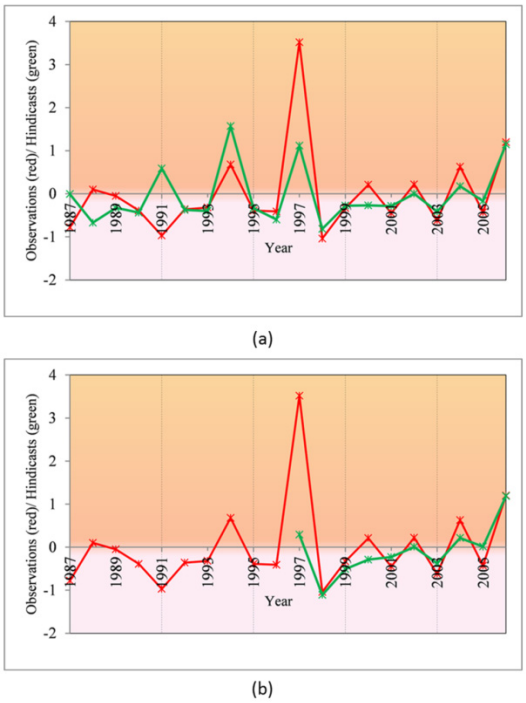

Figure 8. Observed and model predicted standardized regional average SON rainfall total anomalies; (a) Retroactive hindicast technique and (b) Cross-validated hindicast technique

The short-term (SON) rainfall anomaly prediction captured the signs of the rainfall anomaly for 8 out of the 10 years of the retroactive prediction period, corresponding to a "hit rate" of 80%. However, despite the skills of the model in predicting the sign of the SON rainfall anomaly correctly during both the El Niño and La Niña events, the model underestimated the observed severity of the anomaly, especially for the 1997/98 SON period. Moreover, the amount of the overall variance of the regional average SON rainfall total anomaly pattern explained by the model depicted a moderate skill; with R^2 values of 0.423 (R = 0.651) and 0.39 (R = 0.621), for the retroactive design and the cross-validation approach, respectively.

One interesting observation is noted when fitting the relationship between SSTs and regional rainfall anomaly concurrently in time. When the average SON MDI is employed as a predictor, independently, the resulting MLR model (Model #2) explained 35.3% (r=0.59) and 26.4% (r=0.51) of the overall variance of the regional average SON rainfall anomaly for the cross-validated and retroactive approaches, respectively—far more than the other

candidate predictor taken alone, Niño-3.4 SSTs. Hence a simple regression, with the average SON MDI as the only predictor could also be sufficient (Figure 9).

Notwithstanding large amount of the overall variances of the average SON rainfall pattern in the region remained unexplained, overall, the fitted models could be taken for granted, specifically in view of the primary objective of this particular study, which is discriminating the anomalous pattern of rainfall during the three months period preceding the reported outbreak of RVF epidemics for East Africa, for which the model depicted higher skills.

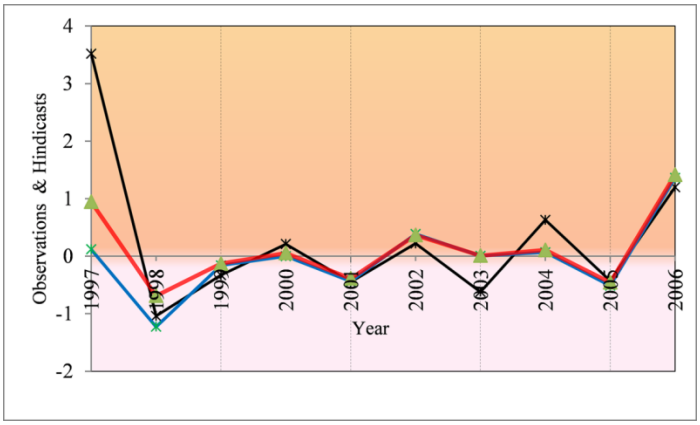

Figure 9. Observed and model predicted standardized regional average SON rainfall anomalies. Dark black line (observed); deep red line (cross-validated forecast); deep blue line (retroactive forecast). The predictor is average SON MDI that is fitted to the regional average SON rainfall anomaly by simple linear regression

4. Conclusions

This paper documents a potential operational prediction of 'rainfall hotspot' areas at finer spatial scale, which can serve as early indicators of high risks for outbreaks of RVF epidemics. Diagnosis of the pattern of the short rainy season (SOND) over the southern and southeastern Ethiopia confirmed stronger correlations among the regional rainfall total anomaly, the convergence of ENSO conditions in the eastern Pacific, and the concurrent warming of SSTs in the western equatorial Indian Ocean region, similar to the rest of RVF endemic countries over the equatorial east Africa region. Examination of trends in annual and seasonal rainfall shows an absence of any systematic patterns of changes in the long term rainfall trend across the region. Thus, yet insignificant, the observed seasonal rainfall trends over the study areas are, thus, attributed to be the result of the large scale teleconnections and the associated atmospheric and oceanic driving forces. Analysis of the regional rainfall anomaly pattern, concurrent with the late 1997/ 2006- and early 1998/ 2007 outbreak periods in the HoA region, indicated that a similar RVF conducive climatic situation had been persisted over the southern and southeastern lowland parts of the country. Accordingly, had the RVFV been entered into the greater mosquito vector populations in this part of the country, it would have taken no longer before the establishment, spread, and the occurrence of RVF disease at an epidemic proportions.

The moderate to high correlations between the regional average rainfall anomaly and the large scale teleconnection variables suggested some predictability skills two to three months preceding outbreaks in neighboring RVF endemic countries. The study demonstrates the capacity of a simple localized climate prediction models in skillfully mapping climatically suitable RVF (rainfall) hotspot areas, based on emerging developments of ENSO and other regional climate indicators. Thus localized climate prediction models are invaluable as early indicators for areas having high risk for RVF potential outbreaks and could be taken as an important and integral part of the disease surveillance. Such models deemed critical in mounting effective localized response against the disease, in accordance with available local resources, and help reduce the impact of outbreaks of vector-borne diseases such as RVF.

Acknowledgments

The author appreciates the helpful comments of the anonymous reviewers. The author is also grateful to the Ethiopian National Meteorological Service Agency for kindly providing daily rainfall data for all the stations in this study, and Mr. Merkebu Kassaw, a GIS expert at Haramaya University, for his invaluable help in plotting the study areas.

References

Abdo-Salem, S., Waret-Szkuta, A., Roger, F., Olive, M. M., Saeed, K., & Chevalier, V. (2010). Risk assessment of the introduction of Rift Valley fever from the Horn of Africa to Yemen via legal trade of small ruminants. *Trop Anim Health Prod, 43*, 471–480. https://doi.org/10.1007/s11250-010-9719-7

Amit, G. D., & Mohammed, Z. (2013). Three-way approach to test data homogeneity: An Analysis of temperature and precipitation series over southwestern Islamic Republic of Iran. *J. Ind. Geophys. Union*, *17*(3), 233-242.

Anyamba, A., Chretienb, J-P., Smalla, J., Tuckera, C. J., Formentyc, P. B., Richardsond, J. H., … Linthicume, K. .J. (2009). Prediction of a Rift Valley fever outbreak. *PNAS*, *106*(3), 955–959. https://doi.org/10.1073/pnas.0806490106

Anyamba, A., Linthicum, K. J., Small, J., Britch, S. C., Pak, E., Rocque, S., … Swanepoel, R. (2010). Prediction, assessment of the Rift Valley fever activity in East and Southern Africa 2006 -2008 and possible vector control strategies. *Am. J. Trop. Med. Hyg., 83*(Suppl 2), 43–51. https://doi.org/10.4269/ajtmh.2010.09-0289

Balkhy, H. H., & Memish, Z. A. (2003). Rift Valley fever: an uninvited zoonosis in the Arabian Peninsula. *Int J Antimicrob Agents*, *21*, 153–157. https://doi.org/10.1016/S0924-8579(02)00295-9

Barnett, V., & Lewis, T. (1994). *Outliers in Statistical Data*. John Wiley and Sons, New York.

Barnston, A. G., van den Dool, H. M., Zebiak, S. E., Barnett, T. P., Ming, Ji., Rodenhuis, D. R., … Livezey, R. E.. (1994). Long-lead seasonal forecasts—Where do we stand? *Bull. Amer. Meteor. Soc., 75*, 2097–2114. https://doi.org/10.1175/1520-0477(1994)075<2097:LLSFDW>2.0.CO;2

Bekele, F. (1997). Ethiopian use of ENSO information in its seasonal forecasts. *Internet J. Afr. Studies*, (2). Retrieved from http://www.ccb.ucar.edu/ijas/ijasno2/bekele.html

Black, E., Slingo, J., & Sperber, K. R. (2003). An observational study of the relationship between excessively strong short rains in coastal east Africa and Indian Ocean SST. *Mon. Wea. Rev.*, *131*, 74–94. https://doi.org/10.1175/1520-0493(2003)131<0074:AOSOTR>2.0.CO;2

Bouna, D. (2015). Rift Valley Fever in the Horn of Africa, East of Africa and the Middle East: A historical overview (animal health), *Rift Valley Fever: New options for trade, prevention and control Conference*, Djibouti, 21 – 23 April 2015.

Box, G. P., & Jenkins, G. M. (1976). *Time-series analysis, forecasting and control* (Rev. ed.). Oakland, California: Holden-Day.

Brockwell, P. J., & Davis, R. A. (1996). *Time Series: Theory and Methods* (2nd ed.). Springer-Verlag, New York, pp. 577.

Buishand, T. A. (1982). Some methods for testing the homogeneity of rainfall records. *J. Hydrol.*, *58*, 11-27. https://doi.org/10.1016/0022-1694(82)90066-X

Cheung, W. H., Senay, G., & Singh, A. (2008). Trends and spatial distribution of annual and seasonal rainfall in Ethiopia. *Int. J. Climatol.*, *28*, 1723–1734. https://doi.org/10.1002/joc.1623

Conrad, V., & Pollak, C. (1950). *Methods in Climatology*. Harvard University Press, Cambridge. https://doi.org/10.4159/harvard.9780674187856

Costa, A. C., & Soares, A. (2009). Trends in extreme precipitation indices derived from a daily rainfall database for the south of Portugal. *Int. J. Climatol.*, *29*, 1956–1975. https://doi.org/10.1002/joc.1834

Daubney, R., & Hudson, J. R. (1931). Enzootic hepatitis or Rift Valley fever: An undescribed virus disease of sheep, cattle and man from East Africa. *J Pathol Bacteriol*, *34*, 545–579. https://doi.org/10.1002/path.1700340418

Davies, F. G. (2008). Epidemiology and ecology of RVF and key drivers for endemicity and epidemics, *Joint FAO-WHO experts consultation on Rift Valley fever outbreaks forecasting models*, Rome, Italy, 29 September–1 October 2008, WHO/HSE/GAR/BDP/2009.2

Davies, F. G. (2010). The historical and recent impact of Rift Valley fever in Africa. *Am J Trop Med Hyg*, *83*, 73-74. https://doi.org/10.4269/ajtmh.2010.83s2a02

Davies, F. G., Linthicum, K. J., & James, A. D. (1985). Rainfall and epizootic Rift Valley Fever. *Bull World Health Organ.*, *63*, 941–943.

Degefu, M. A., Rowell, D. P., & Bewket, W. (2017). Teleconnections between Ethiopian rainfall variability and

global SSTs: observations and methods for model evaluation. *Meteorol Atmos Phys*, *129*, 173–186. https://doi.org/10.1007/s00703-016-0466-9

De-Luı´s, M., Gonza´lez-Hidalgo, J. C., Raventos, J., Sanchez, J. R., & Cortina, J. (1999). Spatial analysis of rainfall trends in the region of Valencia (East Spain). *Int. J. Climatol.*, *20*, 1451–1469. https://doi.org/10.1002/1097-0088(200010)20:12<1451::AID-JOC547>3.0.CO;2-0

Gelan, A., Engida, E., Caria, A. S., & Karugia, J. (2012). The role of livestock in the Ethiopian economy: Policy analysis using a dynamic computable general equilibrium model for Ethiopia. The International Association of Agricultural Economists (IAAEs) Triennial Conference, FOZ DO IGUAÇU, BRAZIL, 18-24 August 2012.

Gikungu, D., Wakhungu, J., Siamba, D., Neyole, E., Muita, R., & Bett, B. (2016). Dynamic risk model for Rift Valley fever outbreaks in Keneya based on climate and disease outbreak data. *Geospat Health.*, *11*(2), 377. https://doi.org/10.4081/gh.2016.377

Gissila, T., Black, E., Grimes, D. I. F., & Slingo, J. M. (2004). Seasonal forecasting of the Ethiopian summer rains. *Int. J. Climatol.*, *24*, 1345–1358. https://doi.org/10.1002/joc.1078

Göktürk, O. M., Bozkurt, D., Sen, Ö. L., & Karaca, M. (2008). Quality control and homogeneity of Turkish precipitation data. *Hydrol. Process*, *22*, 3210–3218. https://doi.org/10.1002/hyp.6915

Gonzalez-Hidalgo, J. C., Lopez-Bustins, J., Stepanek, P., Martin-Vide, J., & De-Luis, M. (2009). Monthly precipitation trends on the Mediterranean fringe of the Iberian Peninsula during the second-half of the twentieth century (1951–2000). *Int. J. Climatol.*, *29*, 1415–1429. https://doi.org/10.1002/joc.1780

Gonzalez-Rouco, J. F., Luis, J. J., Quesada, V., & Valero, F. (2001). Quality control and homogeneity of precipitation data in the southwest of Europe. *J. Climate.*, *14*, 964-978. https://doi.org/10.1175/1520-0442(2001)014<0964:QCAHOP>2.0.CO;2

Hadegu, G., Tesfaye, K., Mamo, G., & Kassa, B. (2013). Trend and variability of rainfall in Tigray, Northern Ethiopia: Analysis of meteorological data and farmers' perception. *Acad. J. Agric. Res.*, *1*(6), 088-100.

Hamill, T. M., & Colucci, S. J. (1997). Verification of Eta-RSM Short-Range Ensemble Forecasts. *Mon. Weather Rev.*, *125*, 1312-1327. https://doi.org/10.1175/1520-0493(1997)125<1312:VOERSR>2.0.CO;2

Hastenrath, S. (1995). Recent advances in tropical climate prediction. *J. Climate*, *8*, 1519–1532. https://doi.org/10.1175/1520-0442(1995)008<1519:RAITCP>2.0.CO;2

Hotez, P. J., & Kamath, A. (2009). Neglected tropical diseases in sub-Saharan Africa: Review of their prevalence, distribution, and disease burden. *PLoS Negl Trop Dis*, *3*: *e412*. https://doi.org/10.1371/journal.pntd.0000412

IFRCRCS. (2010). *Final Report: Sudan Floods.* Retrieved October 19, 2017, from https://reliefweb.int

Kendall, M. G. (1975). *Rank correlation methods*. London, Oxford University.

Korecha, D., & Barnston, A. G. (2007). Predictability of June-September rainfall in Ethiopia. *Mon. Wea. Rev.*, *135*(2), 628–650. https://doi.org/10.1175/MWR3304.1

LaBeaud, A. D. (2008). Why Arboviruses can be neglected tropical diseases? *PLoS Negl Trop Dis*, *2*(6), *e247*. https://doi.org/10.1371/journal.pntd.0000247

LaBeaud, A. D., Ochiai, Y., Peters, C. J., Muchiri, E. M., & King, C. H. (2007). Spectrum of Rift Valley fever virus transmission in Kenya: insights from three distinct regions. *Am J Trop Med Hyg.*, *76*(5), 795–800. https://doi.org/10.4269/ajtmh.2007.76.795

Landman, W. A., Beraki, A., DeWitt, D., & Lötter, D. (2014). SST prediction methodologies and verification considerations for dynamical mid-summer rainfall forecasts for South Africa.

Landman, W. A., DeWitt, D., Lee, D.-E., Beraki, A., & Lötter, D. (2012). Seasonal rainfall prediction skill over South Africa: One- versus two-tiered forecasting systems. *Weather Forecast*, *27*(2), 489-501. https://doi.org/10.1175/WAF-D-11-00078.1

Linthicum, K. J., Anyamba, A., Tucker, C. J., Kelley, P. W., Myers, M. F., & Peters, C. J. (1999). Climate and satellite indicators to forecast Rift Valley fever epidemics in Kenya. *Science*, *285*, 397–400. https://doi.org/10.1126/science.285.5426.397

Mann, H. B. (1945). Nonparametric tests against trend. *Econometrica*, *13*, 245-259. https://doi.org/10.2307/1907187

Mason, S. J., & Graham, N. E. (2002). Areas beneath the relative operating characteristics (ROC) and levels

(ROL) curves: Statistical significance and interpretation. *Q. J. R. Meteorol. Soc.*, *128*, 2145–2166. https://doi.org/10.1256/003590002320603584

Michaelsen, J. (1987). Cross-validation in statistical climate forecast models. *J. Climate Appl. Meteor.*, *26*, 1589–1600. https://doi.org/10.1175/1520-0450(1987)026<1589:CVISCF>2.0.CO;2

Ministry of Agriculture and Rural Development (MoARD), Department of Animal Health Services. (2008, June). *Rift Valley Fever Contingency and Preparedness Plan for Ethiopia*.

National Meteorological Services Agency (NMSA). (1996). Climate and agro-climatic resources of Ethiopia. *Meteor. Res. Report Series*, *1*(1), 137.

Ngongondo, C., Yu-Xu, C., Gottschalk, L., & Alemaw, B. (2011). Evaluation of spatial and temporal characteristics of rainfall in Malawi: a case of data scarce region. *Theor. Appl. Climatol.* https://doi.org/10.1007/s00704-011-0413-0

Ogallo, L. J. (1988). Relationships between seasonal rainfall in East Africa and the Southern Oscillation. *Int. J. Climatol.*, *8*, 31–43. https://doi.org/10.1002/joc.3370080104

Oliver, J. E. (1980). Monthly precipitation distribution: a comparative index. *Prof. Geogr.*, *32*, 300–309. https://doi.org/10.1111/j.0033-0124.1980.00300.x

Partal, T., & Kahya, E. (2006). Trend analysis in Turkish precipitation data. *Hydrol. Processes*, *20*, 2011–2026. https://doi.org/10.1002/hyp.5993

Patz, J. A., Epstein, P. R., Burke, T. A., & Balbus, J. M. (1996). Global climate change and emerging infectious diseases. *JAMA*, *275*(3), 217-23. https://doi.org/10.1001/jama.1996.03530270057032

Peterson, T. C., Easterling, D. R., Karl, T. R., Groisman, P., Nicholls, N., Plummer, N., … Parker, D. (1998). Homogeneity adjustments of in situ atmospheric climate data: A review. *Int. J. Climatol.*, *18*, 1493–1517. https://doi.org/10.1002/(SICI)1097-0088(19981115)18:13<1493::AID-JOC329>3.0.CO;2-T

Peterson, T. C., Vose, R., Schmoyer, R., & Razuvaev, V. (1998). Global Historical Climatology Network (GHCN) quality control of monthly temperature data. *Int. J. Climatol.*, *18*, 1169–1179. https://doi.org/10.1002/(SICI)1097-0088(199809)18:11<1169::AID-JOC309>3.0.CO;2-U

Pettitt, A. N. (1979). A non-parametric approach to the change-point detection. *Applied Statistics*, *28*, 126–135. https://doi.org/10.2307/2346729

Rich, K. M., & Wanyoike, F. (2010). An assessment of the regional and national socio-economic impacts of the 2007 Rift Valley Fever outbreak in Kenya. *Am. J. Trop. Med. Hyg.*, *83*(Suppl 2), 52–57. https://doi.org/10.4269/ajtmh.2010.09-0291

Saji, N. H., Goswami, B. N., Vinayachandran, P. N., & Yamagata, T. (1999). A dipole mode in the tropical Indian Ocean. *Nature, 401*, 360–363. https://doi.org/10.1038/43854

Schonwiese, C. D., & Rapp, J. (1997). Climate trend atlas of Europe based on observation 1891 – 1990. *Int. J. Climatol.*, *18*, 580-595.

Seleshi, Y., & Zanke, U. (2004). Recent changes in rainfall and rainy days in Ethiopia. *Int J Climatol*, *24*, 973–983. https://doi.org/10.1002/joc.1052

Sen, P. K. (1968). Estimates of the regression coefficient based on Kendall's tau. *J. Am. Stat. Assoc.*, *39*, 1379–1389. https://doi.org/10.1080/01621459.1968.10480934

Shanko, D., & Camberlin, P. (1998). The effect of the southwest Indian Ocean tropical cyclones on Ethiopian drought. *Int. J. Climatol.*, *18*, 1373–1378. https://doi.org/10.1002/(SICI)1097-0088(1998100)18:12<1373::AID-JOC313>3.0.CO;2-K

Štěpánek, P., Zahradníček, P., & Fardaet, A. (2013). Experiences with data quality control and homogenization of daily records of various meteorological elements in the Czech Republic in the period 1961–2010. *Quarterly Journal of the Hungarian Meteorological Service*, *117*(1), 123–141.

Stepanek, P., Zahradnicek, P., & Skalak, P. (2009). Data quality control and homogenization of air temperature and precipitation series in the area of the Czech Republic in the period of 1961-2007. *Advances in Science and Research*, *3*, 23-26. https://doi.org/10.5194/asr-3-23-2009

Stern, R., Rijks, D., Dale, I., & Knock, J. (2006). *Instat (interactive statistics) climatic guide*; *Statistical Services Centre*, The University of Reading, Reading, UK, pp. 330.

Teshome, D., Kasye, M., Abiye, A., & Eshetu, A. (2016). A review on Rift Valley fever on animal, human health

and its impact on livestock marketing. *Austin Virol and Retrovirology, 3*(1), 1020.

Thiaw, W. M., Barnston, A. G., & Kumar, V. (1999). Predictions of African rainfall on the seasonal timescale. *J. Geophys. Res.*, *104*, 31589–31597. https://doi.org/10.1029/1999JD900906

Trenberth, K. E., & Paolino, D. A. (1980). The Northern Hemisphere sea-level pressure data set: Trends, errors and discontinuities. *Mon. Wea. Rev.*, *108*, 856–872. https://doi.org/10.1175/1520-0493(1980)108<0855:TNHSLP>2.0.CO;2

Verdin, J., Funk, C., Senay, G., & Choularton, R. (2005). Climate science and famine early warning. *Phil. Trans. R. Soc. B*., *360*, 2155–2168. https://doi.org/10.1098/rstb.2005.1754

Vicente-Serrano, S., Beguería, S., Lopez-Moreno, J. I., García-Verac, M. A., & Stepanek, P. (2010). A complete daily precipitation database for northeast Spain: reconstruction, quality control, and homogeneity. *Int. J. Climatol.*, *30*, 1146–1163. https://doi.org/10.1002/joc.1850

Wijngaard, J. B., Klein-Tank, A. M. G., & Können, G. P. (2003). Homogeneity of 20th century European daily temperature and precipitation series. *Int. J. Climatol.*, *23*, 679–692. https://doi.org/10.1002/joc.906

Wilks, D. S. (2006). *Statistical Methods in the Atmospheric Sciences* (2nd ed.). Academic Press, pp. 648.

Wondosen, F., (2003). *Influence of animal disease and sanitary of regulation of livestock trade and case of export restriction* (10th ed., pp. 1-56), Ethiopian society of state of animal production.

Yenigun, K., Gumus, V., & Bulut, H. (2008). Trends in stream flow of the Euphrates basin, Turkey. *Proc. Inst. Civil Eng. Water Manage*, *161*, 189–198. https://doi.org/10.1680/wama.2008.161.4.189

Yesilırmak, E., Akçay, S., Dagdelen, N., Gürbüz, T., & Sezgin, F. (2008). Quality Control and Homogeneity of Annual Precipitation Data in Büyük Menderes Basin, Turkey. International Meeting on Soil Fertility, Land Management, and Agroclimatology. Turkey, p:225-233.

Yu, P. S., Yang, T. C., & Kuo, C. C. (2006). Evaluating long-term trends in annual and seasonal precipitation in Taiwan. *Water Resour. Manag.*, *20*, 1007–1023. https://doi.org/10.1007/s11269-006-9020-8

Appendix A

Table A1. Environmental and climate data sets used in the study: Sources, lengths of data period, and their specific purposes in the study

Data	Source and Description	Period	Purpose(s)
Observed Rainfall Data	National Meteorology Agency (NMA)	1987-2006	Teleconnection, & input for prediction models development
Nino3.4 SST anomaly index	NOAA_CPC (http://www.cpc.noaa.gov/data/indices/) NINO3.4 SST: is one of the four SST regions used by the National Oceanographic and Atmospheric Administration's/ Climate Prediction Centre (NOAA/CPC) to monitor the phase, amplitude and propagation of ENSO events [34]. URL: http://www.cpc.noaa.gov/products/analysis_monitoring/ensostuff/nino_regions.shtml	1987-2006	Teleconnection, & input for prediction models development
Indian Ocean Dipole Mode (DMI)	Frontier Research Center for Global Change (FRCGC) (FRCGC) The Indian Ocean Dipole (IOD): is a coupled ocean-atmosphere phenomenon in the Indian Ocean. It is normally characterized by anomalous cooling of SST in the south eastern equatorial Indian Ocean and anomalous warming of SST in the western equatorial Indian Ocean. Associated with these changes the normal convection situated over the eastern Indian Ocean warm pool shifts to the west and brings heavy rainfall over the east Africa and severe droughts/forest fires over the Indonesian region.	1987-2006	Teleconnection, & input for prediction models development

Copyrights

Copyright for this article is retained by the author(s), with first publication rights granted to the journal.

This is an open-access article distributed under the terms and conditions of the Creative Commons Attribution license (http://creativecommons.org/licenses/by/4.0/).

P57

Weakened impact of the Atlantic Niño on the future Guinean coast rainfall

Koffi Worou, Hugues Goosse, Thierry Fichefet and Fred Kucharski

Université catholique de Louvain, Earth and Life Institute, Georges Lemaître Centre for Earth and Climate Research, Louvain-la-Neuve, Belgium (koffi.worou@uclouvain.be)

Much of the rainfall variability in the Guinean coast area during the boreal summer is driven by the sea surface temperature (SST) variations in the eastern equatorial Atlantic, amplified by land-atmosphere interactions. This oceanic region corresponds to the center of action of the Atlantic Equatorial mode, also termed Atlantic Niño (ATL3), which is the leading SST mode of variability in the tropical Atlantic basin. In years of positive ATL3, above normal SST conditions in the ATL3 area weaken the sea level pressure gradient between the West African lands and the ocean, which in turn reduces the monsoon flow penetration into Sahel. Subsequently, the rainfall increases over the Guinean coast area. According to observations and climate models, the relation between the Atlantic Niño and the rainfall in coastal Guinea is stationary over the 20th century. While this relation remains unchanged over the 21st century in climate model projections, the strength of the teleconnection is reduced in a warmer climate. The weakened ATL3 effect on the rainfall over the tropical Atlantic (in years of positive ATL3) has been attributed to the stabilization of the atmosphere column above the tropical Atlantic. Analysis of historical and high anthropogenic emission scenario (the Shared Socioeconomic Pathways 5-8.5) simulations from 31 models participating in the sixth phase of the Coupled Model Intercomparison Project suggests an additional role of the Bjerkness feedback. In a warmer climate an anomalous warming of the eastern equatorial Atlantic associated to ATL3 positive phases is less important than in the present day climate conditions. This weakened SST amplitude is associated to weaker anomalous westerlies, which in turn favor the upwelling cooling effect on the eastern equatorial Atlantic. Both the Guinean coast region and the equatorial Atlantic experiment the projected rainfall reduction associated with ATL3, with a higher confidence over the ocean than over the coastal lands. The links between the changes in the ATL3 variability and the changes of the mean state have also been evaluated. The analysis of the future changes has been performed for the near-term (2015-2039), mid-term (2040-2069) and long-term periods (2070-2099), relative to the present-day conditions (1985-2014).

P58

Fidelity in Representing Indian Summer Monsoon rainfall Variability and Teleconnections using Circulation Indices

Yasmin Zahan

with

P. V. Rajesh, B. Abida Choudhury and B. N. Goswami

Department of Physics, Cotton University, Guwahati-781001

Abstract:

A large number of circulation indices has been constructed to represent the Indian summer monsoon to aid diagnosis of teleconnections with Indian summer monsoon rainfall (ISMR), and simulations by climate models based on assumption of strong coupling between rainfall and circulation in past years. Though, a poor correlation is found between the ISMR and circulation indices, raising question on the coupling between monsoon rainfall and circulation. In this study, we have identified and provided the insight of reasons behind the poor correlations. By looking into the periods and variances explained by the oscillatory modes of circulation indices and ISMR, decorrelation between the two can be easily understood. Therefore, all circulation indices underestimate the negative correlation between JJAS SST over the Nino3.4 and ISMR and also fail to simulate the lead-lag relationship between the two. The local response of winds to deep convection over the waters of the Indian Ocean and western Pacific warm pool leads to a strong increasing trend in some of the circulation indices and adds 'noise' in the modes resulting in de-correlation between circulation indices and ISMR.

Keywords:

Indian summer monsoon rainfall (ISMR), Circulation Indices, Coupling between ISMR and circulation, Coupled modes of variability.